Title
Vasoactive intestinal peptide shapes photic communication across the circadian visual system

Author
Vosko, Andrew Martin

Publication Date
2012

Peer reviewed|Thesis/dissertation

UNIVERSITY OF CALIFORNIA

Los Angeles

Vasoactive Intestinal Peptide Shapes Photic Communication across the Circadian Visual System

A dissertation submitted in partial satisfaction of the requirements for the degree Doctor of Philosophy in Neuroscience

by

Andrew Martin Vosko

2012

ABSTRACT OF THE DISSERTATION

Vasoactive Intestinal Peptide
Shapes Photic Communication across the
Circadian Visual System

by

Andrew Martin Vosko
Doctor of Philosophy in Neuroscience
University of California, Los Angeles, 2012
Professor Christopher S. Colwell, Chair

Circadian rhythms affect human health and well-being by temporally organizing biological processes and fitting them to a 24 hour period. In mammals, circadian rhythm generation and organization are regulated by oscillatory networks in the heterogeneous suprachiasmatic nucleus (SCN) of the hypothalamus. Acute light resets the phase of these networks at night by an incompletely understood mechanism that involves changes in the transcriptional status of the immediate early gene *c-fos* and the clock gene *Per1* in individual SCN cells. Neuropeptides, which anatomically define the SCN's functionally distinct core and shell subregions, have also emerged as important players in this light response pathway. The following set of studies examines how one such neuropeptide, vasoactive intestinal peptide (VIP), contributes to the gene expression changes across the SCN network during a successful phase shift. Experiments show

that in response to a phase shifting light pulse, mice genetically deficient in VIP: 1) have acute, blunted molecular responses of c-FOS and *Per1* in the SCN, 2) do not sustain gene expression changes in c-FOS and *Per1* across SCN cells over time, and 3) lack gene expression changes of c-FOS and *Per1* specifically in the SCN shell. Because these effects of VIP may be either acute or chronic due to an organizational or developmental role for VIP, experiments were also carried out to identify anatomical changes in the SCN of mice genetically deficient in VIP. Results suggest that specific changes to the light-input side of the circuit are altered when VIP is absent, indicating an organizational role for this neuropeptide. These changes include increased retinal afferent terminal branching and decreased androgen receptor expression in the retino-recipient region of the SCN. Interestingly, there did not appear to be changes in intra-SCN connectivity in mice lacking VIP, as determined by analysis of Golgi impregnated neurons. These data together suggest that VIP acts not only acutely to affect photic signaling, but it also plays a role in the structuring of the SCN to allow for the efficient flow of photic phase resetting information from retinal inputs across the circadian system.

The dissertation of Andrew Martin Vosko is approved.

James A. Waschek

Stephanie Ann White

Gene D. Block

Ellen M. Carpenter

Christopher S. Colwell, Committee Chair

University of California, Los Angeles

2012

TABLE OF CONTENTS

LIST OF FIGURES

ACKNOWLEDGEMENTS

This work would not have been possible without the financial support from the UCLA Graduate Division Dissertation Year Fellowship Award, the National Institute of Neurological Disorders and Stroke Ruth L. Kirschstein National Research Service Award **(**F31NS063666) and the National Institute of Child Health and Human Development Training Grant (T32HD0007228: "Neuroendocrinology, sex differences and reproduction") at UCLA. I am especially indebted to the UCLA Intellectual and Developmental Disabilities Research Core and the Neuroscience IDP, where I have been provided countless resources and support for completing my research.

I am grateful for the opportunity to have worked with such a large number of bright, motivated and caring individuals who have offered their time and expertise freely and patiently. Each of the members of my Dissertation Committee has gone out of his or her way to extend guidance and advice in the world of scientific research, treating me not only as a student, but also as a colleague and friend. I would especially like to thank Dr. Jim Waschek, Dr. Ellen Carpenter and Dr. Chris Colwell for their constant encouragement and complete support of my research and career. Dr. Waschek offered his lab early on in my graduate career with a lab full of helpful scientists that did not hesitate to help me when needed. Without any questions, Dr. Carpenter openly adopted me into her lab and treated me as her own student to show me the ins and outs of molecular anatomy in the nervous system. Dr. Colwell, the chairman of my committee, was always open to listen to my concerns, always interested in promoting my own research, and actively invested in making me become a productive scientist in the field of chronobiology.

There have been so many friends that I have made since beginning my Ph.D. training to which I will always be indebted. These people have listened to me gripe about the traffic in Los Angeles, the

frustrations of science, and the sometimes unfair curveballs in life. My friends have been a major part of my life both in and outside of the lab, and I am truly lucky to have both worked alongside and enjoyed so much of my time with these great people. I would not have been able to complete this process without their support.

Finally, I have to thank my family for being there, always. My parents have given me the strongest sense of support and confidence any person could ever ask for, and my brothers are also some of my closest friends. Knowing that I have a family as tight and supportive as mine has been invaluable for me throughout all of my studies.

VITA/BIOGRAPHICAL SKETCH

Andrew Martin Vosko is in the interdepartmental graduate program in neuroscience at UCLA. In 2004, he graduated with a B.S. from the University of Michigan, Ann Arbor, holding concentrations both in Biopsychology and Cognitive Science and Japanese Language and Literature. During this time, he began doing circadian rhythms research in the lab of Dr. Theresa Lee, completing an honors thesis investigating molecular rhythms in the diurnal rodent, *Octodon degus*. Andrew also spent a year studying at the University of Tokyo, working in the laboratory of veterinary ethology of Dr. Yuji Mori. Upon returning to Michigan, he worked as a lab technician in both the circadian rhythms lab of Dr. Lee and also the affective neuroscience laboratory of Dr. Kent. Berridge. At UCLA, his research interests have continued in circadian rhythms and have focused on neuroanatomical pathways involved in the circadian visual system.

Publications

Vosko, A.M., Schroeder, A., Loh D., and Colwell, C.S. Vasoactive Intestinal Peptide and the mammalian circadian system. 2007. *General and Comparative Endocrinology* 152: 165-175.

Vosko, A.M., Hagenauer, M.H., Hummer, D.L., and Lee, T.M. *Period* gene expression in the diurnal degu (*Octodon degus*) and nocturnal laboratory rat (*Rattus norvegicus*). 2009. *American Journal of Physiology: Regulatory and Integrative Physiology* 296: R353-61.

Itri, J.N., Vosko, A.M., Schroeder A., Dragich, J.M., Michel, S., and Colwell, C.S. Circadian regulation of a-type potassium currents in the suprachiasmatic nucleus. 2010. *Journal of Neurophysiology* 103: 632-40.

Dragich, J.M., Loh, D.H., Wang, L.M., Vosko A.M., Kudo, T., Nakamura, T.J., Odom, I.H., Tateyama, S., Hagopian, A., Waschek J.A., and Colwell C.S. The role of neuropeptides PACAP and VIP in the photic regulation of gene expression in the suprachiasmatic nucleus. 2010. *European Journal of Neuroscience* 31: 864-75.

Vosko, A.M., Colwell C.S., and Avidan, A.Y. Jet lag syndrome: circadian organization, pathophysiology, and management strategies. 2010. *Nature and Science of Sleep* 2010:

187-198.

Colwell, C.S. and Vosko, A.M. Sleep-wake timing disorders in Review of Sleep Medicine, 3rd Ed. *In press*

Talks and Poster Presentations

"Neuropeptide effects of photic signaling in the SCN". Invited Talk, UCLA Neuroscience Graduate Forum 10/2008

"Peptidergic signaling in photic control of the circadian system". Invited Talk, UCLA Laboratories in Neurondocrinology Meeting 08/2008

"VIP-ergic signaling in the mammalian circadian visual system". Invited Talk, UCLA Neuroscience IDP Retreat 09/11

"*Period* gene expression in the SCN of *Octodon degus*". Poster presentation, Neural Control of Behavior Conference, UCLA. 02/06

"*Period* gene expression in diurnal *Octodon degus* compared to the nocturnal laboratory rat". Poster presentation, Society for Research on Biological Rhythms. 05/06

"*Period* gene expression in diurnal *Octodon degus* compared to the nocturnal laboratory rat". Poster presentation, Society for Research on Biological Rhythms. 05/06

"Circadian regulation of a-type potassium currents in the suprachiasmatic nucleus". Poster presentation, Society for Research on Biological Rhythms. 05/08

"VIP modulates photic signaling in the SCN". Poster presentation, Society for Research on Biological Rhythms. 05/10

"Organizational changes in the circadian visual system of VIP-deficient mice". Poster presentation, UCLA Brain Research Institute Neuroscience Symposium. 11/11

"A role for VIP in circadian visual system organization". Poster presentation, UCSD Center for Chronobiology symposium 02/12

Chapter 1

Introduction to the neurobiology and physiology of circadian rhythms

Introduction

Just as there is intricate spatial organization to biology, there also exists a temporal order that allows for highly complex coordination among the often competing processes necessary to sustain life. At the level of behavior, this can be seen in the cyclicity in which most animals structure the day: separate periods devoted to activity and rest, each having its own set of metabolic needs and physiological demands, and each requiring different adaptations to the surrounding environment.

As temporal order is a fundamental property, multiple mechanisms have evolved in its regulation. Precise and adaptable daily timekeeping is achieved through the interaction between an endogenous oscillator, called a circadian (*circa* meaning "about" and *dia* meaning "day") clock, and external events that influence the clock's function (Dunlap, 1999). The rhythms generated by this clock (or clocks), known as circadian rhythms, are endogenously generated and self-sustained, and they consistently cycle close to, but not exactly, 24 hours. Organisms maintain daily 24 hour rhythms in their natural environments because environmental cues can adjust daily rhythms to a precise 24 hour period. The most powerful of these environmental cues is light (Czeisler *et al.*, 1981).

Circadian rhythms function to maximize success for predation, reproduction, immune function, and restorative processes. However, in a modern, city-dwelling lifestyle, there are artificial environmental cues that constantly expose the brain and body to excessive temporal misalignment and resynchronization, which ultimately has consequences for human health and disease. For instance, shift-workers exposed to alternating day and night shifts severely disrupt rhythms in their sleep-wake behavior, hormone profiles, and autonomic nervous system tone

(Wang *et al.*, 2011). Shift-workers also report having higher rates of GI disorders (Knutsson & Boggild, 2010). Misalignment of the circadian system with the ambient light-dark cycle has also been shown to reduce sleep and alertness (Rajaratnam & Arendt, 2001), alter metabolic and endocrine function (Ha & Park, 2005), increase incidence of cardiovascular morbidity and mortality (Harrington, 1994) and increase the probability of dangerous error (Anch, 1988). Furthermore, seasonal affective disorder (Lewy *et al.*, 2006), age-related dementias (Wu & Swaab, 2007) and both major and bipolar depression (Wirz-Justice, 2009) are responsive to treatments aimed at resynchronizing endogenous rhythms via appropriately timed exposure to light. These data suggest the circadian system has effects that are wide-reaching across different disease states and offers an important therapeutic target, an idea gaining acceptance within and outside of the academic community (Judson, 2009).

Circadian organization

Circadian rhythms are found in organisms from single-celled bacteria to modern man. Mechanistically, circadian systems share a similar set of design principles across kingdoms (Dunlap, 1999). At the molecular level, this includes a feedback loop involving transcription, translation, protein stabilization/destabilization and degradation that takes about 24 hours. In multi-cellular organisms, cells form organizational networks that utilize cellular output signaling to reinforce intracellular molecular rhythms, resulting in reinforced rhythmicity for individual cells in the network (Welsh *et al.*, 2010). Tissue specialization has further yielded structures with altered circadian timekeeping capabilities. This has translated to a system in which ‘master’ and ‘slave’ oscillating structures interact to maintain circadian organization across the body. In

mammals, while each cell contains the machinery and capacity to track circadian time, a complex hierarchy of timekeeping structures is responsible for circadian rhythms in behavior and physiology (see Fig. 1).

At the level of the single, oscillating mammalian cell, a number of 'clock' genes have been isolated and cloned. While theoretically, these genes can be thought of as timekeeping markers in a simple feedback loop that takes about 24 hours to complete, in reality, there are many functional redundancies in individual genes as well as among different interacting loops that utilize different biochemical modulators at each molecular level. This complexity has allowed for the fine-tuning of a robust oscillatory system and also provided the inherent flexibility that allows the molecular clock to be shifted in response to cellular signals. The major players in the transcriptional clock are: *Clock*, *Bmal1*, *Per1*, *Per2*, *Cry1*, *Cry2*, *Rev-Erb* and *Ror*. The basic model of this core molecular oscillator is described below.

CLOCK is the principal transcriptional activator in the feedback loop, both directly and indirectly recruiting the machinery necessary to promote transcription. *Clock* gene expression is relatively constant, but its circadian transcriptional activity is regulated by the cyclicity of the rhythmic expression of the gene *Bmal1*, with which it heterodimerizes (Ripperger & Brown, 2010). CLOCK possesses intrinsic acetylase activity which acts upon BMAL1 to promote DNA binding (Doi *et al.*, 2006), and concomitant to the initial binding to DNA, the CLOCK:BMAL heterodimer is phosphorylated, maintaining the stability of the transcriptional activator complex (this phosphorylation is also expressed in a circadian manner) (Kondratov *et al.*, 2006). CLOCK:BMAL binding is targeted to a *cis*-acting element, called an E-box, which is located in the promoter region of other core 'clock' genes (Ripperger & Brown, 2010).

There are two arms of the molecular feedback loop initiated through CLOCK:BMAL

activation. Studies have shown that the cyclicity expressed in one arm of this loop appears indispensable, while the overall protein levels, and not necessarily their rhythmic expression, are the important factors for the other arm of this loop (Ripperger & Brown, 2010).

The 'clock' genes in the first arm of the loop consist of the *period* genes (*Per1* and *Per2*) and the *cryptochrome* genes (*Cry1* and *Cry2*). As mentioned before, CLOCK:BMAL binds to E-boxes in the *period* and *cryptochrome* promoter regions, initiating their transcription. As each gene is transcribed and then translated, the *period* and *cryptochrome* products form homo- and heterodimers with each other (Reppert & Weaver, 2001). The proteins are modified post-translationally by a series of kinases and phosphatases which affect stability and nuclear translocation (Lowrey *et al.*, 2000; Xu *et al.*, 2005; Partch *et al.*, 2006). Data suggest the PER:CRY dimers, when translocated to the nucleus, repress activity of the CLOCK:BMAL complex (Lee *et al.*, 2001). One proposed mechanism for this is through dephosphorylation of the CLOCK:BMAL1 complex, causing it to become unstable and releasing it from its transcriptional activity (Ripperger & Brown, 2010). The period of CLOCK:BMAL transcriptional activity, as evidenced by *per* and *cry* mRNA expression, is approximately 24 hours (Reppert & Weaver, 2001).

The 'clock' genes in the second feedback loop consist of the REV-ERB and ROR family of orphan nuclear receptors. In this loop, CLOCK:BMAL binds to the E-box element of *Rev-Erbα* or *Rev-Erbβ* initiating transcription (Triqueneaux *et al.*, 2004). After translation, the REV-ERB proteins bind to a *cis*-acting element, called a retinoic acid-related orphan response element (RORE) in the *Bmal1* gene, preventing further transcription of *Bmal1* (Preitner *et al.*, 2002; Ueda *et al.*, 2002). At the same time, there also are retinoid-related orphan receptor (ROR) genes, which, when translated to their protein forms (RORα, RORβ and RORγ), compete with the REV-

ERB proteins in binding to the *Bmal1* RORE. ROR binding promotes *Bmal1* transcription (Akashi & Takumi, 2005; Guillaumond *et al.*, 2005). The balance and circadian rhythmicity of *Bmal1* levels are therefore based on the relative binding of REV-ERB and ROR to the *Bmal1* RORE (Ripperger & Brown, 2010).

Circadian networks and the SCN

The molecular clock is one level at which circadian rhythmicity is regulated. However, another important rhythmic regulator exists at the level of the network. One area illustrating this property is the suprachiasmatic nucleus of the hypothalamus (SCN). While cells throughout the body show oscillatory properties, the clock within the SCN is considered the 'master' oscillator that coordinates daily rhythms in mammals. Lesion studies originally established that the SCN is necessary for behavioral and physiological rhythmicity (Stephan & Zucker, 1972). Subsequent studies have shown that SCN cells are rhythmic both *in vivo* and *in vitro*, these cells begin oscillation *in utero*, they show circadian cycles of metabolism, and transplantation of fetal SCN restores rhythmicity in SCN-lesioned animals (Weaver, 1998; van Esseveldt *et al.*, 2000).

The SCN contains a dense network of oscillating neurons and glia that utilize cell-cell signaling to robustly keep track of time (Welsh *et al.*, 2010). When an SCN is dissociated and separated, individual cells appear to oscillate weakly, as measured by clock gene expression. These oscillations are strengthened when the dissociated cells are placed in high density dispersal cultures, but not at low densities (Webb *et al.*, 2009). This suggests that some type of communication between SCN cells supports robust molecular oscillations. Network strengthening is not inherent in all cell types, however. In fibroblasts, for instance, the same

rhythmic strengthening is not observed when cells are plated at high densities (Welsh *et al.*, 2004). Another interesting observation is that when the SCN becomes molecularly arrhythmic due to *Bmal1* deletion, other clock genes can continue to cycle, but only when the SCN remains intact and not in a dissociated preparation (Ko *et al.*, 2011). This implies that cellular communication may be sufficient for molecular rhythmicity in the SCN. The SCN thus has specific network properties allowing it to function as a robust oscillator.

In addition to molecular oscillations, cells in the SCN exhibit rhythms in electrical activity, providing a measurable rhythmic output and circadian pacemaking signal. These electrical rhythms have been measured both *in vivo* and in SCN slice explants *ex vivo*, illustrating that electrical circadian rhythms are generated and maintained by SCN cells themselves (Welsh *et al.*, 1995). It is important to note that this is a property unique to the SCN, and is another reason the SCN is considered the mammalian 'master' circadian oscillator. SCN electrical rhythms are predicted by molecular rhythmicity within individual SCN cells (Quintero *et al.*, 2003). When dissociated and separated, individual cells again show weak oscillations in electrical activity. Just as when molecular rhythms strengthened when SCN cells were plated at higher densities, so do electrical rhythms (Aton *et al.*, 2005). This is due in part to a synchronizing effect when differently phased cells are within range to communicate with each other. Interestingly, when SCN cells are electrically silenced via application of tetrodotoxin (TTX) to prevent action potential generation, the molecular clocks within individual cells drift out of phase with each other, and the SCN as a structure loses robustness in its clock gene rhythms (Yamaguchi *et al.*, 2003).

Release of neurotransmitters and signaling molecules also follows a circadian rhythm in the SCN. Neuropeptides found in specific SCN subregions: arginine-vasopressin (AVP), gastrin

releasing peptide (GRP) and vasoactive intestinal peptide (VIP), all show daily rhythms in their release from SCN neurons (Nakamura *et al.*, 2001; Francl *et al.*, 2010a; b). In an *ex vivo* SCN slice preparation, GABA-ergic transmission (GABA is the most prominent neurotransmitter in the SCN) is also circadian-regulated (Itri *et al.*, 2004). Therefore, electrical rhythms in spontaneous firing rate from SCN cells not only provide a timekeeping reference for the observer, but through neurotransmitter release, they also provide temporal cues to other cells in the circadian system. These cues are likely communicated both by neural and endocrine mechanisms, having effects all over the brain and body (Antle & Silver, 2005). Other structures in the body, including the liver and adrenal glands, show similar circadian paracrine and endocrine signaling, fitting into a temporally-ordered physiological scheme among organ systems in the mammalian body (Dibner *et al.*, 2010).

Circadian entrainment

Daily entrainment of circadian period to environmental cues is necessary to avoid a persistent drifting of internal rhythms out of phase with the environmental light-dark cycle. In most laboratory studies, entrainment has been shown to result from the discrete effects of light on the circadian clock. The ability for a continuous stimulus, such as light, to discretely affect the clock, is thought to result from the gating of photic sensitivity of the circadian pacemaker to the subjective night (Geier *et al.*, 2005). Light in the early evening causes an organism to delay its rhythm, while light in the late evening/early morning results in an advancing of rhythms (Daan & Pittendrigh, 1976; Johnson *et al.*, 2003; Roenneberg *et al.*, 2003). During the subjective day, light does not appear to shift the clock (Daan & Pittendrigh, 1976; Johnson *et al.*, 2003;

Roenneberg *et al.*, 2003). Thus, early morning and evening light pulses discretely and subtly adjust the circadian clock to align with the environmental light-dark cycle (Daan & Pittendrigh, 1976). These temporally sensitive periods coincide with dawn and dusk transitions.

This model where discrete exposure to light is sufficient to adjust the internal pacemaker to synchronize with the environmental light-dark cycle has been extensively supported through studies of many different species (Johnson *et al.*, 2004). These data have been used to construct an organism's behavioral response graph, called a phase response curve (PRC), to single light pulses administered at different times of the day (DeCoursey, 1960). Different PRCs have shown that both nocturnal and diurnal organisms follow similar time-dependent adjustments of their internal clocks to light, although there are species-specific and small, individually variant characteristics (Smale *et al.*, 2003). An organism's PRC provides an explanation of how stable entrainment to a photoperiod works, based upon that organism's free running period and the ambient light-dark cycle.

In order to achieve stable entrainment through discrete light exposure, the timing of that exposure must coincide with a resulting phase shift of the internal clock that adjusts for the inherent phase difference between the environmental light-dark cycle and the endogenous free running period. For instance, for an animal with a free running period of 23 hours, a stably entraining light pulse must hold back (phase delay) the internal clock by one hour each day to adjust it to a 24 hour schedule. According to that animal's PRC, there will be a time in the early evening when a single light pulse will lead to a one hour delay. While it is likely that there will be other times when that animal will be exposed to light, the PRC also shows that there is a period where discrete light has no shifting effects on the clock at all, called a dead zone, which usually coincides with the time that ambient light is strongest (Daan & Pittendrigh, 1976). Thus,

once the internal clock is phase-locked to a photoperiod that provides a consistent, daily phase shift in the appropriate direction for synchronizing to the environment, stable entrainment can occur (Johnson *et al.*, 2004).

In any circadian system, there is a trade-off between robustness of endogenously generated rhythms and the adaptability of those rhythms to ambient cues (Johnson *et al.*, 2004). In one extreme, the circadian clock is independently strong enough that phase shifting is made more difficult, and it is attainable only during a short window with high intensity light cues resulting in only modest shifts, if at all. At the other end of this spectrum, a very adaptable circadian clock would be able to entrain to any light-dark cycle, even one far beyond the timing of earth's rotation on its axis. In this case, the circadian clock would be much more flexible, but also much less robust. While inter-species variation exists, most organisms lie somewhere in-between the two poles, where there are limits to circadian entrainment based on the magnitude of possible phase shifts (Johnson *et al.*, 2003). When these limits are surpassed, stable entrainment cannot occur, and rhythms lose their adaptive value.

While the discrete effects of light can account for daily entrainment in many cases, the continuous effects of light have also been shown to entrain circadian rhythms to the light-dark cycle. In this way, different light intensities change the free running period of the circadian clock, causing it to speed up or slow down over the course of the day (Daan, 2000). The importance of continuous light effects differs between species, and both discrete and continuous light appear to differentially contribute to certain chronobiological phenomena (Johnson *et al.*, 2004) (see Fig. 2).

As stated in the previous section, circadian timekeeping mechanisms evolved in most mammals to be both precise and adaptable. The multiple levels responsible for rhythm

generation provide a means for these rhythms to maintain precision and robustness around 24 hours. There are also a number of ways for these rhythms to be shifted, making them adaptable. For one, the molecular clock can be pushed forward or back in its circadian cycle through biochemical manipulation. Similarly, so can rhythms in electrical activity and also secreted factors. The following section addresses how circadian rhythms can be shifted to resonate with the appropriate environmental cycles, with a focus on light as the primary entraining agent.

Molecular entrainment

For an external event to shift endogenously generated oscillations, cells must have a way of communicating relevant environmental information as well as a means of regulating responsiveness to such cues. These mechanisms are provided through the cell membrane. At the membrane, ligands that can induce circadian phase shifts can bind to receptors and initiate a cascade of intracellular events that interact with the cell's molecular clock. There are also non-membrane bound receptors that can act on the molecular clock, but these are not addressed in this review. While multiple cell signaling pathways have been implicated in molecular phase shifting and entrainment, most pathways converge on the actions of the cellular transcription factor cyclic adenosine monophosphate [cAMP] response element binding (CREB).

There are at least three major pathways by which CREB signaling is triggered during a phase shift. These are via mitogen activated protein kinases (MAPKs), protein kinase a (PKA) and calcium-calmodulin-dependent protein kinase II (CaMKII) (Golombek & Rosenstein, 2010). Along each of these pathways, a series of second messenger pathways converge on the phosphorylation of CREB at key serine residues. Upon phosphorylation, CREB translocates to

the nucleus and binds to the cAMP response element (CRE) regions on target genes to initiate their transcription (Lonze & Ginty, 2002). In mammals, the binding of CREB to the CREs of the *period* genes (and thus the initiation of their transcription) is believed to be the central mechanism by which the molecular clock resets (Ripperger & Brown, 2010).

Changes in the molecular clock can be tracked in the cells of the SCN. Within five to ten minutes after a phase shifting light pulse, SCN cells exhibit a transient increase in phosphorylated CREB (pCREB) (Ginty *et al.*, 1993). Following this increase, there is also a robust induction of *Per1* message and then protein. Induction of *Per2* follows at a slower rate and may rely on the initial induction of *Per1* or other immediately responsive genes for its activation, but it is also thought to contribute to circadian phase shifts (although its role in phase shifting is less clear) (Ripperger & Brown, 2010). Antisense oligonucleotides to *Creb* have been shown to block both the induction of *Per1* as well as phase shifts in SCN electrical activity (Tischkau *et al.*, 2003). Antisense oligonucleotides to *Per1* have also been shown to block light-induced behavioral phase shifts (Tischkau *et al.*, 2003). Other areas in the body also show CREB-mediated induction of *Per1*, although this transient *Per1* increase has been shown to accompany many phase-resetting pathways, it is thus far indispensible only to photic resetting in the SCN (Tsuchiya & Nishida, 2003).

The increased translation of PER1 is likely the functional link at which molecular phase resetting can be applied directly to the clock itself. By increasing levels of PER1 at different points along the cycle, the molecular clock could respond by either transiently phase shifting ahead, phase lagging, or by lacking any response at all. Conceptually, this can be illustrated by low levels of PER1 rapidly being increased. The sudden accumulation would result in more dimers between PER proteins and their translocation back to the nucleus to shut off the

transcriptional activity of CLOCK:BMAL. If this switch were triggered while the rate of transcription was increasing, the result would be a phase advance, whereas if the induced PER1 increase occurred during a time when transcriptional rate was decreasing, the result would be an extended period of elevated dimers, leading to a phase delay. Importantly, when the PER1 levels are already high, the transient increase in PER1 would have little to no shifting effect on the clock. This is observable both at the molecular and the behavioral levels (Shigeyoshi *et al.*, 1997).

A phase shifting stimulus elicits a number of responses beyond the transcription of clock genes as well. This is because during a phase-resetting stimulus, a cell signaling pathway initiates histone phosphorylation and subsequent chromatin remodeling. This remodeling exposes a large strand of DNA for high levels of transcriptional activity (Crosio *et al.*, 2000). The result is a wave of transcription of genes including *Per1, Per2* (Naruse *et al.*, 2004) and a number of immediate early genes (IEGs), including the proto-onco gene *c-fos* (Crosio *et al.*, 2000). While the transcription and translation of IEGs have been shown to temporally and spatially map light induction of the mammalian SCN in response to a light pulse, their exact role in entrainment is still unclear (Rusak *et al.*, 2002). Regardless, there are a large number of transcriptional changes taking place within a single cell in response to an appropriately timed phase resetting stimulus.

Entrainment across a network

The resetting of each cell's molecular clock has to be coherently and faithfully relayed to other cells within the clock network. Furthermore, depending on the complexity of the circadian system in a given organism, those clock networks have to communicate phase resetting

information to other clock networks in order to synchronize different physiological systems. This is especially pertinent for circadian organization in mammals, where desynchrony among these different networks is thought to contribute to a number of the symptoms found in degenerative and diseased states (Takahashi *et al.*, 2008).

Photoreceptors in the eye are necessary for entrainment of the circadian system (Nelson & Zucker, 1981). Within the eye, the retina is the first relay at which temporal resetting cues are communicated across a clock network. The retina, like the SCN, shows oscillatory activity in clock genes (Ruan *et al.*, 2008), and it also shows a circadian rhythm in melatonin synthesis while isolated in culture (Tosini & Menaker, 1996), suggesting that the retina contains its own circadian clock. In the *ex vivo* preparation, the retina is phase shifted by light, and this appears to be mediated by a dopamenergic mechanism (Ruan et al. 2008). While the mammalian retina both contains oscillatory properties and is the direct recipient of phase shifting light information, it is still unknown whether or not phase shifting the retina itself phase shifts other systems within the body.

As in classical visual perception, mammalian photic entrainment requires conversion of light to an electrochemical signal in the retina. This process requires focused light to reach the back of the retina, where photons come into contact with photopigment-containing rod and cone cells. According to the classical understanding, photopigments in these cells undergo a conformational change in the presence of photons, leading to a change in membrane ionic permeability and subsequent hyperpolarization (Hubbell & Bownds, 1979). This electrical change in rods and cones is then translated to a change in output signals onto bipolar cells. Retinal bipolar cells, in turn, send electrical output signals to adjacent retinal ganglion cells, which are an extension of the central nervous system. These neurons depolarize in response to

visual stimuli and send action potentials along their distal axonal projections, releasing neurotransmitters to the hypothalamus, thalamus and midbrain (Hubbell & Bownds, 1979; Hattar *et al.*, 2006).

Mechanisms behind circadian entrainment differ from the canonical understanding of retinal phototransduction. In mice transgenically degenerate in both rods and cones, circadian entrainment remains intact, suggesting that another photopigment-containing cell carries phase shifting and entrainment information to the circadian clock (Foster *et al.*, 1991). Furthermore, circadian phase shifts are greatest in response to monochromatic light in the blue-green range, which differs from the spectral sensitivity of both rods and cones (Lall *et al.*, 2010; Butler & Silver, 2011). The reasons for these findings is that in the circadian visual system, irradiance coding and detection take place via two mechanisms, one that involves classical rod and cone receptors, and another, predominant mechanism by which phototransduction bypasses rods, cones and bipolar cells, but begins via depolarization of intrinsically photosensitive retinal ganglion cells (ipRGCs) that contain the photopigment melanopsin (Altimus *et al.*, 2010). When rods, cones, and ipRGCs are all absent, circadian photoentrainment does not occur (Hattar *et al.*, 2003).

Tract tracing of the retina reveals that less than 0.1% of all retinal ganglion cell axons travel to the hypothalamus via the retinohypothalamic tract (RHT)(Mason & Lincoln, 1976; Provencio *et al.*, 1998). Most RHT axons synapse onto the SCN in its ventral and mid- posterior subregions (known as the core): an observation that lead to the initial discovery of the SCN as the site of the primary mammalian pacemaker (Moore & Lenn, 1972). Pharmacologically blocking neurotransmitters in the SCN attenuates light-induced phase shifts, suggesting that while light information is initially carried via the retina, phase shifting input is carried through a

neural circuit where the SCN plays an integral role (Kallingal & Mintz, 2010).

The SCN is monosynaptically connected to the retina via ipRGC axons coursing through the RHT (Rollag *et al.*, 2003; Perez-Leon *et al.*, 2006). Unlike other photosensitive cells [rods and cones], ipRGCs depolarize in response to light, they are most sensitive to light in the 480 nm range, and they are most responsive to long exposures of high intensity light (Hankins *et al.*, 2008; Schmidt *et al.*, 2011). In general, these ipRGCs are thought to communicate with the SCN through glutamate and pituitary adenylyl cyclase activating peptide (PACAP) as transmitters, which have been co-localized within ipRGCs (Hannibal, 2002). While glutamate binding to NMDA receptors in the SCN has been shown to be sufficient for causing phase shifts, both PAC1 and non-NMDA glutamate receptors are also known to play a role in mediating the magnitude of phase shifts (Ebling, 1996; Mintz *et al.*, 1999; Hannibal *et al.*, 2001). A basic circuit model of phase shifting involves glutamate released from the RHT binding to NMDA, leading to depolarization and calcium influx in retinorecipient SCN neurons. Within a single, activated neuron, cell signaling pathways are triggered, leading to phosphorylation of CREB, histone modification, initiation of clock gene transcription, and subsequent phase shifting of the molecular clock.

At the same time, another population of ipRGC axons carry photic information to the intergeniculate leaflet of the thalamus (IGL), which sends axons through the geniculohypothalamic tract (GHT) rostrally back to the SCN using gama amino butyric acid (GABA) and neuropeptide y (NPY) as its major transmitters (Reghunandanan & Reghunandanan, 2006). While this pathway does appear to have some role in circadian entrainment, lesion studies have shown that it is not necessary to entrain to a normal light-dark cycle (Pickard *et al.*, 1987). Under intact conditions, however, the SCN receives retinal phase resetting information both

directly and indirectly via a number of different transmitter-releasing systems.

Both RHT and GHT axons terminate just ventrolaterally to the third ventricle in the ventral aspect of the bilateral SCN, functionally distinguishing the ventral SCN as the primary site for photic input to the nucleus (Moore *et al.*, 2002; Reghunandanan & Reghunandanan, 2006). In general, the SCN is quite small and densely packed with neurons and glia connected by many gap junctions and intra-nuclear synapses (Van den Pol, 1980; Antle & Silver, 2005), and so its organization easily provides a pathway for this photic input to be transmitted between its cells. This SCN functional organization is supported by chemoarchitectural and physiological data as well. Differences in visual input synapses, neuropeptide expression and electrical activity patterns all similarly divide the SCN into two primary component parts: the core and the shell (see Fig. 3).

Core and shell subregions functionally divide the SCN into two distinct parts: one responsive to environmental cues and the other that acts as a robust oscillator. The SCN core has been shown to uniquely respond with c-FOS expression in response to a nighttime light pulse (Karatsoreos *et al.*, 2004). Interestingly, the core shows low-amplitude, if any, rhythmicity in c-FOS expression, whereas the SCN shell shows rhythmic c-FOS expression (Schwartz *et al.*, 2000). These effects have also been noted for *period* gene expression, with light-induced expression taking place in the non-oscillating core, and rhythmic oscillation taking place in the SCN shell (Hamada *et al.*, 2001; Karatsoreos *et al.*, 2004; Yan *et al.*, 2007).

Gene expression studies support the idea that the SCN subregions are functionally distinct, but normal entrainment involves communication of temporal cues across each of these areas. For example, all nighttime light pulses induce *Per1* expression in the SCN core, even when behavioral phase shifts are absent. However, only *Per1* and *Per2* expression in the SCN

shell coincides with behavioral phase shifts from light (Yan & Silver, 2002). This suggests that light-induced *period* gene expression spreads from the core to the shell during phase shifting pulses. This idea is further supported by data from a time course *in situ* hybridization study, in which *Per1* expression is increased first in the SCN core following a phase shifting nighttime light pulse and then later increased in the SCN shell (Hamada *et al.*, 2004). Abruptly changing the light dark cycle also results in a change of clock gene expression that occurs first in the core, followed by the shell (Nagano *et al.*, 2003). Taken together, data support a model by which entrainment across the circadian network follows the path of retina → SCN core → SCN shell.

Beyond this pathway, it is also important to consider downstream targets of the SCN in the role of network entrainment. Temporal information from the SCN is communicated to other areas in the brain and also throughout the body, many of which are endogenous oscillators (albeit weaker than the SCN) as well (Guilding *et al.*, 2009). SCN neurons have efferent targets at a number of hypothalamic relay nuclei, including the subparaventricular zone (SPZ) and the dorsomedial nucleus (DMH) (Abrahamson & Moore, 2001; Deurveilher & Semba, 2005). These nuclei, in turn, send projections throughout the subcortical brain to areas that regulate sleep, arousal, feeding, thermoregulation, osmoregulation, reproduction and energy metabolism (Saper *et al.*, 2005; Kalsbeek *et al.*, 2006; Colwell, 2010). Furthermore, the SCN also functions as an endocrine organ, and utilizing the ventricular system, it is likely that diffusible factors from the SCN are used to synchronize cells and systems in the rest of the body (LeSauter & Silver, 1998).

SCN plays multiple roles

The SCN is a model target in neurobiology to understand how sensory information is

integrated into a multitasking, self-sustaining network. However, it is still unclear how the SCN balances its multiple roles. There are clues from oscillation and entrainment theories, but there are many gaps in the literature, especially in the areas that bridge these levels of understanding. The work comprising this dissertation is focused on this particular problem, and it addresses SCN function based on its organization. Specifically, this involves parsing the SCN into its component core and shell subregions and examining how SCN chemoarchitecture defines SCN function.

The retinorecipient SCN core is primarily characterized by neurons expressing VIP (Abrahamson & Moore, 2001). This neuropeptide has been well studied, and recent genetic tools have allowed for a much deeper understanding of its role in the mammalian circadian system. From this work, a model has emerged where VIP acts as a synchronizing agent among single SCN clock cells. However, this model does not include a role for VIP in the equally important process of photic entrainment in the circadian system. The following chapters will focus on the hypothesis that VIP is necessary for the integration of photic information throughout the SCN and is therefore necessary for normal phase shifting and entrainment behaviors in the mammalian circadian system.

VIP

Basic properties

VIP is a neuropeptide in the secretin superfamily (Vaudry *et al.*, 2000), which includes structurally similar PACAP, glucagon and growth hormone-releasing hormone. In mammals,

VIP is expressed in specific subpopulations of neurons in the brain and peripheral nervous system as well as other tissues in the body. In the brain, VIP is expressed in the cortex, hippocampus, amygdala, caudate, posterior pituitary, superior colliculus, dorsal raphe, locus coeruleus and multiple nuclei in both the thalamus and hypothalamus (Brenneman *et al.*, 2000). The pattern of immunoreactive VIP (VIP+) neurons from the hypothalamus to the midbrain could be particularly important for a neuroendocrine role of VIP, as VIP-expressing cells run along the lateral and ventral parts of the third ventricle to the cerebral aqueduct in some species (Korf & Fahrenkrug, 1984; Mikkelsen & Moller, 1988). The broad expression of VIP and characterization of its terminals in many localized circuits indicates that VIP can act as a neurotransmitter and/or neuromodulator. Furthermore, electron microscopy has revealed that VIP-ir neurons contain large dense core vesicles and that VIP is localized to neurosecretory granules of nerve terminals, suggesting that VIP may act as a neurohormone in some species, and its endocrine role may depend on physiological state (Mikkelsen, 1989). VIP+ neurons have also been found to innervate cranial blood vessels, likely acting as a localized vasodilator (Baun *et al.*, 2011). Finally, in astrocytes, VIP has been shown to hydrolyze newly synthesized glycogen (Masmoudi-Kouki *et al.*, 2007). Taken together, these data suggest that VIP serves a variety of signaling and homeostatic functions within the central nervous system.

VIP binding sites are found in the anuran, reptilian, avian, and mammalian brains (Dietl *et al.*, 1990). These peptide receptors are G-protein-coupled receptors with characteristic seven transmembrane domains, three extracellular and intracellular loops, an extracellular amino-terminus and intracellular carboxy-terminus (Harmar, 2001). All members of this family can also regulate cyclic AMP (cAMP) concentrations by coupling to adenylate cyclase (Harmar, 2001). Two receptors, encoded by distinct genes, bind VIP with high affinity: VIP receptor 1 and 2

(VPAC1R and VPAC2R) (Ishihara *et al.*, 1992; Lutz *et al.*, 1993; Usdin *et al.*, 1994). These receptors are so named to reflect the equal binding affinity they have for both VIP and PACAP. VPAC1R and VPAC2R exhibit widespread expression in the brain and mediate most or all of the biological actions of these peptides. No known receptors specifically bind VIP without binding PACAP. Conversely, PACAP binds to another receptor, PAC1, with a 1000-fold affinity over VIP (Shivers *et al.*, 1991).

VIP in the circadian system

Anatomical organization of VIP and its receptors provided early indications that VIP was important for circadian function. Studies in the rat revealed that the SCN had large amounts of VIP- and VIP-receptor-containing neurons (Roberts *et al.*, 1980; Besson *et al.*, 1986; Vertongen *et al.*, 1998). These neurons are primarily located in the ventral aspect of the nucleus (Ibata *et al.*, 1989; Abrahamson & Moore, 2001). Neurons in this region receive retinal input from the RHT and express both VIP and GABA (Buijs *et al.*, 1995). At least one study in rats has directly demonstrated the termination of retinal afferents on VIP expressing cells (Tanaka *et al.*, 1993). Thus, the VIP expressing cells in the ventral SCN are likely an early relay for photic information reaching the SCN.

While the mammalian SCN predominantly lacks expression of the VPAC1R, it may be the most abundant site of expression of the VPAC2R in the central nervous system (Usdin *et al.*, 1994; Sheward *et al.*, 1995; Cagampang *et al.*, 1998; Vertongen *et al.*, 1998). In the mouse SCN, it has been estimated that VPAC2R are co-expressed with ≈30% of VIP expressing and ≈50% of the vasopressin expressing neurons (Kallo *et al.*, 2004b). Clearly, the VIP signal does not have to

travel far to influence SCN neurons in both the core and shell cell populations. The presence of the VPAC2R in the core region also suggests that VIP signals may feed back to regulate VIP secreting cells.

There is some evidence that the levels of VIP and its receptor vary with a circadian oscillation. For example, measurements of VIP release from rat SCN slice cultures revealed circadian oscillations that continued for a number of cycles in constant conditions (Shinohara *et al.*, 2000). Furthermore, in the mouse SCN, the levels of VIP mRNA show a circadian rhythm (Dardente *et al.*, 2004). Similarly, several groups have found that the mRNA coding for the VPAC2R varies with a daily cycle in rodents (Shinohara *et al.*, 1999a; Kallo *et al.*, 2004a). The functional significance of these rhythms is not yet known. For example, it may be that the rhythms in peptide levels are responsible for driving outputs from the circadian system. Alternatively, the presence (but not the rhythm) of the peptide and its receptor may be sufficient to fulfill the functions of this signaling system.

As described above, VIP is expressed in a subpopulation of cells within the SCN. In the central nervous system, it is assumed that these neurons are using this peptide to communicate with specific postsynaptic targets. For example, this assumption predicts that the depolarization of VIP+ neurons by light will cause the release of VIP and co-transmitters including GABA, and the synaptic release of these neurotransmitters will alter the membrane properties of the next set of neurons in the circuit via binding and activation of VPAC2Rs. This assumption has not been directly tested within the SCN. Alternatively, VIP may function as a paracrine signal acting at sites more distant than adjacent postsynaptic neurons. For example, clear rhythms in VIP release from SCN slice cultures (Shinohara *et al.*, 1995; Shinohara *et al.*, 2000) supports a paracrine role for this neuropeptide. Furthermore, a recent study showed that paracrine VIP signaling in the

SCN is sufficient to promote molecular synchrony among desynchronized SCN neurons (Maywood *et al.*, 2011).

In wildtype (WT) animals, VIP has been shown to acutely and directly affect circadian rhythms in the SCN, specifically pointing to a role in phase shifting and entrainment. For instance, microinjection of VIP alone (Piggins *et al.*, 1995) or in combination with other peptides (Albers *et al.*, 1991) can mimic the phase shifting effects of light at night. Application of VIP also phase shifts the circadian rhythm of vasopressin release (Watanabe *et al.*, 2000) and neural activity (Reed *et al.*, 2001) measured *in vitro*. In another study, VIP was shown to greatly enhance the SCN's glutamatergic response, which pharmacologically mimics a photic phase shift (Huang & Pan, 1993). This suggests that the phase shifting action of VIP in the SCN may depend on the other neurotransmitters present. By itself, VIP has been shown to induce *Per1* and *Per2* gene expression during the subjective night in the SCN slice preparation (Nielsen *et al.*, 2002). Also, chronic stimulation of the VPAC2R around the SCN has been shown to lengthen free running period, which could mimic a parametric effect of light input on the circadian clock (Pantazopoulos *et al.*, 2010). Together, these data are in line with a role for VIP in mediating photic phase shifts and entrainment in the SCN.

The exact relationship between light, VIP in the SCN and circadian behaviors is not yet clearly known, as data implicates a complex interaction between acute and chronic effects of light on VIP levels and vice-versa in the circadian system. For one, animals housed in constant light have significantly depressed concentrations of VIP expression in the SCN (Albers *et al.*, 1987). The suppressive effects of light on VIP have also been reported in other studies. Long light pulses cause a decrease in SCN VIP levels, but this effect appears specific for a small range of light intensities with a relatively high threshold (Shinohara *et al.*, 1998). Not only is VIP

expression damped in response to pulses of light, but also to pulses of darkness, and these effects are gated by the circadian clock (Shinohara *et al.*, 1999b). Thus, VIP levels are sensitive to the presence of light and also the interruption of light signaling.

Interestingly, many of the effects of light induced changes of VIP studied to date are long-term organizational effects on SCN VIP expression. Animals temporarily housed under constant lighting conditions as pups have lower levels of VIP in the SCN as adults, and they also have higher activity amplitude and more stable activity than animals reared in 12:12 light-dark cycles and in constant darkness (Smith & Canal, 2009). When mice have had congenitally interrupted retinal signaling due to a mutation resulting in anophthalmia, they show the opposite effect on VIP levels. Instead of decreased VIP levels, they show more diffuse, ectopic labeling of VIP+ cells and also more VIP+ cells overall (Laemle & Rusa, 1992; Ruggiero *et al.*, 2010). Therefore, the presence of retinal inputs appears to pattern SCN expression of VIP+ cells, likely affecting cellular positioning and cell fate determination within the SCN.

Transgenic models shed new light

Recently, transgenic mouse models have provided additional tools to understand the role of VIP and the VPAC2R in the circadian system *in vivo* (Shen *et al.*, 2000; Harmar *et al.*, 2002; Colwell *et al.*, 2003). The development of these models has provided a major contribution in this area, but there are also a few caveats to keep in mind with interpretation. First, these models are congenital knockouts. This means that the phenotypes expressed are the combined result of both the lack of the given gene (VIP and/or VPAC2) and the compensatory responses of the system to the loss of these genes. Nonetheless, both the VPAC2 KO and VIP KO mouse currently offer the

best system available to study the spectrum of molecular through behavioral levels of the VIP-ergic signaling pathway.

Second, knocking out the VPAC2R has effects on non-VIP-ergic signaling. It is possible that the loss of PACAP signaling could contribute to the circadian phenotype associated with VPAC2R KO mice. This is because, as was stated earlier, VPAC2R also recognizes the peptide PACAP with the same affinity as VIP. Analysis of PACAP-deficient mice suggests that PACAP itself is not important for the generation of circadian rhythmicity, and PACAP KO mice primarily present minor abnormalities in the light response of the circadian system (Colwell *et al.*, 2004). Furthermore, the VPAC2 KO mouse recapitulates all of the major circadian phenotypes seen in the VIP KO mouse, suggesting that the primary deficiency in the VPAC2R KO line is via the VIP signaling pathway. Still, the loss of the PACAP signal could contribute to the more severe phenotype seen with VPAC2R KO mice when compared to VIP KO mice (Harmar *et al.*, 2002; Colwell *et al.*, 2003).

Finally, knocking out the VIP ligand could also have effects extraneous to VIP-ergic signaling. This is because the VIP precursor polypeptide contains sequences encoding the peptide histidine-isoleucine (PHI), (Linder *et al.*, 1987). The construct used in making the VIP KO mouse also eliminates PHI, and the loss of PHI could contribute to some of the phenotype associated with VIP KO mice. However, the mRNA coding for VIP and PHI are *not* differentially localized (Linder *et al.*, 1987) and no putative PHI receptors have been described in the mammalian nervous system. Furthermore, since the phenotypes in the VPAC2R KO and VIP KO mouse are quite similar, it appears that the knocking out of PHI has minor, if any, effects on the circadian system. Thus, until more information emerges, the available evidence suggests that the circadian phenotype of the VIP KO mouse is due to the loss of VIP.

Oscillatory abnormalities in transgenic mice

Data from both VPAC2R KO and VIP KO mice suggest that VIP-ergic signaling is necessary for molecular clock gene rhythmicity. In constant dim red light, a condition which unmasks the endogenous circadian clock, VPAC2R KO mice show uniformly low and arrhythmic expression of *Per1*, *Per2*, and *Cry1* (although not *Bmal1*) in the SCN as measured by *in situ* hybridization, while WT controls exhibit robust rhythms (Harmar *et al.*, 2002). Similarly, under constant dark conditions, the rhythmic expression of *Per1* and *Bmal1* mRNA are lost in the VIP KO SCN, but expression of *Per2* remains rhythmic (Loh *et al.*, 2011). In subsequent studies, both VIP KO and VPAC2R KO mice have been crossed into mouse lines carrying either the *Per1::luciferase* or *Per1::GFP* transgenes in order to measure *ex vivo* real-time clock gene expression (Maywood *et al.*, 2006; Ciarleglio *et al.*, 2009). SCN slice cultures from these mice exhibit low levels of *Per1* expression that do not express the robust circadian variation seen control explants. Furthermore, not only are fewer of these cells rhythmic, the normal synchrony of *Per1* expression between cells is also lost. However, in another optical reporting model where KO mice were crossed with PER2:LUC knock-in mice, clock gene expression in the SCN appears to remain rhythmic (Hughes *et al.*, 2011; Loh *et al.*, 2011). This discrepancy indicates that some clock genes are more sensitive to the loss of VIP signaling than others.

The observation that molecular clock synchrony between neurons is disrupted without VIP or its receptor suggests that VIP-ergic signaling has some role in communicating temporal output of individually oscillating cells in the SCN. One means by which VIP-VPAC2R signaling may affect this synchrony is through its effects on SCN electrical activity. VIP KO and VPAC2R

KO mice fail to exhibit the midday peak in electrical activity that is characteristic of impulse rhythms from SCN brain slices (Cutler *et al.*, 2003; Brown *et al.*, 2007). Furthermore, the loss of the rhythms in electrical activity is most pronounced in mutant mice having the most severe disruption in their behavioral rhythms (Brown *et al.*, 2007). Using high-density dispersed cultures of SCN neurons grown on a microelectrode array, Herzog and colleagues found that both the ability of the population of SCN cells to remain synchronized as well as the ability of single cells to generate oscillations are both compromised in VIP KO and VPAC2R KO mice (Aton *et al.*, 2005). Importantly, in VIP KO mice, the daily administration of a VPAC2R agonist is sufficient to restore robust rhythmicity to the SCN neural population. It is not yet known if tonic application of this agonist would also rescue circadian rhythms in SCN cultures or if phasic application is necessary. Regardless, these data point to electrical rhythm deficits that mirror the molecular rhythm deficits in these transgenic mice.

Finally and importantly, all VPAC2R KO and VIP KO mice also exhibit disruptions in their ability to express a coherent circadian rhythm in locomotor activity in constant conditions (Harmar *et al.*, 2002; Colwell *et al.*, 2003). In many cases, the transgenic mice exhibit wheel-running behavior that is arrhythmic on the circadian time scale. The remainder of the mutant mice express a rhythm with a significantly shortened period that lacks coherence and statistical power due to variability in activity onset and expansion of the duration of wheel running activity. The extent of the arrhythmic phenotype varies from animal to animal and between transgenic models, with VPAC2R KO mice exhibiting the most disrupted rhythms. Recent evidence suggests that one explanation for the variability in phenotype is that GRP has some ability to compensate for the loss of VIP-ergic signaling (Brown *et al.*, 2005). These behavioral results indicate that VIP and the VPAC2R are critical for the generation of behavioral rhythmicity in

mice.

Light resetting abnormalities in transgenic mice

At the level of molecular resetting, the majority of data related to the effects of VIP on light-induced gene expression come from studies using the VPAC2R KO mouse. These studies suggest that VIP-ergic signaling is involved in both amplifying light-induced gene responses and also in gating these responses to occur in the subjective night. VPAC2R KO mice fail to show an induction of PER1 in the SCN in response to a 6-hour light pulse at night, while WT controls show upregulated PER1-ir in response to the same pulse (Harmar *et al.*, 2002). In contrast, it was also recently stated that *Per1* mRNA is induced by a light pulse during subjective night in VPAC2R KO mice, but to a lesser extent than in WT mice (Maywood *et al.*, 2007). This protein-mRNA discrepancy might be due to a difference in time course required for maximal expression for either the protein or mRNA, or it may be due to some translational modification. Interestingly, Maywood et al. (2007) also reported an induction of *Per1* during the subjective day in these mice, as did another study (Hughes *et al.*, 2004). In WT mice, light does not normally induce *Per1* expression during the day (Shigeyoshi *et al.*, 1997). Light induced expression of c-FOS is also observed during both the day and night in the VPAC2R KO mouse (Hughes et al., 2004) suggesting that there is a general lack of photic gating of gene expression in the absence of VIP. VIP KO mice also show this lack of gating in *Per1* and c-FOS responses during the day (Dragich *et al.*, 2010). These differences in light responses of the transgenic mice may uncover a mechanism involving VIP by which light normally acts to reset the circadian clock.

One means by which VIP affects light induced gene expression may be by altering

electrical properties in SCN neurons. Evidence suggests that certain electrical properties of pacemaking neurons have to be maintained for the normal expression of clock genes and circadian rhythm generation. In the SCN, membrane hyperpolarization reversibly abolishes the rhythmic expression of *Per1* (Lundkvist *et al.*, 2005). Using a bioluminescence assay based on *Per1* transcription, another study showed that TTX (which blocks action potentials) damps *Per1* rhythmicity in individual SCN neurons and decreases levels of *Per1* transcripts and proteins (Yamaguchi *et al.*, 2003). Therefore, the electrical properties of individual neurons appear to regulate gene expression in the SCN.

The gene expression phenotypes of VPAC2 KO mice (Harmar *et al.*, 2002; Hughes *et al.*, 2004; Maywood *et al.*, 2007) and VIP KO mice (Chapter 2) are likely related to 1) altered properties of SCN neurons regulating spontaneously evoked firing and/or 2) altered responses of SCN neurons to afferent signals. Data from VPAC2 KO mice suggest that both of these mechanisms are at work. SCN neurons in these mice are hyperpolarized (Pakhotin *et al.*, 2006). This observation has led to the hypothesis that a night-like state in which SCN neurons are both inactive (hyperpolarized) and excitable may underlie the gene expression responses observed in VPAC2R KO mice (Pakhotin *et al.*, 2006; Maywood *et al.*, 2007). According to this hypothesis, in the absence of VIP-ergic signaling, the SCN does not display electrical properties normally found during the day (eg. increased resting membrane potential and firing rate). Therefore, a light pulse during the day is interpreted by the SCN like a light pulse at night, and so light induces the expression of c-FOS and *Per1*. This hypothesis has never been directly tested, but data supporting this idea come from studies showing that population day-night differences in electrical activity are lost in SCN neurons from both VPAC2 KO and VIP KO mice (Cutler *et al.*, 2003; Brown *et al.*, 2007).

At a behavioral level, the loss of VIP/VPAC2 alters the relationship of the circadian oscillator to the environment (Fig. 4.). This phenotype is best seen in the experiments in which VPAC2R KO or VIP KO animals are released into constant darkness (DD) from a light-dark (LD) cycle. A normally entrained animal will start its activity from a phase predicted from the prior LD cycle and, for a nocturnal organism, the activity will start from a phase near the beginning of nocturnal activity in LD. For example, WT mice begin their free-running rhythm within 30 minutes of the time of lights-off in the prior LD cycle. In contrast, VIP KO animals start their activity about 8 to 10 hours before the time of the prior lights-off (Colwell *et al.*, 2003). The shorter period cannot account for this large shift in activity onset, and most of this response is likely due to an alteration in the processes that couple the oscillator to the environment. This idea is supported by the altered phase angle of entrainment seen in VIP KO mice entrained to a single light pulse per cycle (Colwell *et al.*, 2003). Similarly, the VPAC2R KO mice also exhibit an extremely large advance in activity onset after release into DD (Harmar *et al.*, 2002).

Research targets

Numerous studies to date have implicated a role for VIP-ergic signaling in relation to both the robust generation of circadian rhythmicity as well as the circadian system's response to environmental light input. However, there does not yet appear to be a comprehensive understanding linking VIP in circadian maintenance and entrainment mechanisms. Specifically, it is unknown whether or not the deficits in rhythm generation from the loss of VIP are the cause of the deficits in phase shifting behaviors, or if alternately, entrainment deficits result from an

independent but parallel dysfunction in the system. The following chapters in this dissertation set out to further utilize the VIP KO mouse and determine the different levels at which its entrainment and phase shifting behaviors and physiology are altered so that this gap in understanding can be filled. The first set of experiments defines a specific role for VIP in SCN core-shell communication in response to phase shifting light exposure. Following, a non-acute role for VIP is examined, in which VIP-mediated organizational changes in the basic anatomy of the circadian visual system might be affecting the function of the circadian network. Not only will these experiments help clarify the role of this neuropeptide, they will also improve our understanding of how SCN neurons communicate with each other in the intact mammalian circadian system. In addition to the direct benefits for human health, knowledge from these findings may be extended to our understanding of how neuropeptides modulate and incorporate sensory signals in other neural systems as well.

Fig. 1. Organization of circadian rhythms

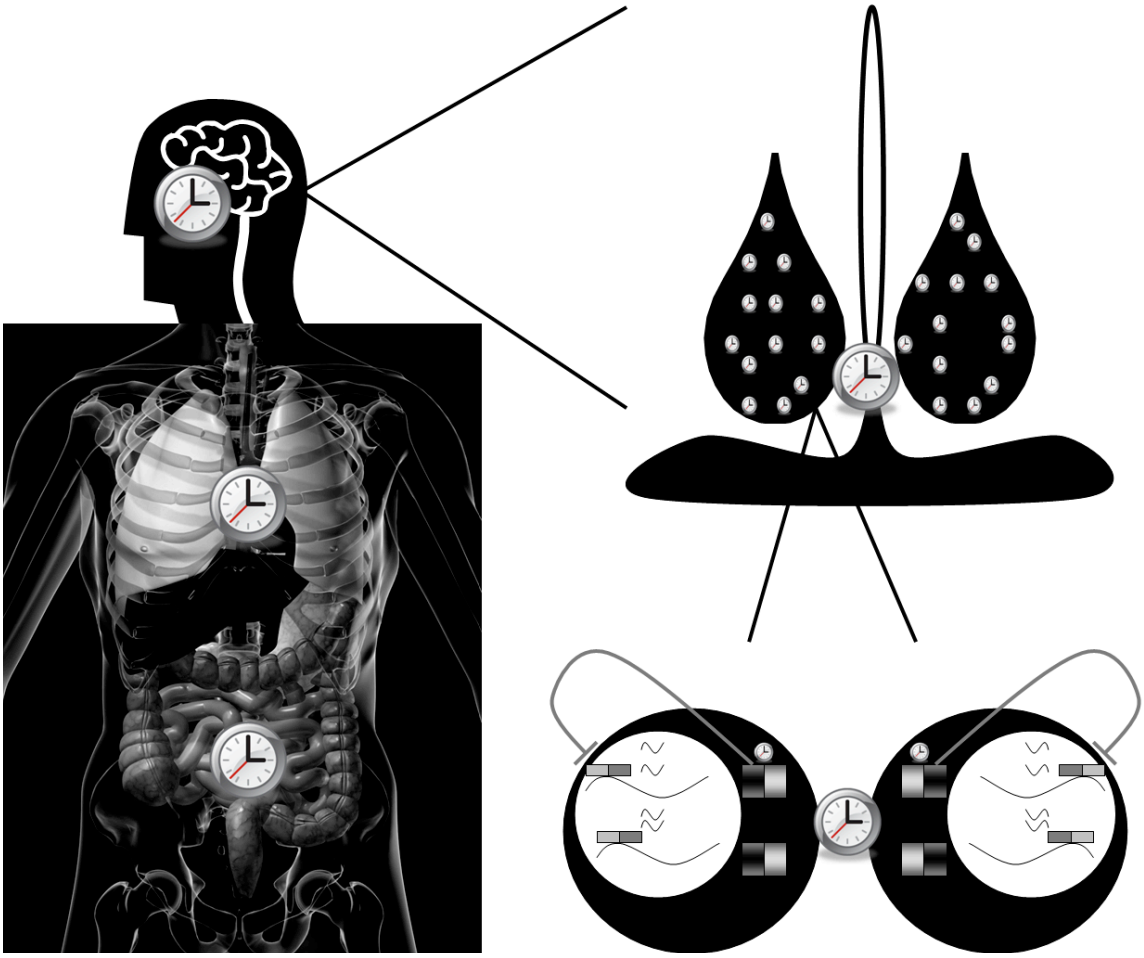

Circadian rhythms are generated by networks hierarchically organized throughout the body. Each cell contains the molecular machinery to express rhythms in gene expression through a transcriptional-translational feedback loop that has a cycle length of about 24 hours. Rhythms in individual cells become more robust through intercellular communication in structures like the mammalian suprachiasmatic nucleus (SCN). Within the SCN, groups of synchronized cells form networks to reinforce robust rhythmic release of electrochemical and humoral synchronizing cues. These cues help maintain temporal structure across all of the body's oscillatory networks to regulate essential biological functions.

Fig. 2. Non-parametric and parametric mechanisms of entrainment

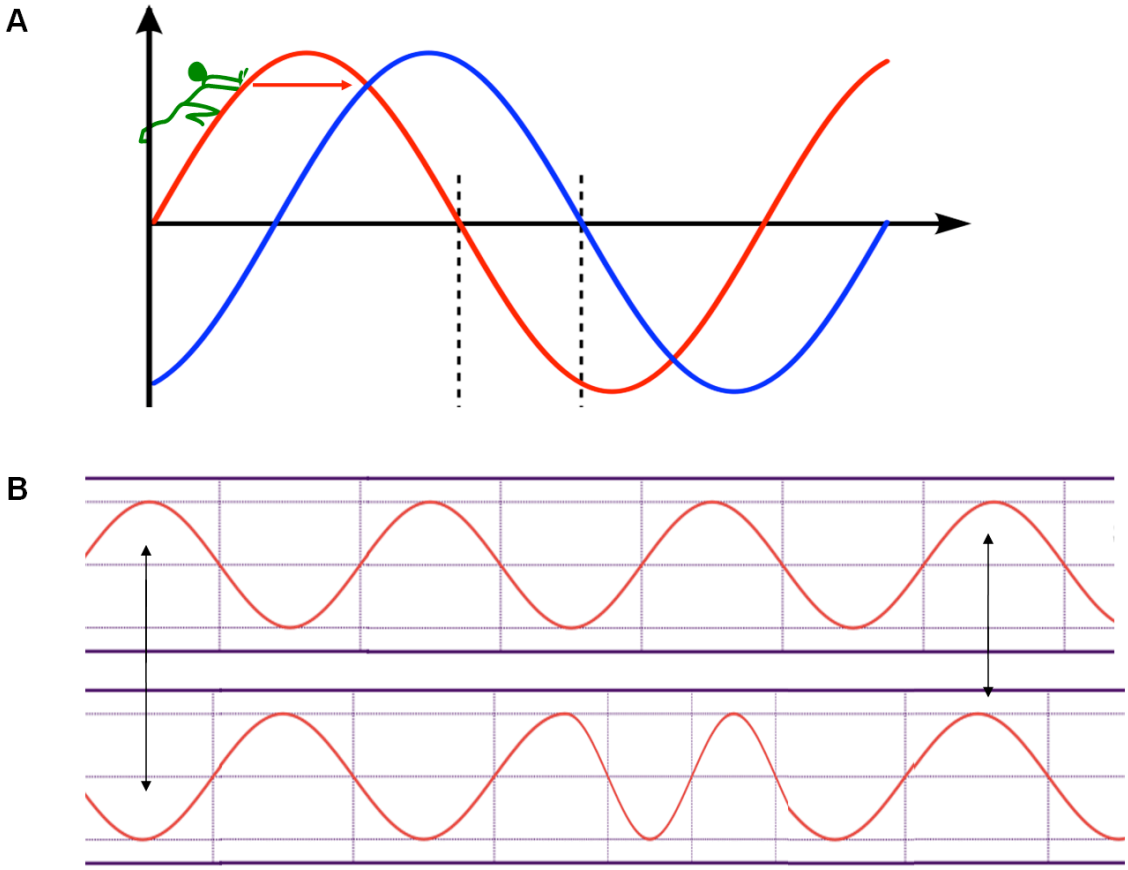

Oscillators can entrain to other oscillators by one of two basic mechanisms. (A) In non-parametric entrainment, an acute force aligns the phase of one oscillator so that it becomes phase-locked to the other. As long as that force is applied in a periodic manner to provide the same magnitude shift in the correct direction, stable entrainment can occur. This is predominantly how the environmental light-dark cycle entrains the circadian clock. (B) In parametric entrainment, some continuous force changes the period of one oscillator so that it can align with the correct phase and period of another oscillator. The influence of parametric entrainment on the circadian clock is variable between species.

Fig. 3. The SCN can be divided into two component parts, the core and the shell

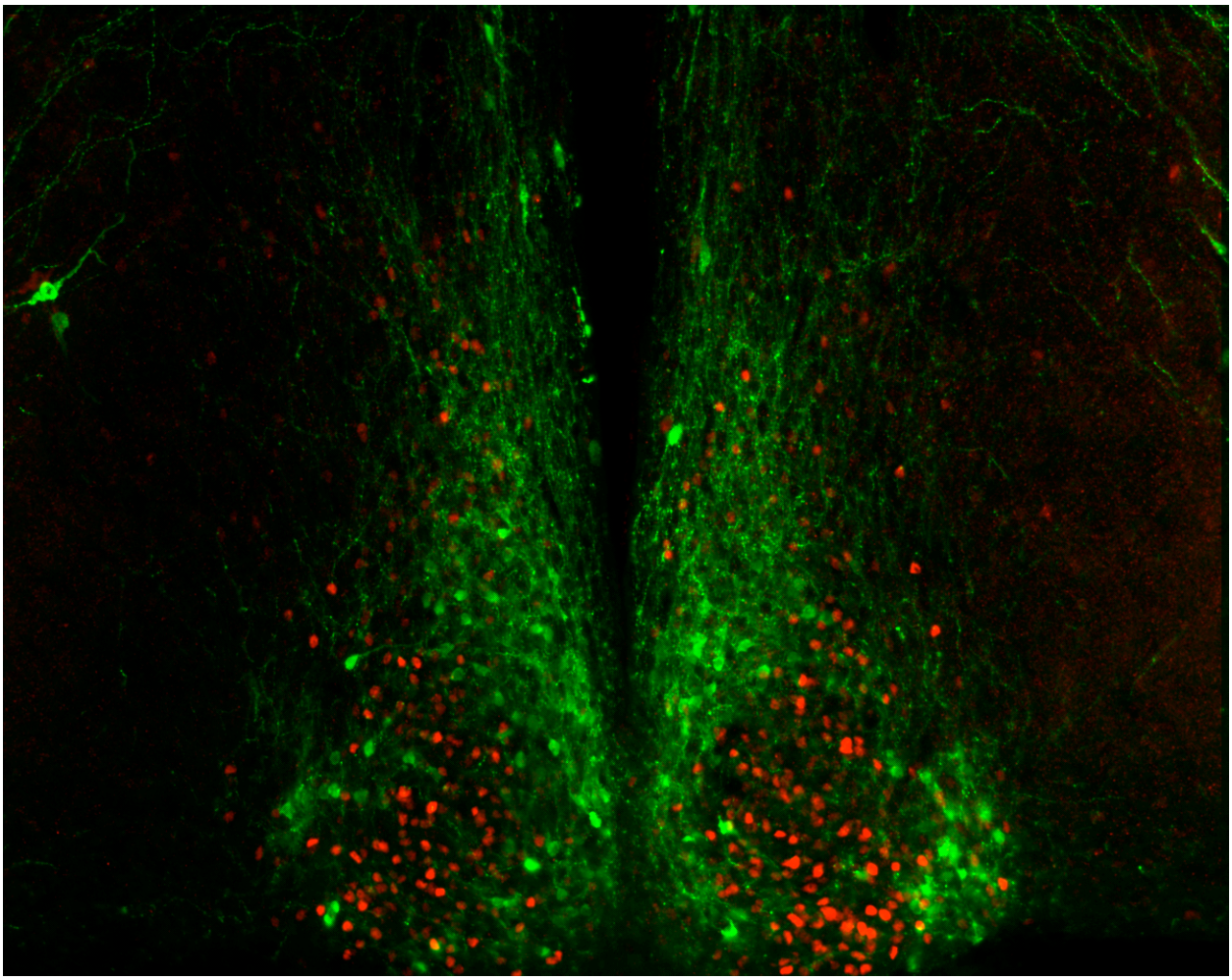

Both functionally and chemocarchitecturally, different subregions of the SCN display different properties. A photomicrograph of a coronal slice through the mid SCN shows the SCN shell is characterized by clusters of vasopressin-expressing cell bodies and fibers (in green). These cells are thought to contain the most robustly oscillating networks in the nucleus. The dense cell body clusters in the ventro-middle aspect of the SCN is known as the core, and this is where most retinal afferents terminate to provide visual information to the hypothalamus. Here, expression of the protein product of the proto-oncogene *c-Fos* is up-regulated due to a phase shifting light pulse that was delivered one hour earlier (in red).

Fig. 4. VIP KO mice have robust entrainment and phase-shifting deficiencies

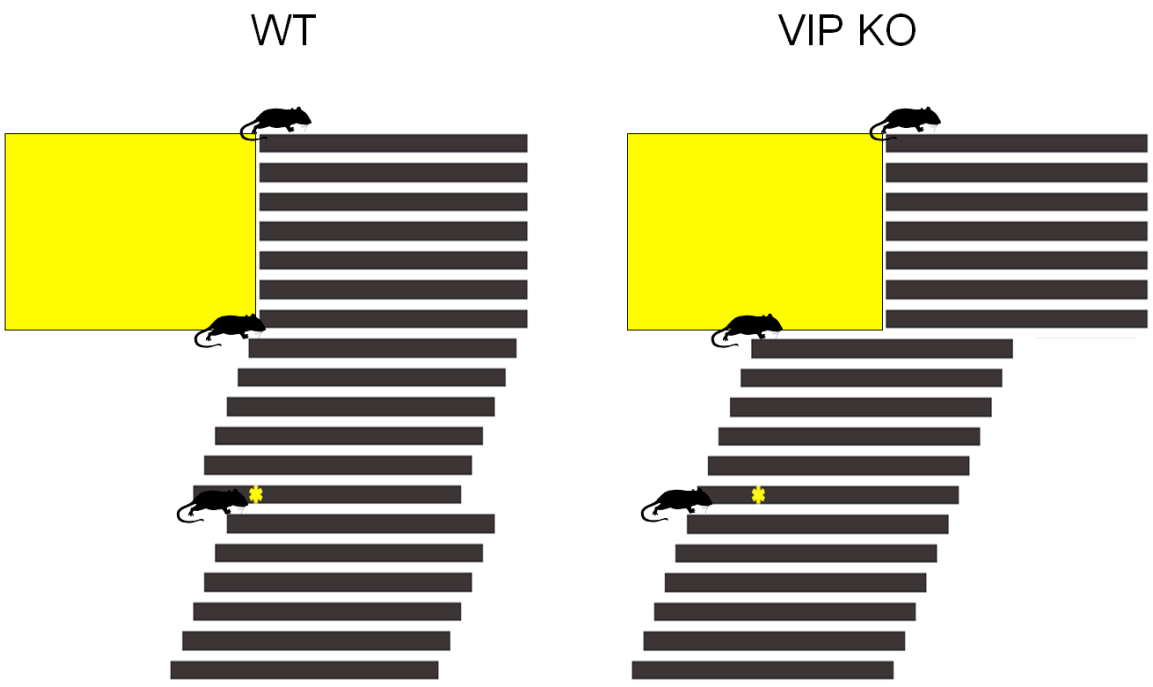

Schematic of single-plotted actograms of locomotor activity comparing the entrainment and phase shifting phenotypes of WT and VIP KO mice. In a normal light-dark cycle, VIP KO mice exhibit nocturnal activity similar to WT mice (inactive light period depicted by yellow, gray bars indicate activity). Upon release into constant darkness, WT mice begin activity at a phase predicted by the previous day's light offset. In contrast, VIP KO mice begin their active period in constant darkness with a 6-8 hour phase advance from the previous day's light offset. Furthermore, when exposed to a brief light pulse at night that normally elicits a phase delay in WT mice (depicted by yellow asterisk), VIP KO mice fail to shift.

Abrahamson, E.E. & Moore, R.Y. (2001) Suprachiasmatic nucleus in the mouse: retinal innervation, intrinsic organization and efferent projections. *Brain Res*, **916**, 172-191.

Akashi, M. & Takumi, T. (2005) The orphan nuclear receptor ROR[alpha] regulates circadian transcription of the mammalian core-clock Bmal1. *Nat Struct Mol Biol*, **12**, 441-448.

Albers, H.E., Liou, S.Y., Stopa, E.G. & Zoeller, R.T. (1991) Interaction of colocalized neuropeptides: functional significance in the circadian timing system. *J Neurosci*, **11**, 846-851.

Albers, H.E., Minamitani, N., Stopa, E. & Ferris, C.F. (1987) Light selectively alters vasoactive intestinal peptide and peptide histidine isoleucine immunoreactivity within the rat suprachiasmatic nucleus. *Brain Res*, **437**, 189-192.

Altimus, C.M., Guler, A.D., Alam, N.M., Arman, A.C., Prusky, G.T., Sampath, A.P. & Hattar, S. (2010) Rod photoreceptors drive circadian photoentrainment across a wide range of light intensities. *Nat Neurosci*, **13**, 1107-1112.

Anch, A.M. (1988) *Sleep : a scientific perspective*. Prentice Hall, Englewood Cliffs, N.J.

Antle, M.C. & Silver, R. (2005) Orchestrating time: arrangements of the brain circadian clock. *Trends Neurosci*, **28**, 145-151.

Aton, S.J., Colwell, C.S., Harmar, A.J., Waschek, J. & Herzog, E.D. (2005) Vasoactive intestinal polypeptide mediates circadian rhythmicity and synchrony in mammalian clock neurons. *Nat Neurosci*, **8**, 476-483.

Baun, M., Hay-Schmidt, A., Edvinsson, L., Olesen, J. & Jansen-Olesen, I. (2011) Pharmacological characterization and expression of VIP and PACAP receptors in isolated cranial arteries of the rat. *Eur J Pharmacol*, **670**, 186-194.

Besson, J., Sarrieau, A., Vial, M., Marie, J.C., Rosselin, G. & Rostene, W. (1986) Characterization and autoradiographic distribution of vasoactive intestinal peptide binding sites in the rat central nervous system. *Brain Res*, **398**, 329-336.

Brenneman, D., Hill, J. & Gozes, I. (2000) Vasoactive Intestinal Peptide in the Central Nervous System. In Bloom, F.E., Kupfer, D.J. (eds) *Psychopharmacology: the Fourth Generation of Progress*. Raven Press, New York.

Brown, T.M., Colwell, C.S., Waschek, J.A. & Piggins, H.D. (2007) Disrupted neuronal activity rhythms in the suprachiasmatic nuclei of vasoactive intestinal polypeptide-deficient mice. *J Neurophysiol*, **97**, 2553-2558.

Brown, T.M., Hughes, A.T. & Piggins, H.D. (2005) Gastrin-releasing peptide promotes suprachiasmatic nuclei cellular rhythmicity in the absence of vasoactive intestinal polypeptide-VPAC2 receptor signaling. *J Neurosci*, **25**, 11155-11164.

Buijs, R.M., Wortel, J. & Hou, Y.X. (1995) Colocalization of gamma-aminobutyric acid with vasopressin, vasoactive intestinal peptide, and somatostatin in the rat suprachiasmatic nucleus. *J Comp Neurol*, **358**, 343-352.

Butler, M.P. & Silver, R. (2011) Divergent photic thresholds in the non-image-forming visual system: entrainment, masking and pupillary light reflex. *Proceedings of the Royal Society B: Biological Sciences*, **278**, 745-750.

Cagampang, F.R., Sheward, W.J., Harmar, A.J., Piggins, H.D. & Coen, C.W. (1998) Circadian changes in the expression of vasoactive intestinal peptide 2 receptor mRNA in the rat suprachiasmatic nuclei. *Brain Res Mol Brain Res*, **54**, 108-112.

Ciarleglio, C.M., Gamble, K.L., Axley, J.C., Strauss, B.R., Cohen, J.Y., Colwell, C.S. & McMahon, D.G. (2009) Population encoding by circadian clock neurons organizes circadian behavior. *J Neurosci*, **29**, 1670-1676.

Colwell, C.S. (2010) Preventing dehydration during sleep. *Nat Neurosci*, **13**, 403-404.

Colwell, C.S., Michel, S., Itri, J., Rodriguez, W., Tam, J., Lelievre, V., Hu, Z., Liu, X. & Waschek, J.A. (2003) Disrupted circadian rhythms in VIP- and PHI-deficient mice. *Am J Physiol Regul Integr Comp Physiol*, **285**, R939-949.

Colwell, C.S., Michel, S., Itri, J., Rodriguez, W., Tam, J., Lelievre, V., Hu, Z. & Waschek, J.A. (2004) Selective deficits in the circadian light response in mice lacking PACAP. *Am J Physiol Regul Integr Comp Physiol*, **287**, R1194-1201.

Crosio, C., Cermakian, N., Allis, C.D. & Sassone-Corsi, P. (2000) Light induces chromatin modification in cells of the mammalian circadian clock. *Nat Neurosci*, **3**, 1241-1247.

Cutler, D.J., Haraura, M., Reed, H.E., Shen, S., Sheward, W.J., Morrison, C.F., Marston, H.M., Harmar, A.J. & Piggins, H.D. (2003) The mouse VPAC2 receptor confers suprachiasmatic nuclei cellular rhythmicity and responsiveness to vasoactive intestinal polypeptide in vitro. *Eur J Neurosci*, **17**, 197-204.

Czeisler, C.A., Richardson, G.S., Zimmerman, J.C., Moore-Ede, M.C. & Weitzman, E.D. (1981) Entrainment of human circadian rhythms by light-dark cycles: a reassessment. *Photochem Photobiol*, **34**, 239-247.

Daan, S. (2000) Colin Pittendrigh, Jurgen Aschoff, and the Natural Entrainment of Circadian Systems. *Journal of Biological Rhythms*, **15**, 195-207.

Daan, S. & Pittendrigh, C.S. (1976) A Functional analysis of circadian pacemakers in nocturnal rodents. *Journal of Comparative Physiology A: Neuroethology, Sensory, Neural, and Behavioral Physiology*, **106**, 253-266.

Dardente, H., Menet, J.S., Challet, E., Tournier, B.B., Pevet, P. & Masson-Pevet, M. (2004) Daily and circadian expression of neuropeptides in the suprachiasmatic nuclei of nocturnal and diurnal rodents. *Brain Res Mol Brain Res*, **124**, 143-151.

DeCoursey, P.J. (1960) Phase Control of Activity in a Rodent. *Cold Spring Harbor Symposia on Quantitative Biology*, **25**, 49-55.

Deurveilher, S. & Semba, K. (2005) Indirect projections from the suprachiasmatic nucleus to major arousal-promoting cell groups in rat: implications for the circadian control of behavioural state. *Neuroscience*, **130**, 165-183.

Dibner, C., Schibler, U. & Albrecht, U. (2010) The mammalian circadian timing system: organization and coordination of central and peripheral clocks. *Annu Rev Physiol*, **72**, 517-549.

Dietl, M.M., Hof, P.R., Martin, J.L., Magistretti, P.J. & Palacios, J.M. (1990) Autoradiographic analysis of the distribution of vasoactive intestinal peptide binding sites in the vertebrate central nervous system: a phylogenetic study. *Brain Res*, **520**, 14-26.

Doi, M., Hirayama, J. & Sassone-Corsi, P. (2006) Circadian regulator CLOCK is a histone acetyltransferase. *Cell*, **125**, 497-508.

Dragich, J.M., Loh, D.H., Wang, L.M., Vosko, A.M., Kudo, T., Nakamura, T.J., Odom, I.H., Tateyama, S., Hagopian, A., Waschek, J.A. & Colwell, C.S. (2010) The role of the neuropeptides PACAP and VIP in the photic regulation of gene expression in the suprachiasmatic nucleus. *Eur J Neurosci*.

Dunlap, J.C. (1999) Molecular bases for circadian clocks. *Cell*, **96**, 271-290.

Ebling, F.J. (1996) The role of glutamate in the photic regulation of the suprachiasmatic nucleus. *Prog Neurobiol*, **50**, 109-132.

Foster, R.G., Provencio, I., Hudson, D., Fiske, S., De Grip, W. & Menaker, M. (1991) Circadian photoreception in the retinally degenerate mouse (rd/rd). *J Comp Physiol A*, **169**, 39-50.

Francl, J.M., Kaur, G. & Glass, J.D. (2010a) Regulation of vasoactive intestinal polypeptide release in the suprachiasmatic nucleus circadian clock. *Neuroreport*, **21**, 1055-1059.

Francl, J.M., Kaur, G. & Glass, J.D. (2010b) Roles of light and serotonin in the regulation of gastrin-releasing peptide and arginine vasopressin output in the hamster SCN circadian clock. *Eur J Neurosci*, **32**, 1170-1179.

Geier, F., Becker-Weimann, S., Kramer, A. & Herzel, H. (2005) Entrainment in a model of the mammalian circadian oscillator. *J Biol Rhythms*, **20**, 83-93.

Ginty, D.D., Kornhauser, J.M., Thompson, M.A., Bading, H., Mayo, K.E., Takahashi, J.S. &

Greenberg, M.E. (1993) Regulation of CREB phosphorylation in the suprachiasmatic nucleus by light and a circadian clock. *Science*, **260**, 238-241.

Golombek, D.A. & Rosenstein, R.E. (2010) Physiology of circadian entrainment. *Physiol Rev*, **90**, 1063-1102.

Guilding, C., Hughes, A.T., Brown, T.M., Namvar, S. & Piggins, H.D. (2009) A riot of rhythms: neuronal and glial circadian oscillators in the mediobasal hypothalamus. *Mol Brain*, **2**, 28.

Guillaumond, F., Dardente, H., Giguere, V. & Cermakian, N. (2005) Differential control of Bmal1 circadian transcription by REV-ERB and ROR nuclear receptors. *J Biol Rhythms*, **20**, 391-403.

Ha, M. & Park, J. (2005) Shiftwork and metabolic risk factors of cardiovascular disease. *J Occup Health*, **47**, 89-95.

Hamada, T., Antle, M.C. & Silver, R. (2004) Temporal and spatial expression patterns of canonical clock genes and clock-controlled genes in the suprachiasmatic nucleus. *Eur J Neurosci*, **19**, 1741-1748.

Hamada, T., LeSauter, J., Venuti, J.M. & Silver, R. (2001) Expression of Period genes: rhythmic and nonrhythmic compartments of the suprachiasmatic nucleus pacemaker. *J Neurosci*, **21**, 7742-7750.

Hankins, M.W., Peirson, S.N. & Foster, R.G. (2008) Melanopsin: an exciting photopigment. *Trends Neurosci*, **31**, 27-36.

Hannibal, J. (2002) Neurotransmitters of the retino-hypothalamic tract. *Cell Tissue Res*, **309**, 73-88.

Hannibal, J., Jamen, F., Nielsen, H.S., Journot, L., Brabet, P. & Fahrenkrug, J. (2001) Dissociation between light-induced phase shift of the circadian rhythm and clock gene expression in mice lacking the pituitary adenylate cyclase activating polypeptide type 1 receptor. *J Neurosci*, **21**, 4883-4890.

Harmar, A.J. (2001) Family-B G-protein-coupled receptors. *Genome Biol*, **2**, REVIEWS3013.

Harmar, A.J., Marston, H.M., Shen, S., Spratt, C., West, K.M., Sheward, W.J., Morrison, C.F., Dorin, J.R., Piggins, H.D., Reubi, J.C., Kelly, J.S., Maywood, E.S. & Hastings, M.H. (2002) The VPAC(2) receptor is essential for circadian function in the mouse suprachiasmatic nuclei. *Cell*, **109**, 497-508.

Harrington, J.M. (1994) Shift work and health--a critical review of the literature on working hours. *Ann Acad Med Singapore*, **23**, 699-705.

Hattar, S., Kumar, M., Park, A., Tong, P., Tung, J., Yau, K.W. & Berson, D.M. (2006) Central

projections of melanopsin-expressing retinal ganglion cells in the mouse. *J Comp Neurol*, **497**, 326-349.

Hattar, S., Lucas, R.J., Mrosovsky, N., Thompson, S., Douglas, R.H., Hankins, M.W., Lem, J., Biel, M., Hofmann, F., Foster, R.G. & Yau, K.W. (2003) Melanopsin and rod-cone photoreceptive systems account for all major accessory visual functions in mice. *Nature*, **424**, 76-81.

Huang, S.K. & Pan, J.T. (1993) Potentiating effects of serotonin and vasoactive intestinal peptide on the action of glutamate on suprachiasmatic neurons in brain slices. *Neurosci Lett*, **159**, 1-4.

Hubbell, W.L. & Bownds, M.D. (1979) Visual transduction in vertebrate photoreceptors. *Annu. Rev. Neurosci.*, **2**, 17-34.

Hughes, A.T., Fahey, B., Cutler, D.J., Coogan, A.N. & Piggins, H.D. (2004) Aberrant gating of photic input to the suprachiasmatic circadian pacemaker of mice lacking the VPAC2 receptor. *J Neurosci*, **24**, 3522-3526.

Hughes, A.T., Guilding, C. & Piggins, H.D. (2011) Neuropeptide signaling differentially affects phase maintenance and rhythm generation in SCN and extra-SCN circadian oscillators. *PLoS One*, **6**, e18926.

Ibata, Y., Takahashi, Y., Okamura, H., Kawakami, F., Terubayashi, H., Kubo, T. & Yanaihara, N. (1989) Vasoactive intestinal peptide (VIP)-like immunoreactive neurons located in the rat suprachiasmatic nucleus receive a direct retinal projection. *Neurosci Lett*, **97**, 1-5.

Ishihara, T., Shigemoto, R., Mori, K., Takahashi, K. & Nagata, S. (1992) Functional expression and tissue distribution of a novel receptor for vasoactive intestinal polypeptide. *Neuron*, **8**, 811-819.

Itri, J., Michel, S., Waschek, J.A. & Colwell, C.S. (2004) Circadian rhythm in inhibitory synaptic transmission in the mouse suprachiasmatic nucleus. *J Neurophysiol*, **92**, 311-319.

Johnson, C.H., Elliot, J., Foster, R., Honma, K. & Kronauer, R. (2004) Fundamental properties of circadian rhythms. In Dunlap, J.C., Loros, J.J., DeCoursey, P.J. (eds) *Chronobiology: Biological Timekeeping*. Sinauer Associates, Inc., Sunderland, MA, pp. 67-106.

Johnson, C.H., Elliott, J.A. & Foster, R. (2003) Entrainment of Circadian Programs. *Chronobiology International*, **20**, 741-774.

Judson, O. (2009) Enter the chronotherapists *The New York Times*. New York Times Company, New York, pp. Opinionator: exclusive online commentary from the times.

Kallingal, G.J. & Mintz, E.M. (2010) An NMDA antagonist inhibits light but not GRP-induced phase shifts when administered after the phase-shifting stimulus. *Brain Research*, **1353**,

106-112.

Kallo, I., Kalamatianos, T., Piggins, H.D. & Coen, C.W. (2004a) Ageing and the diurnal expression of mRNAs for vasoactive intestinal peptide and for the VPAC2 and PAC1 receptors in the suprachiasmatic nucleus of male rats. *J Neuroendocrinol*, **16**, 758-766.

Kallo, I., Kalamatianos, T., Wiltshire, N., Shen, S., Sheward, W.J., Harmar, A.J. & Coen, C.W. (2004b) Transgenic approach reveals expression of the VPAC2 receptor in phenotypically defined neurons in the mouse suprachiasmatic nucleus and in its efferent target sites. *Eur J Neurosci*, **19**, 2201-2211.

Kalsbeek, A., Palm, I.F., La Fleur, S.E., Scheer, F.A., Perreau-Lenz, S., Ruiter, M., Kreier, F., Cailotto, C. & Buijs, R.M. (2006) SCN outputs and the hypothalamic balance of life. *J Biol Rhythms*, **21**, 458-469.

Karatsoreos, I.N., Yan, L., LeSauter, J. & Silver, R. (2004) Phenotype matters: identification of light-responsive cells in the mouse suprachiasmatic nucleus. *J Neurosci*, **24**, 68-75.

Knutsson, A. & Boggild, H. (2010) Gastrointestinal disorders among shift workers. *Scand J Work Environ Health*, **36**, 85-95.

Ko, C.H., Yamada, Y.R., Welsh, D.K., Buhr, E.D., Liu, A.C., Zhang, E.E., Ralph, M.R., Kay, S.A., Forger, D.B. & Takahashi, J.S. (2011) Emergence of noise-induced oscillations in the central circadian pacemaker. *PLoS Biol*, **8**, e1000513.

Kondratov, R.V., Shamanna, R.K., Kondratova, A.A., Gorbacheva, V.Y. & Antoch, M.P. (2006) Dual role of the CLOCK/BMAL1 circadian complex in transcriptional regulation. *FASEB J*, **20**, 530-532.

Korf, H.W. & Fahrenkrug, J. (1984) Ependymal and neuronal specializations in the lateral ventricle of the Pekin duck, Anas platyrhynchos. *Cell Tissue Res*, **236**, 217-227.

Laemle, L.K. & Rusa, R. (1992) VIP-like immunoreactivity in the suprachiasmatic nuclei of a mutant anophthalmic mouse. *Brain Res*, **589**, 124-128.

Lall, G.S., Revell, V.L., Momiji, H., Al Enezi, J., Altimus, C.M., Guler, A.D., Aguilar, C., Cameron, M.A., Allender, S., Hankins, M.W. & Lucas, R.J. (2010) Distinct contributions of rod, cone, and melanopsin photoreceptors to encoding irradiance. *Neuron*, **66**, 417-428.

Lee, C., Etchegaray, J.-P., Cagampang, F.R.A., Loudon, A.S.I. & Reppert, S.M. (2001) Posttranslational Mechanisms Regulate the Mammalian Circadian Clock. *Cell*, **107**, 855-867.

LeSauter, J. & Silver, R. (1998) Output signals of the SCN. *Chronobiol Int*, **15**, 535-550.

Lewy, A.J., Lefler, B.J., Emens, J.S. & Bauer, V.K. (2006) The circadian basis of winter

depression. *Proc Natl Acad Sci U S A*, **103**, 7414-7419.

Linder, S., Barkhem, T., Norberg, A., Persson, H., Schalling, M., Hokfelt, T. & Magnusson, G. (1987) Structure and expression of the gene encoding the vasoactive intestinal peptide precursor. *Proc Natl Acad Sci U S A*, **84**, 605-609.

Loh, D.H., Dragich, J.M., Kudo, T., Schroeder, A.M., Nakamura, T.J., Waschek, J.A., Block, G.D. & Colwell, C.S. (2011) Effects of vasoactive intestinal peptide genotype on circadian gene expression in the suprachiasmatic nucleus and peripheral organs. *J Biol Rhythms*, **26**, 200-209.

Lonze, B.E. & Ginty, D.D. (2002) Function and Regulation of CREB Family Transcription Factors in the Nervous System. *Neuron*, **35**, 605-623.

Lowrey, P.L., Shimomura, K., Antoch, M.P., Yamazaki, S., Zemenides, P.D., Ralph, M.R., Menaker, M. & Takahashi, J.S. (2000) Positional syntenic cloning and functional characterization of the mammalian circadian mutation tau. *Science*, **288**, 483-492.

Lundkvist, G.B., Kwak, Y., Davis, E.K., Tei, H. & Block, G.D. (2005) A calcium flux is required for circadian rhythm generation in mammalian pacemaker neurons. *J Neurosci*, **25**, 7682-7686.

Lutz, E.M., Sheward, W.J., West, K.M., Morrow, J.A., Fink, G. & Harmar, A.J. (1993) The VIP2 receptor: molecular characterisation of a cDNA encoding a novel receptor for vasoactive intestinal peptide. *FEBS Lett*, **334**, 3-8.

Masmoudi-Kouki, O., Gandolfo, P., Castel, H., Leprince, J., Fournier, A., Dejda, A., Vaudry, H. & Tonon, M.C. (2007) Role of PACAP and VIP in astroglial functions. *Peptides*, **28**, 1753-1760.

Mason, C.A. & Lincoln, D.W. (1976) Visualization of the retino-hypothalamic projection in the rat by cobalt precipitation. *Cell Tissue Res*, **168**, 117-131.

Maywood, E.S., Chesham, J.E., O'Brien, J.A. & Hastings, M.H. (2011) A diversity of paracrine signals sustains molecular circadian cycling in suprachiasmatic nucleus circuits. *Proc Natl Acad Sci U S A*, **108**, 14306-14311.

Maywood, E.S., O'Neill, J.S., Chesham, J.E. & Hastings, M.H. (2007) Minireview: The circadian clockwork of the suprachiasmatic nuclei--analysis of a cellular oscillator that drives endocrine rhythms. *Endocrinology*, **148**, 5624-5634.

Maywood, E.S., Reddy, A.B., Wong, G.K., O'Neill, J.S., O'Brien, J.A., McMahon, D.G., Harmar, A.J., Okamura, H. & Hastings, M.H. (2006) Synchronization and maintenance of timekeeping in suprachiasmatic circadian clock cells by neuropeptidergic signaling. *Curr Biol*, **16**, 599-605.

Mikkelsen, J.D. (1989) Immunohistochemical localization of vasoactive intestinal peptide (VIP) in the circumventricular organs of the rat. *Cell Tissue Res*, **255**, 307-313.

Mikkelsen, J.D. & Moller, M. (1988) Vasoactive intestinal peptide in the hypothalamohypophysial system of the Mongolian gerbil. *J Comp Neurol*, **273**, 87-98.

Mintz, E.M., Marvel, C.L., Gillespie, C.F., Price, K.M. & Albers, H.E. (1999) Activation of NMDA receptors in the suprachiasmatic nucleus produces light-like phase shifts of the circadian clock in vivo. *J Neurosci*, **19**, 5124-5130.

Moore, R.Y. & Lenn, N.J. (1972) A retinohypothalamic projection in the rat. *The Journal of Comparative Neurology*, **146**, 1-14.

Moore, R.Y., Speh, J.C. & Leak, R.K. (2002) Suprachiasmatic nucleus organization. *Cell Tissue Res*, **309**, 89-98.

Nagano, M., Adachi, A., Nakahama, K., Nakamura, T., Tamada, M., Meyer-Bernstein, E., Sehgal, A. & Shigeyoshi, Y. (2003) An abrupt shift in the day/night cycle causes desynchrony in the mammalian circadian center. *J Neurosci*, **23**, 6141-6151.

Nakamura, W., Honma, S., Shirakawa, T. & Honma, K. (2001) Regional pacemakers composed of multiple oscillator neurons in the rat suprachiasmatic nucleus. *Eur J Neurosci*, **14**, 666-674.

Naruse, Y., Oh-hashi, K., Iijima, N., Naruse, M., Yoshioka, H. & Tanaka, M. (2004) Circadian and light-induced transcription of clock gene Per1 depends on histone acetylation and deacetylation. *Mol Cell Biol*, **24**, 6278-6287.

Nelson, R.J. & Zucker, I. (1981) Absence of extraocular photoreception in diurnal and nocturnal rodents exposed to direct sunlight. *Comparative Biochemistry and Physiology Part A: Physiology*, **69**, 145-148.

Nielsen, H.S., Hannibal, J. & Fahrenkrug, J. (2002) Vasoactive intestinal polypeptide induces per1 and per2 gene expression in the rat suprachiasmatic nucleus late at night. *Eur J Neurosci*, **15**, 570-574.

Pakhotin, P., Harmar, A.J., Verkhratsky, A. & Piggins, H. (2006) VIP receptors control excitability of suprachiasmatic nuclei neurones. *Pflugers Arch*, **452**, 7-15.

Pantazopoulos, H., Dolatshad, H. & Davis, F.C. (2010) Chronic stimulation of the hypothalamic vasoactive intestinal peptide receptor lengthens circadian period in mice and hamsters. *Am J Physiol Regul Integr Comp Physiol*, **299**, R379-385.

Partch, C.L., Shields, K.F., Thompson, C.L., Selby, C.P. & Sancar, A. (2006) Posttranslational regulation of the mammalian circadian clock by cryptochrome and protein phosphatase 5. *Proc Natl Acad Sci U S A*, **103**, 10467-10472.

Perez-Leon, J.A., Warren, E.J., Allen, C.N., Robinson, D.W. & Lane Brown, R. (2006) Synaptic inputs to retinal ganglion cells that set the circadian clock. *Eur J Neurosci*, **24**, 1117-1123.

Pickard, G.E., Ralph, M.R. & Menaker, M. (1987) The intergeniculate leaflet partially mediates effects of light on circadian rhythms. *J Biol Rhythms*, **2**, 35-56.

Piggins, H.D., Antle, M.C. & Rusak, B. (1995) Neuropeptides phase shift the mammalian circadian pacemaker. *J Neurosci*, **15**, 5612-5622.

Preitner, N., Damiola, F., Lopez-Molina, L., Zakany, J., Duboule, D., Albrecht, U. & Schibler, U. (2002) The orphan nuclear receptor REV-ERBalpha controls circadian transcription within the positive limb of the mammalian circadian oscillator. *Cell*, **110**, 251-260.

Provencio, I., Cooper, H.M. & Foster, R.G. (1998) Retinal projections in mice with inherited retinal degeneration: implications for circadian photoentrainment. *J Comp Neurol*, **395**, 417-439.

Quintero, J.E., Kuhlman, S.J. & McMahon, D.G. (2003) The biological clock nucleus: a multiphasic oscillator network regulated by light. *J Neurosci*, **23**, 8070-8076.

Rajaratnam, S.M. & Arendt, J. (2001) Health in a 24-h society. *Lancet*, **358**, 999-1005.

Reed, H.E., Meyer-Spasche, A., Cutler, D.J., Coen, C.W. & Piggins, H.D. (2001) Vasoactive intestinal polypeptide (VIP) phase-shifts the rat suprachiasmatic nucleus clock in vitro. *Eur J Neurosci*, **13**, 839-843.

Reghunandanan, V. & Reghunandanan, R. (2006) Neurotransmitters of the suprachiasmatic nuclei. *J Circadian Rhythms*, **4**, 2.

Reppert, S.M. & Weaver, D.R. (2001) Molecular analysis of mammalian circadian rhythms. *Annu Rev Physiol*, **63**, 647-676.

Ripperger, J.A. & Brown, S.A. (2010) Transcriptional Regulation of Circadian Clocks. In Albrecht, U. (ed) *The Circadian Clock*. Springer, New York, pp. 37-78.

Roberts, G.W., Woodhams, P.L., Bryant, M.G., Crow, T.J., Bloom, S.R. & Polak, J.M. (1980) VIP in the rat brain: evidence for a major pathway linking the amygdala and hypothalamus via the stria terminalis. *Histochemistry*, **65**, 103-119.

Roenneberg, T., Daan, S. & Merrow, M. (2003) The art of entrainment. *J Biol Rhythms*, **18**, 183-194.

Rollag, M.D., Berson, D.M. & Provencio, I. (2003) Melanopsin, ganglion-cell photoreceptors, and mammalian photoentrainment. *J Biol Rhythms*, **18**, 227-234.

Ruan, G.X., Allen, G.C., Yamazaki, S. & McMahon, D.G. (2008) An autonomous circadian clock in the inner mouse retina regulated by dopamine and GABA. *PLoS Biol*, **6**, e249.

Ruggiero, L., Allen, C.N., Brown, R.L. & Robinson, D.W. (2010) Mice with early retinal degeneration show differences in neuropeptide expression in the suprachiasmatic nucleus. *Behav Brain Funct*, **6**, 36.

Rusak, B., Guido, M.E. & Semba, K. (2002) Chapter VI Immediate-early gene expression in the analysis of circadian rhythms and sleep. In Kaczmarek, L., Robertson, H.A. (eds) *Handbook of Chemical Neuroanatomy*. Elsevier, pp. 147-170.

Saper, C.B., Scammell, T.E. & Lu, J. (2005) Hypothalamic regulation of sleep and circadian rhythms. *Nature*, **437**, 1257-1263.

Schmidt, T.M., Do, M.T., Dacey, D., Lucas, R., Hattar, S. & Matynia, A. (2011) Melanopsin-positive intrinsically photosensitive retinal ganglion cells: from form to function. *J Neurosci*, **31**, 16094-16101.

Schwartz, W.J., Carpino, A., Jr., de la Iglesia, H.O., Baler, R., Klein, D.C., Nakabeppu, Y. & Aronin, N. (2000) Differential regulation of fos family genes in the ventrolateral and dorsomedial subdivisions of the rat suprachiasmatic nucleus. *Neuroscience*, **98**, 535-547.

Shen, S., Spratt, C., Sheward, W.J., Kallo, I., West, K., Morrison, C.F., Coen, C.W., Marston, H.M. & Harmar, A.J. (2000) Overexpression of the human VPAC2 receptor in the suprachiasmatic nucleus alters the circadian phenotype of mice. *Proc Natl Acad Sci U S A*, **97**, 11575-11580.

Sheward, W.J., Lutz, E.M. & Harmar, A.J. (1995) The distribution of vasoactive intestinal peptide2 receptor messenger RNA in the rat brain and pituitary gland as assessed by in situ hybridization. *Neuroscience*, **67**, 409-418.

Shigeyoshi, Y., Taguchi, K., Yamamoto, S., Takekida, S., Yan, L., Tei, H., Moriya, T., Shibata, S., Loros, J.J., Dunlap, J.C. & Okamura, H. (1997) Light-induced resetting of a mammalian circadian clock is associated with rapid induction of the mPer1 transcript. *Cell*, **91**, 1043-1053.

Shinohara, K., Funabashi, T. & Kimura, F. (1999a) Temporal profiles of vasoactive intestinal polypeptide precursor mRNA and its receptor mRNA in the rat suprachiasmatic nucleus. *Brain Res Mol Brain Res*, **63**, 262-267.

Shinohara, K., Funabashi, T., Mitushima, D. & Kimura, F. (2000) Effects of gap junction blocker on vasopressin and vasoactive intestinal polypeptide rhythms in the rat suprachiasmatic nucleus in vitro. *Neurosci Res*, **38**, 43-47.

Shinohara, K., Honma, S., Katsuno, Y., Abe, H. & Honma, K. (1995) Two distinct oscillators in the rat suprachiasmatic nucleus in vitro. *Proc Natl Acad Sci U S A*, **92**, 7396-7400.

Shinohara, K., Tominaga, K. & Inouye, S.T. (1998) Luminance-dependent decrease in vasoactive intestinal polypeptide in the rat suprachiasmatic nucleus. *Neurosci Lett*, **251**, 21-24.

Shinohara, K., Tominaga, K. & Inouye, S.T. (1999b) Phase dependent response of vasoactive intestinal polypeptide to light and darkness in the suprachiasmatic nucleus. *Neurosci Res*, **33**, 105-110.

Shivers, B.D., Gorcs, T.J., Gottschall, P.E. & Arimura, A. (1991) Two high affinity binding sites for pituitary adenylate cyclase-activating polypeptide have different tissue distributions. *Endocrinology*, **128**, 3055-3065.

Smale, L., Lee, T. & Nunez, A.A. (2003) Mammalian diurnality: some facts and gaps. *J Biol Rhythms*, **18**, 356-366.

Smith, L. & Canal, M.M. (2009) Expression of circadian neuropeptides in the hypothalamus of adult mice is affected by postnatal light experience. *J Neuroendocrinol*, **21**, 946-953.

Stephan, F.K. & Zucker, I. (1972) Circadian rhythms in drinking behavior and locomotor activity of rats are eliminated by hypothalamic lesions. *Proc Natl Acad Sci U S A*, **69**, 1583-1586.

Takahashi, J.S., Hong, H.K., Ko, C.H. & McDearmon, E.L. (2008) The genetics of mammalian circadian order and disorder: implications for physiology and disease. *Nat Rev Genet*, **9**, 764-775.

Tanaka, M., Ichitani, Y., Okamura, H., Tanaka, Y. & Ibata, Y. (1993) The direct retinal projection to VIP neuronal elements in the rat SCN. *Brain Res Bull*, **31**, 637-640.

Tischkau, S.A., Mitchell, J.W., Tyan, S.H., Buchanan, G.F. & Gillette, M.U. (2003) Ca2+/cAMP response element-binding protein (CREB)-dependent activation of Per1 is required for light-induced signaling in the suprachiasmatic nucleus circadian clock. *J Biol Chem*, **278**, 718-723.

Tosini, G. & Menaker, M. (1996) Circadian rhythms in cultured mammalian retina. *Science*, **272**, 419-421.

Triqueneaux, G., Thenot, S., Kakizawa, T., Antoch, M.P., Safi, R., Takahashi, J.S., Delaunay, F. & Laudet, V. (2004) The orphan receptor Rev-erbalpha gene is a target of the circadian clock pacemaker. *J Mol Endocrinol*, **33**, 585-608.

Tsuchiya, Y. & Nishida, E. (2003) Mammalian cultured cells as a model system of peripheral circadian clocks. *J Biochem*, **134**, 785-790.

Ueda, H.R., Chen, W., Adachi, A., Wakamatsu, H., Hayashi, S., Takasugi, T., Nagano, M., Nakahama, K., Suzuki, Y., Sugano, S., Iino, M., Shigeyoshi, Y. & Hashimoto, S. (2002)

A transcription factor response element for gene expression during circadian night. *Nature*, **418**, 534-539.

Usdin, T.B., Bonner, T.I. & Mezey, E. (1994) Two receptors for vasoactive intestinal polypeptide with similar specificity and complementary distributions. *Endocrinology*, **135**, 2662-2680.

Van den Pol, A.N. (1980) The hypothalamic suprachiasmatic nucleus of rat: intrinsic anatomy. *J Comp Neurol*, **191**, 661-702.

van Esseveldt, K.E., Lehman, M.N. & Boer, G.J. (2000) The suprachiasmatic nucleus and the circadian time-keeping system revisited. *Brain Res Brain Res Rev*, **33**, 34-77.

Vaudry, D., Gonzalez, B.J., Basille, M., Yon, L., Fournier, A. & Vaudry, H. (2000) Pituitary adenylate cyclase-activating polypeptide and its receptors: from structure to functions. *Pharmacol Rev*, **52**, 269-324.

Vertongen, P., Schiffmann, S.N., Gourlet, P. & Robberecht, P. (1998) Autoradiographic visualization of the receptor subclasses for vasoactive intestinal polypeptide (VIP) in rat brain. *Ann N Y Acad Sci*, **865**, 412-415.

Wang, X.S., Armstrong, M.E., Cairns, B.J., Key, T.J. & Travis, R.C. (2011) Shift work and chronic disease: the epidemiological evidence. *Occup Med (Lond)*, **61**, 78-89.

Watanabe, K., Vanecek, J. & Yamaoka, S. (2000) In vitro entrainment of the circadian rhythm of vasopressin-releasing cells in suprachiasmatic nucleus by vasoactive intestinal polypeptide. *Brain Res*, **877**, 361-366.

Weaver, D.R. (1998) The suprachiasmatic nucleus: a 25-year retrospective. *J Biol Rhythms*, **13**, 100-112.

Webb, A.B., Angelo, N., Huettner, J.E. & Herzog, E.D. (2009) Intrinsic, nondeterministic circadian rhythm generation in identified mammalian neurons. *Proc Natl Acad Sci U S A*, **106**, 16493-16498.

Welsh, D.K., Logothetis, D.E., Meister, M. & Reppert, S.M. (1995) Individual neurons dissociated from rat suprachiasmatic nucleus express independently phased circadian firing rhythms. *Neuron*, **14**, 697-706.

Welsh, D.K., Takahashi, J.S. & Kay, S.A. (2010) Suprachiasmatic nucleus: cell autonomy and network properties. *Annu Rev Physiol*, **72**, 551-577.

Welsh, D.K., Yoo, S.H., Liu, A.C., Takahashi, J.S. & Kay, S.A. (2004) Bioluminescence imaging of individual fibroblasts reveals persistent, independently phased circadian rhythms of clock gene expression. *Curr Biol*, **14**, 2289-2295.

Wirz-Justice, A. (2009) From the basic neuroscience of circadian clock function to light therapy for depression: on the emergence of chronotherapeutics. *J Affect Disord*, **116**, 159-160.

Wu, Y.H. & Swaab, D.F. (2007) Disturbance and strategies for reactivation of the circadian rhythm system in aging and Alzheimer's disease. *Sleep Med*, **8**, 623-636.

Xu, Y., Padiath, Q.S., Shapiro, R.E., Jones, C.R., Wu, S.C., Saigoh, N., Saigoh, K., Ptacek, L.J. & Fu, Y.H. (2005) Functional consequences of a CKIdelta mutation causing familial advanced sleep phase syndrome. *Nature*, **434**, 640-644.

Yamaguchi, S., Isejima, H., Matsuo, T., Okura, R., Yagita, K., Kobayashi, M. & Okamura, H. (2003) Synchronization of cellular clocks in the suprachiasmatic nucleus. *Science*, **302**, 1408-1412.

Yan, L., Karatsoreos, I., Lesauter, J., Welsh, D.K., Kay, S., Foley, D. & Silver, R. (2007) Exploring spatiotemporal organization of SCN circuits. *Cold Spring Harb Symp Quant Biol*, **72**, 527-541.

Yan, L. & Silver, R. (2002) Differential induction and localization of mPer1 and mPer2 during advancing and delaying phase shifts. *Eur J Neurosci*, **16**, 1531-1540.

Chapter 2

Vasoactive intestinal peptide is necessary for normal gene expression responses to photic phase shifting stimuli in the suprachiasmatic nucleus

Introduction

The circadian timekeeping system provides temporal structure to nearly all biological processes, including gene transcription, cellular metabolism, immune response, gut motility and the sleep-wake cycle (Dunlap, 2004; Hoogerwerf, 2009; Keller *et al.*, 2009). Circadian rhythms not only promote adaptive fitness by predicting and priming our systems for periodic changes in the environment, they are emerging as an important therapeutic target for improving quality of life. In the biomedical research community, there is now a major focus on the mechanisms by which circadian rhythms are generated, propagated and regulated in order to improve our understanding of the chronobiological factors involved in human health and disease.

Each eukaryotic cell contains the machinery and capacity to track circadian time, yet circadian rhythms are predominantly organized by hierarchical networks that span different tissues and physiological systems (Welsh *et al.*, 2010). In mammals, the suprachiasmatic nucleus of the hypothalamus (SCN) contains the master oscillatory network necessary for coordinating daily rhythms throughout the body (Reppert & Weaver, 2002). SCN neurons communicate temporal information to a number of hypothalamic relay nuclei that send their projections throughout the subcortical brain to regulate sleep, arousal, feeding, thermoregulation, osmoregulation, reproduction and energy metabolism (Abrahamson & Moore, 2001; Deurveilher & Semba, 2005; Saper *et al.*, 2005; Kalsbeek *et al.*, 2006; Colwell, 2010). As an endocrine organ, the SCN also secretes diffusible factors that synchronize cells and systems through humoral pathways (LeSauter & Silver, 1998).

The SCN receives photic cues though retinal input directly via the retinohypothalamic tract (RHT) and indirectly via the geniculohypothalamic tract (GHT). These light-input pathways

synchronize the SCN to the environmental light-dark cycle, with the RHT playing the predominant role for this process (Harrington & Rusak, 1986). Light is the most powerful environmental cue to which circadian rhythms synchronize (Czeisler *et al.*, 1981), and without appropriately timed light cues, individual circadian rhythms would drift out of phase both with each other and with the external environment (Johnson *et al.*, 2003). Such desynchrony has been linked to increased risk for mental illness, autoimmune disorders, and cancer (Hedstrom *et al.*, ; Lewy *et al.*, 2006; Schernhammer *et al.*, 2006).

In synchronizing circadian oscillators to light, afferent signals first reset the molecular oscillation of clock genes in individual SCN neurons, and this resetting normally occurs at night. The major synaptic transmitter in the light input pathway is the excitatory amino acid glutamate, and in response to a resetting light stimulus, glutamate is released directly onto SCN neurons from a subpopulation of retinal ganglion cells (RGCs) (Gooley *et al.*, 2001). In addition to glutamate, these RGCs also express the neuropeptide pituitary adenylyl cyclase activating peptide (PACAP) (Hannibal *et al.*, 2000), and PACAP has been shown to modulate glutamatergic signaling in the SCN (Michel *et al.*, 2006). It is thought that excitatory neurotransmission alters the electrical activity of retino-recipient SCN neurons, leading to an activation of different intracellular signaling cascades and transcriptional activation (Reppert & Weaver, 2002; also see Fig. 1). Specifically, glutamatergic signals, primarily acting through N-Methyl-D-aspartic acid (NMDA) receptors, trigger an influx of Ca^{2+} that initiates a number of signal transduction pathways, including protein kinase A (PKA), mitogen-activated protein kinase (MAPK), and calcium-calmodulin dependent protein kinase II (CAMKII). Recently, a pathway involving the exchange protein activated by cAMP (EPAC) has also been implicated in cyclic AMP (cAMP)-based circadian signaling (O'Neill *et al.*, 2008), but a direct role has yet to

be established for EPAC in light-based resetting of the circadian system.

These signaling pathways converge on the phosphorylation of cAMP response element binding protein (CREB) at both serine residues 133 and 142 (Ser133 and Ser142) (Gau *et al.*, 2002), leading to the nuclear translocation and transcriptional activity of phosphorylated CREB upon certain genes carrying a cAMP response element (CRE) in their promoter regions. These genes include the immediate early gene *c-fos* and the clock gene *Per1* (Rusak *et al.*, 2002; Travnickova-Bendova *et al.*, 2002). This transcriptional activation can be seen as increases in both *c-fos* and *Per1* mRNA and subsequently c-FOS and PER1 protein in the SCN following phase-resetting light pulses, optic nerve stimulation, and glutamate-induced phase shifts (Shigeyoshi *et al.*, 1997; Rusak *et al.*, 2002; Meijer & Schwartz, 2003). These molecular light responses are necessary to cause light-induced phase shifts in physiology and behavior (Kornhauser *et al.*, 1990; Wollnik *et al.*, 1995; Albrecht *et al.*, 2001).

Both indirect and direct photic cues first reach the mouse SCN bilaterally in the ventro-medial aspect of the nucleus. Thus, there is a functional distinction that the ventro-medial SCN is the primary site for photic input to the nucleus (Moore *et al.*, 2002; Reghunandanan & Reghunandanan, 2006). In general, the SCN is quite small and densely packed with neurons and glia connected by many gap junctions and intra-nuclear synapses (Van den Pol, 1980; Antle & Silver, 2005), and its organization easily provides a pathway for this photic input to be transmitted between its cells. Differences in visual input synapses, neuropeptide expression and electrical activity patterns all similarly divide the SCN into two primary component parts: the core and the shell.

Core and shell distinctions functionally divide the SCN into one subregion that is responsive to environmental cues and another that acts as a robust oscillator. The SCN core has

been shown to uniquely respond with c-FOS expression in response to a nighttime light pulse (Karatsoreos *et al.*, 2004). Interestingly, the core shows low-amplitude, if any, rhythmicity in c-FOS expression, whereas the SCN shell shows rhythmic c-FOS expression (Schwartz *et al.*, 2000). These effects have also been noted for *period* gene expression, with light-induced expression taking place in the non-oscillating core, and rhythmic oscillation taking place in the SCN shell (Hamada *et al.*, 2001; Karatsoreos *et al.*, 2004; Yan *et al.*, 2007).

Gene expression studies support the idea that the SCN subregions are functionally distinct, but normal entrainment involves communication of temporal cues across each of these areas. For example, all nighttime light pulses induce *Per1* expression in the SCN core, even when behavioral phase shifts are absent. However, only *Per1* and *Per2* expression in the SCN shell coincides with behavioral phase shifts from light (Yan & Silver, 2002). This suggests that light-induced *period* gene expression spreads from the core to the shell during phase shifting pulses. This idea is further supported by data from a time course *in situ* hybridization study, in which *Per1* expression is increased first in the SCN core following a phase shifting nighttime light pulse and then later increased in the SCN shell (Hamada *et al.*, 2004). Abruptly changing the light dark cycle also results in a change of clock gene expression that occurs first in the core, followed by the shell (Nagano *et al.*, 2003). Taken together, gene expression data related to molecular clock resetting support a model by which entrainment across the circadian network follows the path of retina → SCN core → SCN shell.

Neurons in the shell region can be anatomically distinguished by their robust expression of vasopressin (AVP), and neurons in the core can be characterized by the presence of vasoactive intestinal peptide (VIP) (Abrahamson & Moore, 2001; Morin, 2007). Because the cell bodies of VIP-expressing neurons are found in the retino-recipient SCN core, VIP is well-situated to play a

role in the photic resynchronization pathway of SCN neurons. A role for VIP in photic resetting has been supported with data from a number of studies. Microinjection of VIP around the SCN (Piggins *et al.*, 1995) can mimic the behavioral phase shifting effects of light *in vivo*, and application of VIP can also phase shift SCN neural activity *in vitro* (Reed *et al.*, 2001). *In vitro* application of VIP to SCN-containing slices also induces *Per1* expression in SCN neurons (Nielsen *et al.*, 2002), and optic nerve stimulation, (resulting in RHT activation) has been shown to increase VIP release around the SCN (Shibata *et al.*, 1994). Importantly, in a recent *in vivo* study, both nighttime light and NMDA injected into the SCN were shown to result in VIP release in the SCN (Francl *et al.*, 2010).

Other evidence supporting a role for VIP-ergic signaling in photic resetting comes from transgenic mice. Mice overexpressing the major VIP receptor found in the SCN, VPAC2, show faster resynchronization to changes in the light cycle than WT controls (Shen *et al.*, 2000). In contrast, activity in VPAC2R KO mice (Harmar *et al.*, 2002) and VIP KO mice (Colwell *et al.*, 2003) (also see Chapter 1, Fig. 4) is abnormally, if at all, synchronized to the ambient light-dark cycle. It is also worth noting that VIP KO mice do not exhibit the behavioral phase shift normally seen in WT controls in response to a nighttime light pulse (see Chapter 1, Fig. 4). Together, these data suggest that VIP is an important signal for circadian rhythm synchronization to the environmental light-dark cycle.

Analyzing light-induced gene expression is one approach to track both the molecular mechanisms and the circuits involved in circadian entrainment *in vivo*. To date, the majority of data related to the effects of VIP on light-induced gene expression come from studies using the VPAC2R KO mouse. These studies suggest that VIP-ergic signaling is involved in both amplifying light-induced gene responses and also in gating these responses to occur in the

subjective night. VPAC2R KO mice fail to show an induction of PER1 protein in the SCN in response to a 6-hour light pulse at night, while WT controls show up-regulated PER1 immunoreactivity in response to the same pulse (Harmar *et al.*, 2002). In contrast, the same group later presented data that *Per1* mRNA is induced by a light pulse during subjective night in VPAC2R KO mice, but to a lesser extent than in WT mice (Maywood *et al.*, 2007). This protein-mRNA discrepancy might be due to a difference in time course required for maximal expression for either the protein or mRNA, or it may be due to some translational modification. Nonetheless, investigations with the VPAC2R KO model suggest that there is a blunted gene expression response accompanying a diminished phase shifting capacity when VIP-ergic signaling is dysfunctional.

It is important to note that while data from VPAC2R KO mice have been useful in establishing a model for neuropeptidergic signaling within the SCN, a role for VIP itself is still incompletely defined. This is because the observations of VPAC2R KO mice may not be solely based on VIP-ergic signaling. VPAC2 is a receptor that also has high affinity for PACAP (Lutz *et al.*, 1993), another neuropeptide released from SCN afferents, and it is possible that the observed effects of VPAC2 deficiency result from a lack of both VIP and PACAP signaling. This is important to rule out, as PACAP has known modulating effects on photic and glutamatergic transmission in the SCN (Chen *et al.*, 1999; Colwell *et al.*, 2004). The more severe behavioral phenotypes of VPAC2R KO mice as compared to VIP KO mice provide some support for this possibility (Harmar *et al.*, 2002; Colwell *et al.*, 2003).

Since data support that VIP-ergic signaling modulates the circadian system's responses to light, we sought to test the hypothesis that VIP itself plays a major role for the integration of photic information throughout the SCN. Using a combination of *in situ* hybridization and

immunohistochemistry, we determined how a ubiquitous genetic deficiency in VIP affected the retina → SCN core → SCN shell pathway of phase resetting in mammals. In the following set of studies, we first obtain "snapshots" of whole SCN *Per1*and c-FOS expression using well-established, quantifiable techniques. We then expanded our investigation to include carefully defined SCN subregional topography and multiple time points, mapping out spatial and temporal expression profiles of photic gene induction in mice with and without VIP.

Materials and Methods

Animals

Adult male (2-5 months) WT C57Bl/6 mice and mice lacking the gene encoding for the neuropeptides VIP and peptide histidine isoleucine (PHI) were obtained from a breeding facility at the University of California, Los Angeles. Male mice were housed individually, and their wheel-running activity was recorded as revolutions per 3 minute interval. Mice were exposed to a 12:12 hour light-dark (LD) cycle for 2-3 weeks (light intensity ≈ 700 lux) and placed into constant darkness (DD) for 7-14 days to assess their free-running activity pattern. Animals were given a 10 minute light pulse (light intensity ≈ 50 lux) at circadian time (CT) 16 based on wheel running activity records (CT 12 was defined as activity onset) and sacrificed after either 30, 60, 90, or 120 minutes under anesthesia (n=3-5 in each condition). For preliminary time course studies, animals (n=1-2) were also sacrificed at 15, 45, and 240 minutes following the light pulse. Control animals were culled at the same time without a light pulse. Brains were removed and frozen, slide mounted at 20 μM, and then refrozen until hybridization or immunofluorescence.

Experimental protocols used in this study were approved by the UCLA Animal Research Committee, and all recommendations for animal use and welfare, as dictated by the UCLA Division of Laboratory Animals and the guidelines from the National Institutes of Health, were followed.

Per1 radioisotopic in situ hybridization

A plasmid (pCRII; Invitrogen, Carlsbad, CA, USA) containing the cDNA for *Per1* (340–761 nucleotides, accession number AF022992) was generously provided by Dr. D. Weaver (University of Massachusetts), and insert identity was confirmed by sequencing using the M13R primer. To generate antisense and sense templates for hybridization, plasmids were linearized overnight, phenol-chloroform extracted, ethanol precipitated and re-suspended in diethyl pyrocarbonate (DEPC)-treated water. Riboprobes were synthesized from 1 μg of template cDNA in a reaction mixture containing 100 μCi of UTP ^{35}S (1250 Ci/mmol; Perkin Elmer, Wellesley, MA, USA), 5X transcription buffer (Promega, Madison, WI, USA), 0.1 M dithiothreitol (DTT; Promega), 10 mM of each rATP, rCTP, rGTP, 40 U RNase Inhibitor, and the appropriate RNA transcriptase (SP6, or T7) for 3 hours at 37°C. The *in vitro* transcription reaction was DNase I treated, unincorporated nucleotides were removed using the RNase-free microfuge spin columns (Bio-Spin 30; Biorad, Hercules, CA, USA) and probe yields were calculated by scintillation counting.

On the first day of hybridization, slides were warmed to room temperature, briefly washed in phosphate buffered saline (PBS) and fixed in 4% paraformaldehyde, air-dried and blocked by acetylation with acetic anhydride, followed by a series of dehydration steps in

ethanol. After drying, slides were placed in pre-hybridization buffer [50% formamide, 3 M NaCl, 20 mM ethylenediaminetetraacetic acid (EDTA), 400 mM Tris, pH 7.8, 0.4% sodium dodecyl sulfate (SDS), 2X Denhardt's, 500 mg/mL tRNA and 50 mg/mL polyA RNA] for 1 hour at 55°C. Sections were then hybridized overnight at 55°C in humidified chambers in hybridization buffer (50% formamide, 10% dextran sulfate, 3 M NaCl, 20 mM EDTA, 400 mM Tris, pH 7.8, 0.4% SDS, 2X Denhardt's, 500 mg/mL tRNA, 50 mg/mL polyA RNA and 40 mM DTT), where each slide was incubated with 1–4 million cpm/70 mL of a riboprobe. Following hybridization, the slides were washed for 15 minutes in 4X standard sodium citrate (SSC) at 55°C, in 2X SSC for 1 hour at room temperature, and then RNase A (20 μg/mL) treated at 37°C for 30 minutes to remove unbound probe. To further reduce non-specific hybridization, slides were washed twice in 2X SSC at 37°C, and for 1 hour in 0.1X SSC at 62–67°C. Slides were serially dehydrated in ethanol containing 0.3 M ammonium acetate and exposed to Kodak Biomax MR film (Kodak, Rochester, NY, USA) along with a ^{14}C slide standard (American Radiolabeled Chemicals, St Louis, MO, USA). The slides were counterstained with cresyl violet to reference SCN boundaries based on well-established anatomical landmarks. Densitometric analysis of hybridization intensity was done as described using NIH Image software (Shearman *et al.*, 1997; Chaudhury *et al.*, 2008; Wang *et al.*, 2009). Sections were visualized under a dissecting microscope. Sense probe hybridization showed no positive staining.

Per1 digoxigenin in situ hybridization histochemistry

Digoxigenin-labeled riboprobes were generated from 1 μg of template cDNA (described above) in a reaction mixture containing 2 μl of 10X concentrated digoxigenin (DIG) RNA

Labeling Mix (Roche Applied Science Indianapolis, IN, USA), 2 µl of 10X concentrated Transcription Buffer (Roche Applied Science, Indianapolis, IN, USA), 40 U Rnase Block (Stratagene, La Jolla, CA, USA), and 2 µl of the appropriate RNA transcriptase (SP6, or T7; Roche Applied Science, Indianapolis, IN, USA) for 2 hours at 37°C. The *in vitro* transcription reaction was terminated by the addition of 2 µl of 0.2 M EDTA and precipitated with 2.5 µl of 4 M LiCl and 100% ethanol overnight at -20°C. Precipitate was extracted with 70% ethanol and reconstituted in 100 µl of sterile water. Probe yield estimates were determined using relative densities of known concentrations of untranscribed, linearized plasmid in gel electrophoresis and also from serial dilutions of cross-linked riboprobe bound to alkaline phosphatase-conjugated anti-DIG antibody (Roche Applied Science, Indianapolis, IN, USA) visualized with 4-Nitro blue tetrazolium (NBT) and 5-Bromo-4-chloro-3-indolyl phosphate (BCIP) (Roche Applied Science, Indianapolis, IN, USA).

On the first day of hybridization, slides were warmed to room temperature and fixed in 4% paraformaldehyde. Following brief washes in PBS, slides were placed in prehybridization buffer (50% formamide, 5X SSC, 1% SDS, 0.2% Tween-20, 0.1% heparin, and 50 ng/mL Torula RNA at 60°C for 1- 2 hours. Sections were then hybridized overnight at 60°C in hybridization buffer (50% formamide, 5X SSC, 1% SDS, 0.2% Tween-20, 0.1% heparin, and 50 ng/mL Torula RNA), and ≈ 50-100 pg/µL of riboprobe) in sealed slide mailers. Following hybridization, slides were washed briefly in 5X SSC and then for 1 hour in 0.2X SSC at 60°C to remove unbound probe. Slides were then briefly washed with maleic acid buffer (0.1M maleic acid, 0.15M NaCl) and blocked in 20% heat-treated sheep serum in maleic acid buffer. After blocking, slides were incubated with 1:500 anti-DIG antibody conjugated to alkaline phosphatase (Roche Applied Science, Indianapolis, IN, USA) in a humid chamber at 4°C overnight.

After antibody incubation, slides were washed in maleic acid buffer and then in tris buffer (0.1 M Tris (pH 9.5), 0.1 M NaCl, and 5 mM $MgCl_2$). For revelation, slides were incubated in a color reaction solution (tris buffer, 0.3375% NBT, 0.35% BCIP, 1mM levimasole) at room temperature overnight in a humid chamber. After revelation, slides were washed with PBS and color was preserved via a final incubation in 4% paraformaldehyde containing EDTA. Slides were then coverslipped and imaged on an Olympus microscope using Axiovision software (Carl Zeiss Inc., Thornwood, NY) for analysis. Sense probe hybridization showed no positive staining.

Vasopressin immunofluorescence

Brains were processed as described above, and alternate sections were used to delineate SCN subregions chemoarcheticurally. Sections were fixed in 4% paraformaldehyde at room temperature, washed with PBS, and incubated in blocking solultion (3% normal goat serum (NGS), 0.1% Triton X-100 in PBS). After blocking, sections were incubated with a guinea pig polyclonal antibody raised against arginine-vasopressin (AVP, Bachem, Torrance, CA) diluted to 1:1000 in blocking solution at $4^{o}C$ for 4 days. Sections were then washed and incubated with Alexa Fluor® 568-conjugated goat anti-guinea pig IgG antisera (Molecular Probes, Eugene, OR), diluted to 1:300 with blocking solution at room temperature. If tissue was processed for double immunostaining, primary antibody incubation was carried out with both the primary AVP antibody and a rabbit polyclonal antibody raised against androgen receptor (AR) (Santa Cruz Biotechnology, Santa Cruz, CA) diluted at 1:150. Also, during the secondary antibody incubation, Alexo Fluor® 488-conjugated secondary antisera (Molecular Probes, Eugene, OR),

diluted at 1:200, was additionally used. After incubation with secondary antibody, sections were again washed with PBS, coverslipped with Vectashield Mounting Media containing 4',6-Diamidino-2-Phenylindole, Dihydrochloride (DAPI, Vector Laboratories, Burlingame, CA), and stored in the dark at 4^{o}C until imaged.

c-FOS immunofluorescence

Brains were processed as described above, and alternate sections were used whenever available. Sections were fixed in 4% paraformaldehyde at room temperature, washed with PBS, and incubated in blocking solultion (1% bovine serum albumin (BSA), 0.3% Triton X-100, 20% NGS). After blocking, sections were incubated with a rabbit polyclonal antibody raised against c-FOS (Calbiochem, La Jolla, CA) diluted to 1:10,000 in carrier solution (1% BSA, 0.3% Triton X-100, 5% NGS in PBS) at 4^{o}C for 6 days. Sections were then washed and incubated with goat anti-rabbit IgG (Jackson Immunoresearch , West Grove, PA) diluted to 1:200 with carrier solution. Sections were washed with PBS, coverslipped with Vectashield Mounting Media containing DAPI and then stored in the dark at 4^{o}C until imaged.

c-FOS immunohistochemistry with 3,3'-diaminobenzidene (DAB)

Mice were anesthetized and perfused with PBS followed by 4% paraformaldehyde. Brains were dissected, post-fixed at 4°C overnight and cryoprotected in 30% sucrose. Immunohhistochemistry was performed on free-floating 30 μm sections. Sections were washed with PBS, quenched with 2% H_2O_2, washed with PBS and then incubated in blocking solution

(10% NGS in PBS). After blocking, sections were incubated with rabbit polyclonal antiera (see above) diluted at 1:30,000 in PBS overnight at 4°C. Sections were then washed with PBS and incubated with biotinylated goat anti-rabbit antibody at 1:2000 for 2 hours. Sections were washed again in PBS and dipped in AB solution (Vector Labs, Burlingame, CA, USA) for 1 hour, washed, and then placed in filtered 0.05% 3,3'-Diaminobenzidine (DAB) in PBS containing 1:10,000 30% H_2O_2. After desired color was reached, sections were washed, mounted and left to dry overnight. Following ethanol dehydration, sections were coverslipped.

Quantification and statistical analysis

SCN sections were imaged and SCN borders were determined by DAPI and AVP distribution dorsal to the optic chiasm in the anterior hypothalamus. For each SCN, a template was created to define core and shell subregions delineated by AVP expression. This delineation was confirmed by additionally double immunostaining against AR to confirm that a lack of AVP signal coincided with the SCN core. Templates from adjacent sections were superimposed onto both *Per1*+ and c-FOS+ sections and the resulting mid-SCN image (unilateral) for each animal was counted by an experimenter blind to condition. In ≈ 15% of the cases, an alternate section was unavailable and a standardized template was used to delineate subregions. The data sets were analyzed by two-way analysis of variance (ANOVA), with genotype and light exposure as factors. If significant group differences were detected ($p < 0.05$) by ANOVA, then the Holm–Sidak method for pair-wise multiple comparisons was used. For all tests, values were considered significantly different if $p < 0.05$. All tests were performed using Sigmastat software (version 3.5, Systat Software, San Jose, CA, USA). Values are shown as mean ± SEM.

Results

Light-induced Per1 expression in the SCN is strongly affected by VIP

We first used radioisotopic *in situ* hybridization to quantify SCN *Per1* induction in response to a phase delaying light pulse at night (CT 16). Previous data from our lab has shown that VIP KO mice have behavioral deficits in response to light at this time. Experimental mice expressing stable, rhythmic wheel running activity in constant darkness were exposed to white light (1.5×10^{-1} $\mu W/cm^2$; 10 minute duration) and brains were collected and processed for *in situ* hybridization 60 minutes after the beginning of the light pulse.

Two-way ANOVA revealed effects of genotype ($p = 0.01$), light treatment ($p = 0.001$) and interaction of genotype x light treatment ($p = 0.01$), on *Per1* expression levels in the mouse SCN at CT 16 (Fig. 2). *Post hoc* analyses revealed that both WT and VIP KO mice have a significant induction of *Per1* following a light pulse at CT 16 (WT: $p = 0.0001$; VIP KO: $p = 0.03$). The magnitude of this light induction was, however, significantly reduced in VIP KO mice compared to WT controls ($p = 0.01$). There were no statistically significant untreated *Per1* expression level differences at CT 16 between the two genotypes ($p = 0.70$).

To establish how light-induced *Per1* expression parameters varied over space and time, we investigated distribution profiles of *Per1* in the SCN over an extended time series in WT mice. We performed digoxigenin hybridization histochemistry on the SCN at 15, 30, 45, 60, 120, and 240 minutes after a CT 16 light pulse (n = 1-2 at each time point; Fig. 3). *Per1* mRNA begins to appear around 30 min after the beginning of the light pulse, with well-defined

expression in a subpopulation of cells in the ventro-middle region of the nucleus around 45 to 60 min after the initial pulse. Message expression spreads across the nucleus, largely dissipates by 120 minutes following the pulse, and disappears by 4 hours after initial exposure. Based on the data from this expression profile, we chose to specifically compare SCN *Per1* at 30, 60, and 120 minutes following the CT 16 light pulse in WT and VIP KO mice. Converting SCN photomicrographs to heat maps where relative densities of mRNA distribution are expressed on a color scale, it appears that SCN from VIP KO mice express far less *Per1* mRNA at the later time points following the light pulse and altered distribution of *Per1* across the SCN (Fig. 4).

For initial quantification, optical density measurements of *Per1* from digoxigenin *in situ* hybridization were performed across the rostro-caudal axis of the SCN (Fig. 5). In the rostral SCN, two-way ANOVA revealed no significant effects of genotype ($p = 0.693$), light treatment ($p = 0.983$) or interaction of genotype x light treatment ($p = 0.42$), on *Per1* expression levels. However, in the middle SCN, WT mice showed significantly higher *Per1* induction than VIP KO mice ($p = 0.005$), but there were no reported significant effects of light treatment ($p = 0.99$) or interaction of genotype x light treatment ($p = 0.20$). *Post hoc* analyses revealed that the WT SCN had significantly higher *Per1* induction 90 minutes after the CT 16 light pulse ($p = 0.01$) and a trend toward significantly higher induction 120 minutes after the pulse ($p = 0.06$). In the caudal SCN, like in the middle SCN, WT mice showed significantly higher *Per1* induction than VIP KO mice ($p = 0.04$), but there were no reported significant effects of light treatment ($p = 0.50$) or interaction of genotype x light treatment ($p = 0.82$).

Using optical density measures confers the advantage of detecting relative mRNA levels within individual cells. However, when using chromogenic revelation (despite its advantages for providing spatial detail), inter-trial variability and non-linear color-density relationships limit

interpretation of densitometric results. For the sake of these experiments, we used optical density measures to hone in on a target for more rigorous and appropriate quantification methods. Since the majority of WT and VIP KO *Per1* expression differences occurred in the middle SCN (relative to the rostro-caudal axis), and also since at the level of the middle SCN, in particular, there is clear evidence of a retino-recipient region as well as a defined chemoarchitectural classification of core and shell (Fig. 7), we systematically used the middle SCN for further cell counting analysis.

Two-way ANOVA revealed significantly higher *Per1*+ cell counts in the SCN of WT mice compared to VIP KO mice ($p < 0.001$), as well as significant differences of *Per1*+ counts due to light treatment ($p < 0.001$) and interaction effects of genotype x light treatment ($p = 0.011$) (Fig. 6). *Post hoc* analyses revealed that WT mice have a significant increase of *Per1*+ cells at all sampled times (30 minutes: $p = 0.024$; 60 minutes: $p < 0.001$; 90 minutes $p < 0.001$; 120 minutes $p = 0.032$) following a CT 16 light pulse. In contrast, VIP KO mice showed a significant increase in *Per1*+ cells at only 30 minutes ($p = 0.06$) and 60 minutes ($p = 0.014$) following the light pulse. There were no statistically significant untreated *Per1*+ cell count differences at CT 16 between the two genotypes ($p = 0.67$). At 60 minutes and 90 minutes after light pulse, however, there were significantly higher numbers of *Per1*+ cells in the SCN of WT mice (60 minutes: $p = 0.005$; 90 minutes: $p < 0.001$). At 120 minutes following the light pulse, there was a strongly significant trend for higher *Per1*+ cell counts in WT mice compared to VIP KO mice ($p = 0.052$).

We hypothesized that differences could be better uncovered if compared across SCN subregions rather than treating the SCN as a homogenous structure. Therefore, we used a number of anatomical markers to best demarcate and divide the SCN for further analyses (Fig. 7).

Traditionally, the SCN is defined by a dense cluster of cell bodies around the third ventricle just above the optic chiasm, visualized by either a nissl stain or a fluorescence emitting nuclear intercolating agent such as DAPI (Fig. 7A). Cell bodies in the ventral SCN that express VIP have been traditionally used to define part of the SCN core, while VIP-expressing fibers course through the core and to a larger extent, the shell. Since these studies were performed on mice deficient in VIP, we had to choose other markers for SCN classification. AVP expression in the SCN has been used both to define global SCN boundaries and also specifically, borders of the SCN shell (Fig. 8B) (Karatsoreos & Silver, 2007). Between DAPI and AVP expression, we proposed that we could define the boundaries of the complete SCN, the shell of the SCN, and by inductive reasoning, the core of the SCN (where AVP+ cells were absent). To support our reasoning, we also performed immunohistochemistry for androgen receptor (AR) expression, an established marker for the SCN core (Karatsoreos & Silver, 2007) (Fig. 8C). This confirmed that the non-AVP+ region of the SCN was a reasonable and reliable marker for the SCN core. Using alternate sections (20 μm) to those used for the digoxigenin *Per1 in situ* hybridization, we created unilateral SCN templates for each animal of SCN core and shell based on AVP+ staining (Figs. 8D, E).

WT and VIP KO mice differed greatly in the spatio-temporal expression profiles of *Per1*. In WT SCN, *Per1* is photically induced in two separate waves: one in the core followed by one in the shell (Fig. 9A). The majority of light-induced *Per1* expression is in the SCN core, as has been previously reported (Hamada *et al.*, 2004). However, there is also steady increase of *Per1* from 30 to 90 minutes in the shell following the light pulse. This wave-like pattern of core followed by shell increase has also been reported previously (Yan & Silver, 2002; Hamada *et al.*, 2004), and it has been hypothesized as a necessary step for behavioral phase shifts of locomotor

activity in mammals (Yan & Silver, 2002).

In VIP KO mice, the waves of *Per1* induction followed a different pattern. First, there was an immediate response to the light pulse with a sizable induction of *Per1* by 30 minutes after the initial pulse in the SCN core. However, the hybridization signal decreased steadily through time, at least an hour earlier when compared to WT mice (Fig. 9B). There appears to be a very slight increase of *Per1* in the VIP KO shell, and although its profile has a slight waxing and waning waveform, its levels consistently hover close to untreated controls.

Two-way ANOVA revealed significantly higher *Per1*+ cell counts through both the SCN core and shell in WT mice compared to VIP KO mice (core: $p = 0.015$; shell: $p < 0.001$), as well as significant differences in *Per1*+ cell counts due to light treatment (core: $p < 0.001$; shell: $p < 0.001$) and interaction effects of genotype x light treatment (core: $p = 0.028$; shell: $p = 0.009$) (Fig. 9, 10). *Post hoc* analyses revealed that WT mice have a significant increase in *Per1*+ cells in the core at 60 minutes ($p < 0.001$) and 90 minutes ($p < 0.001$) and in the shell at all times sampled following the light pulse (30 minutes: $p = 0.004$; 60 minutes: $p = 0.001$; 90 minutes: $p < 0.001$; 120 minutes: $p = 0.028$) following a CT 16 light pulse. In contrast, VIP KO mice only show significant increase in *Per1*+ cells at 30 minutes following the light pulse and only in the core ($p = 0.01$). There were no statistically significant untreated *Per1*+ cell count differences at CT 16 between the two genotypes (core: $p = 0.95$; shell: $p = 0.17$). At 60 minutes and 90 minutes after light pulse, there were significantly higher numbers of *Per1*+ cells in the both subregions of the SCN in WT mice compared with VIP KO mice, and this difference extended to 120 minutes after pulse in the SCN shell (60 minutes core: $p = 0.011$; shell: $p = 0.018$; 90 minutes core: $p = 0.014$; shell: $p < 0.001$; 120 minutes shell $p = 0.005$).

Light-induced c-FOS expression in the SCN is strongly affected by VIP

In order to determine the effects of VIP on other genetic markers of photic induction, we also used immunohistochemistry, first with chromogenic revelation (DAB), to quantify SCN c-FOS induction in response to a CT 16 light pulse (Fig. 11). Two-way ANOVA revealed effects of genotype ($p = 0.001$), light treatment ($p = 0.001$) and interaction of genotype x light treatment ($p = 0.001$) on c-FOS+ cell counts in the mouse SCN at CT 16. *Post hoc* analyses reveal that both WT and VIP KO mice have a significant induction of c-FOS following a light pulse at CT 16 (WT: $p = 0.0001$; VIP KO: $p = 0.0001$). The magnitude of this light induction was, however, significantly reduced in VIP KO mice compared to WT controls ($p = 0.0001$).

To establish how light-induced c-FOS expression parameters varied over space and time, we investigated distribution profiles of c-FOS in the SCN over an extended time series in WT mice. We performed immunohistochemistry with fluorescent revelation on the SCN at 45, 60, 90 and 120 minutes after a phase delaying light pulse (n = 1-2 at each time point; Fig. 12). C-FOS begins to appear ≈ 45 min after the beginning of the light pulse, with well-defined expression in a subpopulation of cells in the ventro-middle region of the nucleus around 60 to 90 minutes after the initial pulse. Expression patterns show a spread across the nucleus beginning by 120 minutes following the pulse. Based on the data from this expression profile, we chose to specifically compare SCN c-FOS at 60 and 120 minutes following the CT 16 light pulse in WT and VIP KO mice (Fig. 12). It appears that SCN from VIP KO mice express far less c-FOS at both time points following the light pulse (Fig. 13).

WT and VIP KO mice differ in the SCN expression profiles of c-FOS (Fig. 14). In WT SCN, there is a large photic induction of c-FOS in both the SCN core and shell that occurs in

parallel waves (Fig. 14A). In VIP KO mice, on the other hand, there is very little light-induced c-FOS expression at all, although there is a small increase in the core specifically 60 minutes following the light pulse (Fig. 14B). The shell remains unchanged throughout the time course of analysis.

Two-way ANOVA revealed significantly higher c-FOS+ cell counts through both the SCN core and shell in WT mice compared to VIP KO mice (core: $p < 0.001$; shell: $p < 0.001$), as well as significant differences in c-FOS+ cell counts due to light treatment (core: $p < 0.001$; shell: $p = 0.002$) and interaction effects of genotype x light treatment (core: $p = 0.024$; shell: $p = 0.018$) (Figs. 15, 16). *Post hoc* analyses revealed that WT mice have a significant induction of c-FOS at 60 minutes (core: $p < 0.001$; shell: $p < 0.001$) and 120 minutes (core: $p < 0.001$; shell: $p = 0.003$) following a CT 16 light pulse. In contrast, VIP KO mice only show significant induction of c-FOS at 60 minutes following the light pulse and only in the SCN core ($p = 0.005$). There were no statistically significant untreated c-FOS+ cell count differences at CT 16 between the two genotypes (core: $p = 0.70$; shell: $p = 0.49$). At both 60 minutes and 120 minutes after light pulse, there were significantly higher numbers of c-FOS+ cells in both subregions of the SCN in WT mice, (60 minutes core: $p = 0.002$; shell: $p < 0.001$; 120 minutes core: $p < 0.001$; shell: $p = 0.002$).

Discussion

In this set of studies, we investigated how VIP deficiency affects light-induced gene expression across the SCN network in response to a phase delaying stimulus. Since VIP KO mice exhibit impaired behavioral phase shifting responses to light at this time, we sought to

carefully characterize molecular responses across the SCN network in order to infer mechanistically how VIP participates in the process of entrainment in the circadian system.

Our results indicate that following a CT 16 light pulse: 1) There is a lower magnitude induction of *Per1* and c-FOS in the SCN when VIP is absent, 2) the duration of photically induced *Per1* and c-FOS expression is considerably shortened in the SCN when VIP is absent, 3) VIP absence does not prevent gene expression responses from reaching the SCN core, but it does correlate with a near complete lack of photic gene induction in the SCN shell.

In the past, VIP has been viewed as a synchronizing output signal between SCN neurons that allows the SCN to oscillate as a robust, single pacemaker by aligning inter-neuronal phase relationships of its 20,000+ independent clocks (Aton & Herzog, 2005; Maywood *et al.*, 2007). At the same time, the loss of VIP-ergic signaling has also been shown to result in damped responses to photic resetting in the SCN (Hughes *et al.*, 2004). While these two phenomena have been tacitly treated as separate effector pathways of VIP-ergic signaling, they both include the same integral steps found in photic entrainment.

During entrainment, sensory afferents transmit irradiance-encoded light input to retino-recipient SCN neurons and provide synchronizing cues to them that allow SCN phase alignment to the environmental light-dark cycle (Berson, 2003). These second order neurons, in turn, must synchronize downstream SCN cells to the newly shifted phase of the retino-recipient neurons (Yan *et al.*, 2007; Golombek & Rosenstein, 2010). If VIP does in fact synchronize the phases of SCN neurons, then loss of VIP-ergic signaling should result in deficits in light entrainment and the neuronal signals that correlate with photic resetting in individual clock cells along each point in this pathway. Thus, the two distinct observations referenced above are each consistent with a synchronizing role for VIP. Our data are the first to show that during photic resetting, the cells

most strongly affected by the loss of VIP are those in the largely non-retino-recipient SCN shell, and this deficit is most clearly demonstrated over the subsequent two hours that follow a phase-resetting light pulse.

VIP deficiency reduces photically-induced Per1 and c-FOS expression in the SCN

Consistent across four different neuroanatomical techniques for two different markers, we show that photically induced gene expression is largely damped in the SCN of VIP KO mice compared to WT controls. The reason why two forms of *in situ* hybridization and immunohistochemistry were employed was because the more traditionally used radioistopic *in situ* hybridization and chromogenic immunohistochemistry were not sufficient to examine all of the spatio-temporal propagation effects we wished to document. However, we had to first validate our techniques with the more traditional methods in order to directly compare our results with other data in the available literature, particularly with the VPAC2R KO mouse model. The consistent trends in both c-FOS and *Per1* we found across all techniques allow us to make these important comparisons.

We chose to analyze the expression of *Per1* because its induction is part of a signal transduction pathway activated by glutamatergic retinal input to the SCN (Akiyama *et al.*, 1999). Induction of SCN *Per1* leads to shifts in the circadian molecular clockwork and also tightly correlates to behavioral phase shifts in locomotor activity (Shigeyoshi *et al.*, 1997). The fast induction and depletion of *Per1* by light also makes it a useful anatomical marker with a relatively detailed temporal resolution for cells in which molecular clock resetting is likely to take place (Shigeyoshi *et al.*, 1997; Hamada *et al.*, 2004).

Previous studies have shown that *Per1* expression is altered in mice lacking the VPAC2 receptor. Maywood et al. (2007) have reported that SCN *Per1* shows reduced induction in VPAC2R KO mice in response to a nighttime light pulse compared to WT mice (Maywood *et al.*, 2007). While acute *Per1* transcription appears reduced in the VPAC2R KO SCN, expression of PER1 protein 6+ hours after a nighttime light pulse is strikingly absent in these same mice (Harmar *et al.*, 2002). This would indicate that acute *Per1* mRNA expression in the SCN is not solely predictive of the subsequent PER1 protein expression (and likely molecular clock resetting) in the VPAC2R KO model.

Expression of the immediate early gene c-FOS is another product of the signal transduction pathway triggered by retinal input to the SCN. Traditionally, both *Per1* and c-FOS have each been used to determine the status of resetting in the SCN clock. *Per1* induction is considered a molecular correlate of clock resetting itself, and c-FOS induction is thought to serve as a molecular stamp of a recently 'activated' (at the level of second messenger recruitment) neuron (Rusak *et al.*, 2002). Since SCN neuronal firing and molecular clock resetting are both integral to inducing phase shifts, both *Per1* and c-FOS usually show similar expression profiles in response to light. To this end, c-FOS expression in the SCN highly correlates with phase shifts and has been shown to strongly modulate the magnitude of these shifts (Wollnik *et al.*, 1995) yet is not necessary for inducing a phase shift (Honrado *et al.*, 1996). We looked at gene expression profiles of both genes, as their functions may be dissociable. Furthermore, the time course for c-FOS translation and stability is slower and longer than that for *Per1* mRNA, and this time discrepancy offers another vantage point from which to analyze the effects of VIP-ergic signaling on photic gene expression profiles.

There are two different reports of c-FOS expression from the VPAC2R KO mice with

conflicting results. In their first published characterization, VPAC2R KO mice were reported to not have a significant induction of c-FOS following a phase delaying light pulse. However looking at the counts of c-FOS+ cells, it does appear as if there is relatively increased c-FOS expression, despite the lack of statistical significance at the $\alpha = 0.05$ level. A more recent study reported that there was significant photically induced c-FOS expression in the VPAC2R KO SCN across both the subjective day and night, although these levels were not directly compared to WT levels (Hughes *et al.*, 2004).

Here we describe that both light induced *Per1* and c-FOS expression levels are decreased in VIP KO mice. Considering that there is a time lag between expression profile changes of *Per1* mRNA and c-FOS protein, both markers tell a consistent story with their blunted levels. As *Per1* mRNA is highest in the VIP KO SCN at 30 minutes following the light pulse, c-FOS is highest at 60 minutes. In both cases, levels are greatly decreased compared to WT mice, but even at these lower levels, it suggests that there is both second messenger activation and activity toward molecular clock resetting in VIP KO mice. It is the magnitude at which these processes are taking place that differs between the genotypes.

At a functional level, this difference in magnitude has been implicated in phase shifting differences in different physiological paradigms. For instance, in the SCN of aged rodents, both *Per1* and c-FOS responses to light have been shown to decrease with a concomitant decrease in behavioral phase shift magnitude (Benloucif *et al.*, 1997; Kolker *et al.*, 2003). Furthermore, stronger light stimuli have been shown to correlate with both increased SCN c-FOS expression as well as greater magnitude phase shifts in young animals (Travnickova *et al.*, 1996). Our data could thus fit in a similar model by which a blunted gene expression response would indicate a blunted magnitude (or, if small enough, a blocked) phase shift in the clock.

VIP deficiency shortens the duration of Per1 and c-FOS responses in the SCN

This is the first set of studies to report the large impact that VIP-ergic signaling has on the temporal profile of photically induced gene expression in the SCN. Our data show that in the absence of VIP, the most dramatic differences in photically induced gene expression occur when considerable time has elapsed after the light pulse (see Figs. 4, 13). The importance of the current data stress that while there is a gene expression signal to track in the absence of VIP, this is only visible in the earliest phases of the SCN response to light.

Nearly all light induced gene expression studies in the SCN target one specific time point in order to compare maximal gene expression between conditions or backgrounds. In the mouse SCN, for instance, c-FOS has been shown to peak between 60 and 120 minutes following a light pulse, and *Per1* has been shown to peak slightly earlier (Colwell & Foster, 1992; Shigeyoshi *et al.*, 1997). This type of comparison assumes that the maximally induced levels of protein or transcript are related to specific downstream physiological and behavioral changes, such as circadian phase shifts. This is not necessarily the case, however, as there are paradigms in which both c-FOS and *Per1* can be induced in the SCN without accompanying phase shifts (Aronin *et al.*, 1990; Yan & Silver, 2002). Furthermore, maximal expression at one time point does not account for other factors, such as molecular stability or degradation rates, both of which will likely affect the downstream actions of these photically induced molecules. For instance, in the *drosophila* clock, the post-transcriptional regulation of *period* follows a circadian rhythm and further contributes to rhythmic expression of other clock genes (So & Rosbash, 1997).

The most robust response that VIP KO mice show is that after an initial induction of *Per1*

in response to light, mRNA levels drop sharply, whereas they remain elevated for at least another 30 to 60 minutes in WT mice. The rapid induction and depletion of *Per1* in the mouse SCN in response to light (Fig. 3) suggests that the initial light response in both genotypes induces transcriptional changes in SCN cells. The remaining question is: what is causing the major phenotypic difference? VIP deficiency could be contributing to: 1) an increased level of mRNA degradation, 2) a large decrease in transcriptional activity subsequent to the initial photic signal, and/or 3) a lack of molecular resetting signals propagated between SCN cells. Because our experiments did not track dynamic changes in gene expression within individual SCN cells over time, we cannot determine beyond inference the involvement of the first two processes. The process of phase resetting signal propagation across SCN cells is addressed later, as there are noted deficiencies in core to shell gene expression in the SCN of VIP KO mice.

The half-life of *Per1* is thought to be just slightly less than 1 hour in WT mice (Wilsbacher *et al.*, 2002). Looking at *Per1* expression levels in the VIP KO SCN (including its subregional divisions), it appears that the degradation rate *in vivo* does not fall outside of the normal degradation rate as reported in WT mice (see Figs. 3,8). While this observation is not conclusive due to the possible contribution of other processes (eg. increased transcription rates at the same time as increased degradation), the early, confined window of blunted *Per1* expression supports that increased transcriptional activity is unlikely. In both cases, an *in vitro* analysis will be necessary to determine the possible contributions of prolonged transcriptional activity and mRNA degradation rates, similar to what was performed in the *drosophila* system (So & Rosbash, 1997).

The c-FOS data provides other clues as to what molecular process may be altered in the VIP KO SCN that lead to deficits in phase shifting. Firstly and importantly, the c-FOS

expression patterns in the WT SCN follow a predicted temporal profile based on the expression patterns of *Per1*. According to our understanding of the molecular processes that occur within the cell following a phase resetting light pulse, both *c-fos* and *Per1* transcription are initiated by CREB. Since *c-fos* is an immediate early gene, transcription takes place rapidly to produce highly labile mRNA which are rapidly translated to proteins. *Per1,* while not a considered an immediate early gene, is still transcribed relatively quickly, but its rate slightly lags that of *c-fos*. C-FOS protein translation, then slightly lags *Per1* transcription, but precedes *Per1* translation by many hours. Thus, following a light pulse, our data shows the expected result that *Per1* is expressed at high levels at the early stages following a light pulse (Figs. 3,8) and c-FOS takes slightly longer to induce elevated expression, but c-FOS levels remain relatively high over the first and second hours post-induction (Fig. 14).

These c-FOS patterns replicate patterns in data from an earlier study in the mouse SCN (Colwell & Foster, 1992) as well as fall within the confines of the reported trend that c-FOS protein half-life is somewhere around 2 hours (Curran *et al.*, 1984). It is thus particularly interesting that the VIP KO mouse shows a small induction of c-FOS at 60 minutes with levels falling dramatically by 120 minutes after the light pulse. Again, since these experiments did not specifically or directly test transcriptional, post-transcriptional, translational, or post-translational effects of VIP deficiency, those studies need to be carried out *in vitro* to appropriately establish the type of modification at each stage. One important clue within the data from this study, however, is that c-FOS levels are reduced by more than half within 60 minutes (half of the c-FOS half-life) in the VIP KO SCN. This would suggest that protein stability is altered in the absence of VIP. This possibility is further supported by data in which VIP has been shown to alter the stability of another protein, interleukin-4 (IL-4), in mouse T-lymphocytes (Wang *et al.*,

1996). If VIP-ergic signaling does have a role in altering protein stability, this may explain, in part, why in VPAC2R KO mice PER1 protein levels did not appear to be increased following a light pulse, while *Per1* transcript levels did (Harmar *et al.*, 2002; Maywood *et al.*, 2007).

Because VIP KO deficits in gene expression extend both to *Per1* mRNA and c-FOS protein, it suggests that there is likely a process upstream of both transcription and translation affecting cells in the SCN in these animals. As c-FOS has been used as a marker for second messenger pathway activation, subsequent studies could start at this point and try to determine the specific second messenger pathways that are likely altered in the absence of VIP-ergic signaling. In the SCN, it is canonically thought that VIP binds to the G-protein coupled VPAC2 receptor, which activates adenylyl cyclase. Cylic AMP is then generated, resulting in the recruitment PKA and then the subsequent phosphorylation of CREB, which promotes gene transcription (Vosko *et al.*, 2007). Recently, however, it was suggested that the VPAC2 receptor also interacts with calmodulin, and in the nervous system, it has been demonstrated that this interaction affects c-FOS expression (Falktoft *et al.*, 2009). There are many targets available to further determine effects on second messenger signaling pathways, including Ca^{2+} entry, CAMKII activation, phosphorylated CREB expression and PKA activity.

There have been two other reports in mammals tracking the temporal profiles of gene expression after phase delaying light pulses. The first examined gene expression in the hamster SCN and reported an ordered induction of gene expression over a number of hours, similar to the WT mouse *Per1* results reported here (Hamada *et al.*, 2004). The other, more recent study, compared temporal profiles between WT and mutant mice deficient in a subunit for a sodium channel that is expressed in the SCN (Han *et al.*, 2012). Interestingly, the mutant mice in this study showed marked decreases in relative SCN *Per1* expression that were most pronounced ≈

90 minutes following the light pulse (the furthest time point examined). Even more importantly, these mice did not successfully exhibit behavioral phase shifts to the same light pulse that induced behavioral phase shifts in WT mice. Our data, taken together with these data, suggest a correlation between extended light induced gene expression in the SCN and successful behavioral phase shifting.

VIP deficiency maps to a lack of photic gene induction in the SCN shell

The other major finding in this study is how the loss of VIP-ergic signaling differentially affects light induced gene expression in different subregions of the SCN.

Numerous reports support that the SCN is a heterogeneous structure comprised of multiple functional subunits (Abrahamson & Moore, 2001; Morin, 2007; Yan *et al.*, 2007), yet light induced gene expression studies tend to treat the SCN as a singular, homogenous nucleus. One reason for this treatment is likely due to the difficulty in finding consistent ways to divide the SCN. For instance, the core and shell regions in rats, hamsters and mice are differentially distributed topographically and have different chemoarchitectrual properties (Morin, 2007). In some cases, a simple geographical delineation (dorsal v. ventral) can be employed, but this is often insufficient when cell populations of interest lie in a plane that regularly crosses these boundaries, such as in the mouse. Furthermore, depending on the angle at which a coronal section was sliced, geographic subdivisions of the SCN can appear very different than their typical representation from model neuroanatomy. In order to accurately define the mouse SCN and its subregions, a thorough analysis across the different planes of the SCN was necessary.

The current set of studies first determined the targeted area of interest according to a

rostro-caudal analysis of the gene expression data. Since changes in gene expression over time and differences between the genotypes were most pronounced in the middle SCN, we performed a detailed analysis among coronal sections of this area. Furthermore, the middle SCN corresponds with comparatively dense retinal innervation (see Chapter 3) and also well-defined delineation by chemoarchitectural markers (AVP and AR), so it seemed most appropriate for further examination. We used alternate sections to carefully define SCN subregions in each section and map out the spread of photically induced gene expression across both the core and shell.

In WT mice, the phase delaying light pulse resulted in two waves of propagation of *Per1* expression in the SCN. The first wave began in the SCN core, followed by a second wave in the SCN shell. These patterns mimic those shown in a similar study done in the hamster (Hamada *et al.*, 2004) and are consistent with the circuit model of the SCN in which photic information first reaches the SCN via the RHT signal to the core, and then from the core to the shell (Abrahamson & Moore, 2001). Statistical analyses also revealed a small but significant early induction of *Per1* in the shell as well. This is likely due to the fact that *Per1* baseline levels in the shell are low enough that very small increases are statistically significant. This result is also anatomically plausible, as others have noted that retinal afferents are not strictly limited to the ventral-most regions, but some can extend through more dorsal aspects of the SCN as well (Abrahamson & Moore, 2001; Hattar *et al.*, 2002). Our data indicate that retinal afferent terminals, can, in fact, extend to the shell subregion, but the majority are concentrated in the vicinity of the core (see Chapter 3).

In VIP KO mice, the order of *Per1* expression waves differs considerably. The wave in the core is both damped and highly skewed to the earliest time points examined (around 30

minutes), and core *Per1* levels decrease continuously over all the time points that follow. The shell, unlike the core, shows no induction over any of the time points following the light pulse. Therefore, when VIP-ergic signaling is absent, the core is affected in such a way that there is a weaker *Per1* response that rapidly diminishes. In the shell, there is no observable gene expression response at all. The lack of *Per1* induction in the SCN shell would indicate that the molecular clockwork, and likely, the components of the cellular network in SCN shell, do not receive the appropriate signals to induce a phase delay. Between the blunted response in the core and the lack of response in the shell, one interpretation for the lack of light induced behavioral phase delays in VIP KO mice is that gene expression changes are of insufficient strength to promote behavioral shifts.

The spatial expression profiles from this study are consistent with other data supporting that light induced *Per1* in the core is not sufficient to cause a phase shift from an acute shifting stimulus. Yan and Silver (2002) showed that in the middle of the night, light induces *Per1* expression in the core, but it does not induce subsequent behavioral phase shifts. It was only when *period* genes were induced both in the core and shell that there was a also a behavioral phase shift (Yan & Silver, 2002). In another study involving a sodium channel mutant mouse, researchers were able to show that non-shifting mutant mice lacked shell induction of *Per1*, but core induction persisted (Han *et al.*, 2012). Taken together, these data suggest that light induced gene expression in the SCN core may occur without observable behavioral changes, whereas core-to-shell expression is a more consistent predictor of successful phase shifting behavior.

Finally, the observation that VIP KO mice have specific deficits in shell gene expression suggests that photic resetting signals are insufficiently propagated within the SCN in the absence of VIP. Both *Per1* and c-FOS show photic induction in the core of the VIP KO SCN, albeit to a

lesser extent than in the WT SCN. Since the SCN is normally organized such that VIP-ergic cell bodies are concentrated in the ventral-most core and VIP-ergic fibers course through the rest of the nucleus, VIP likely plays a role in relaying photic information from its retino-recipient area (core) to its surrounding oscillatory network in the shell. The lack of core-to-shell spread in VIP KO mice might also suggest that part of the lower magnitude gene expression response observed in both VIP KO and VPAC2R KO mice is due to an intra-SCN impairment in inducing appropriate second messenger pathways and molecular clock resetting in the efferent targets of retino-recipient cells. This should be reflected in differences in SCN electrophysiological properties and possibly anatomical changes in SCN circuitry in VIP KO mice.

The concentrated placement of VIP-containing neurons around the retino-recipient SCN has long suggested a role for this neuropeptide in the photic resetting of the circadian system. This study, using mice genetically deficient in VIP, points specifically to a role for VIP in mediating the core-to-shell spread of phase resetting information within the SCN. While further experiments will be necessary to uncover the mechanisms by which VIP may be acting, one important point to test will be if and how the genetic loss of VIP could alter the circadian visual system in both acute activity, and alternatively, through long-term changes that may arise during development.

Fig. 1. Schematic of SCN cellular signaling in response to phase resetting photic input

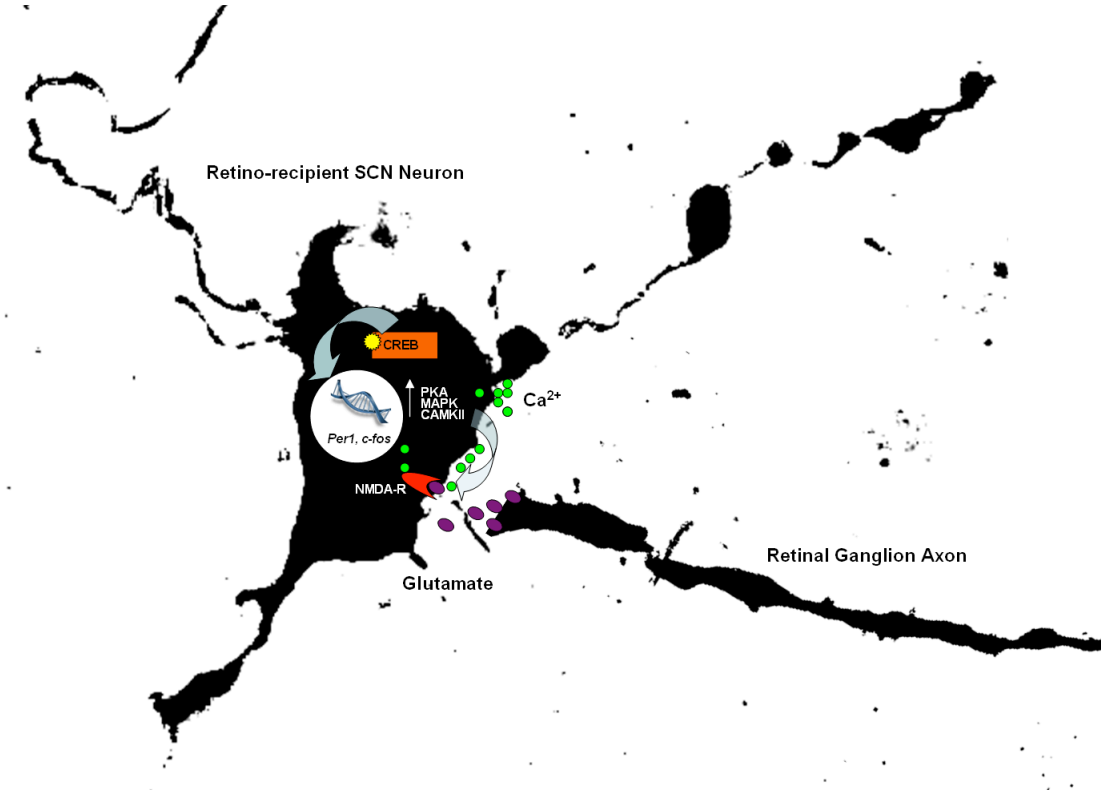

Upon exposure to nighttime light or stimulation of the retinohypothalamic tract, retinal ganglion cell axons release glutamate, binding postsynaptically to N-methyl-D-aspartate receptors (NMDAR) on retinorecipient SCN neurons in the SCN core. NMDAR conformational change allows an intracellular influx of Ca^{2+}, which induces intracellular signaling through the protein kinase a (PKA), mitogen-activated protein kinase (MAPK) and calcium-calmodulin dependent protein kinase II (CAMKII) cascades, all of which converge on the phosphorylation of cAMP response element binding protein (CREB). Phosphorylated CREB translocates to the nucleus and binds to the cAMP response element (CRE) regions on a number of target genes, including *Per1* and *c-fos*, to initiate their transcription. This transcription is thought to reset the molecular clock of an individual cell and synchronize its phase appropriately to the environmental light cue.

Fig. 2. VIP KO mice show reduced magnitude SCN *Per1* expression to a CT 16 light pulse

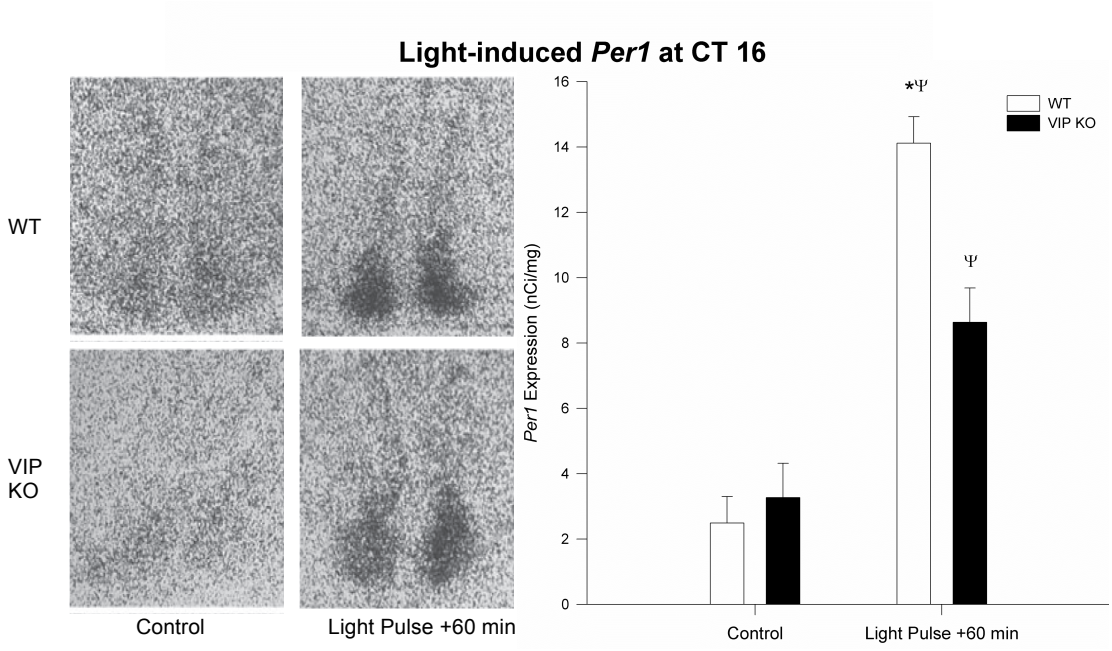

Radioisotopic *in situ* hybridization reveals a reduction in *Per1* mRNA in response to a CT 16 light pulse. (A) Photomicrographs of autoradiograms taken from SCN in mice one hour after a 10 minute light pulse at CT 16, alongside SCN from time-matched control mice receiving no light. (B) While both wild type (WT) and vasoactive intestinal peptide knockout (VIP KO) mice show a significant induction of *Per1* from the light pulse compared to controls (denoted by ψ), WT mice show a significantly higher magnitude induction than VIP KO mice (denoted by *).

Fig. 3. SCN *Per1* expression shows a characteristic spatio-temporal profile following a CT 16 light pulse in WT mice

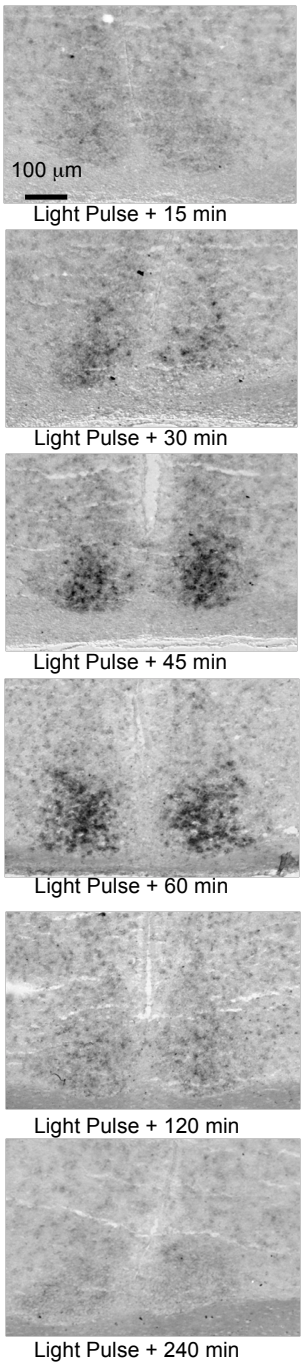

SCN photomicrographs following digoxigenin *in situ* hybridization histochemistry for *Per1* reveal a time course of induction in WT mice at CT 16. Message begins to appear around 30 minutes after the beginning of the light pulse, with well-defined expression in a subpopulation of cells in the ventro-middle region of the nucleus around 45 to 60 minutes after the initial pulse. Message expression spreads across the nucleus and disappears by 4 hours after the initial pulse.

Fig. 4. VIP is essential for sustained *Per1* expression in the SCN following a CT 16 light pulse

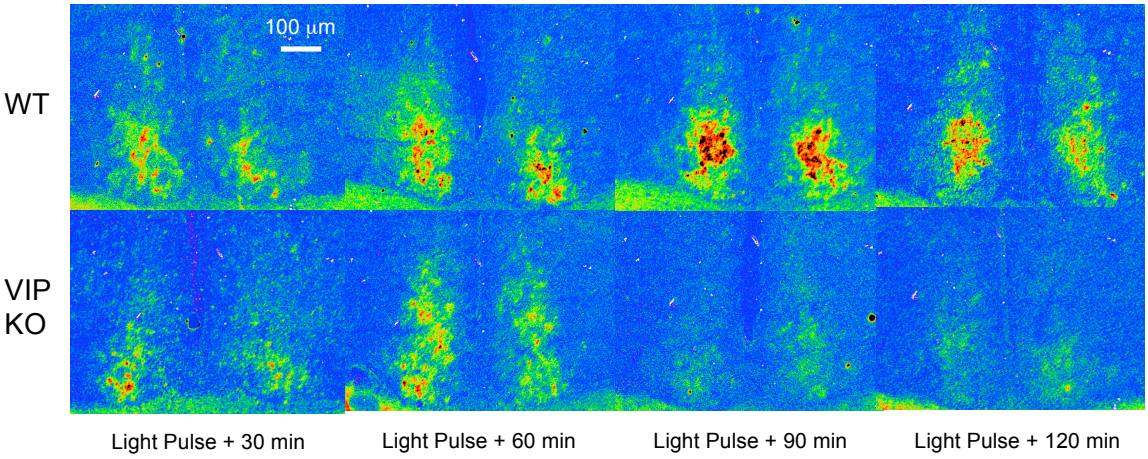

Photomicrographs from *Per1* hybridization histochemistry were converted to pseudo-color with Image J software to show a time course of relative gene expression in the SCN of WT and VIP KO mice following a CT 16 light pulse. There was an initial induction of *Per1* in response to the light pulse in both WT and VIP KO mice. However, only in WT mice is this signal sustained and strongly concentrated in the ventro-middle SCN subregion.

Fig. 5. *Per1* expression is most pronounced in the middle SCN along its rostro-caudal axis

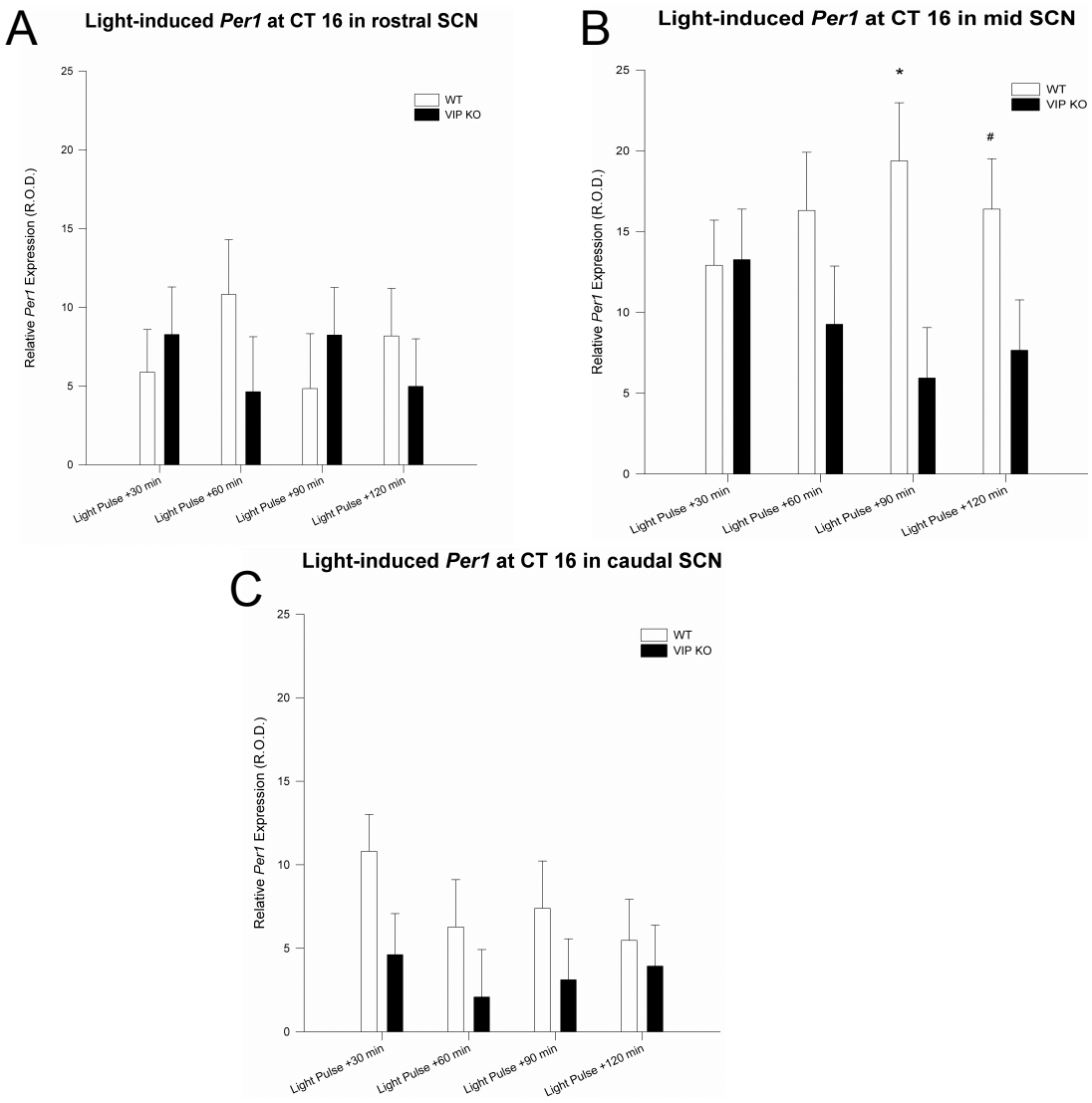

Optical density measures for *Per1* from WT and VIP KO SCN undergoing hybridization histochemistry show highest expression of mRNA in the middle SCN compared with levels taken from rostral or caudal SCN. (A) There are no genotypic differences, low expression levels and high variability of *Per1* levels in the rostral SCN. (B) In the middle SCN, *Per1* levels appear highest, with WT mice significantly showing higher levels than VIP KO mice overall, and *post hoc* tests showing this specifically at 90 minutes following the pulse. At 120 minutes following the light pulse, there is a strongly significant trend of higher *Per1* levels in the WT SCN (p = 0.06, denoted by #). (C) In the caudal SCN, *Per1* levels are again low, but they are statistically higher in WT mice than in VIP KO mice.

Fig. 6. *Per1*+ cell quantification shows sustained *Per1* induction in WT but not in VIP KO mice

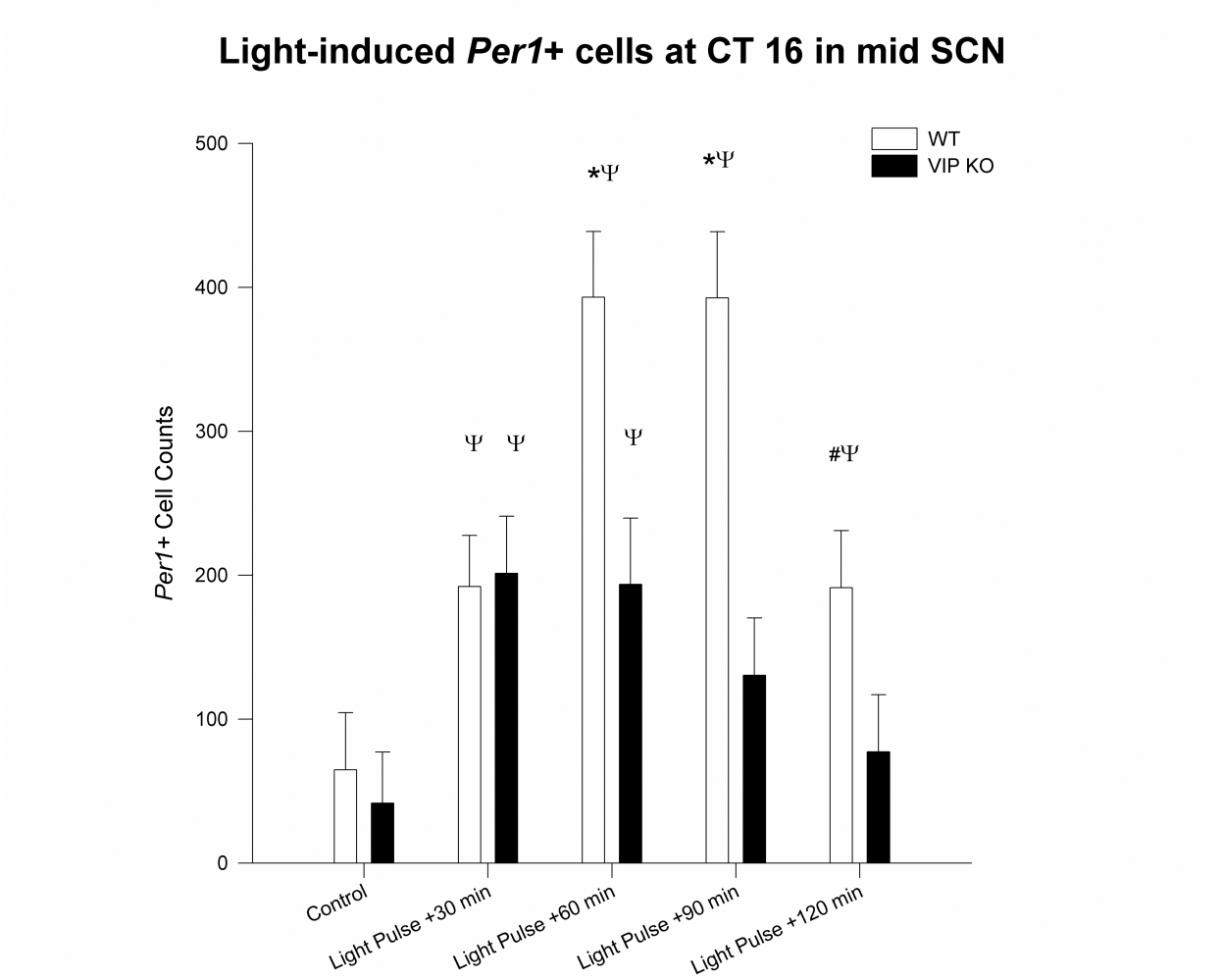

Cell counting of *Per1*+ cells following hybridization histochemsitry reveals that *Per1* is significantly induced by a CT 16 light pulse at all time points measured in WT mice, but only at 30 and 60 minutes post pulse in VIP KO mice (denoted by ψ). *Post hoc* analyses reveal greater *Per1*+ cell counts in WT mice compared with VIP KO mice at both 60 and 90 minutes following the light pulse (denoted by *). At 120 minutes following the light pulse, there is a strongly significant trend of higher *Per1* levels in the WT SCN ($p = 0.052$, denoted by #).

Fig. 7. SCN chemoarchitecture delineates core and shell for quantifying *Per1* propagation

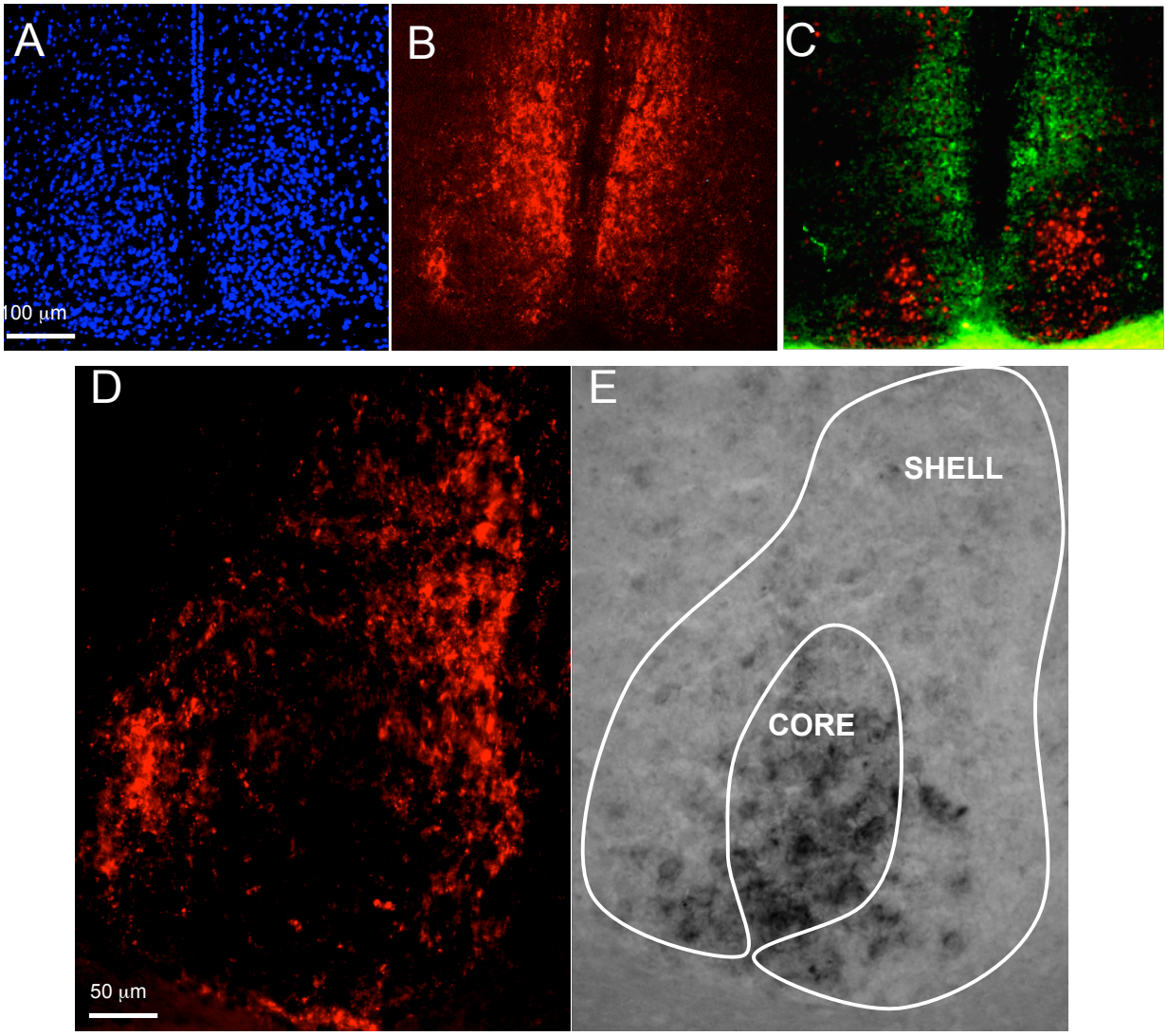

Different SCN markers were used to create core and shell templates to overlay on alternately stained *Per1*-expressing SCN photomicrographs. (A) 4',6-Diamidino-2-Phenylindole, Dihydrochloride (DAPI) traditionally localizes the SCN and its landmarks based on dense cell body staining around the third ventricle, just above the optic chiasm. (B) Arginine-vasopressin (AVP) is used to delineate SCN boundaries as well as demarcate the SCN shell. We proposed the ventro-middle subregion absent of AVP expression was sufficient to define the core as well. (C) Double labeling for AVP (green) and androgen receptor (AR) (red), an accepted SCN core chemoarchitectural marker, confirms that this ventro-middle subregion would fulfill the criteria for labeling it as core. (D and E) Templates were drawn around the AVP+ SCN area to define core and shell, and templates were overlaid onto alternate sections (20 μm) to apply to quantification of *Per1* expression across SCN subregions.

Fig. 8. *Per1* is propagated in separate core and shell waves in WT mice, but not in VIP KO mice

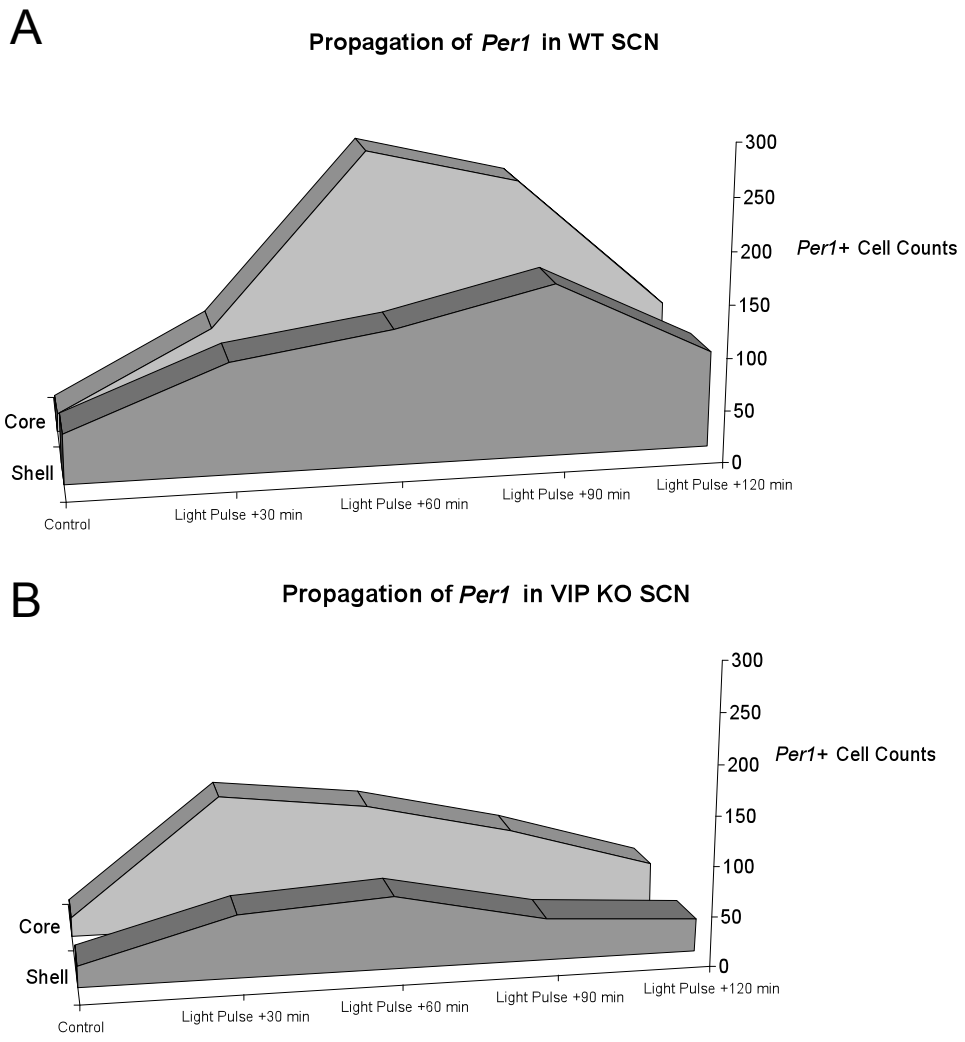

Graphical representation of *Per1* spread shows differences in signal propagation between WT and VIP KO mice. (A) After a CT 16 light pulse, WT mice show a high amplitude, rapid wave of *Per1* expression in the core, and a slower, lower amplitude induction of *Per1* in the shell. (B). VIP KO mice, however, show a blunted, brief wave of *Per1* expression in the core and a near complete lack of *Per1* induction in the shell.

Fig. 9. *Per1*+ cell quantification shows lower magnitude core *Per1* induction in VIP KO mice

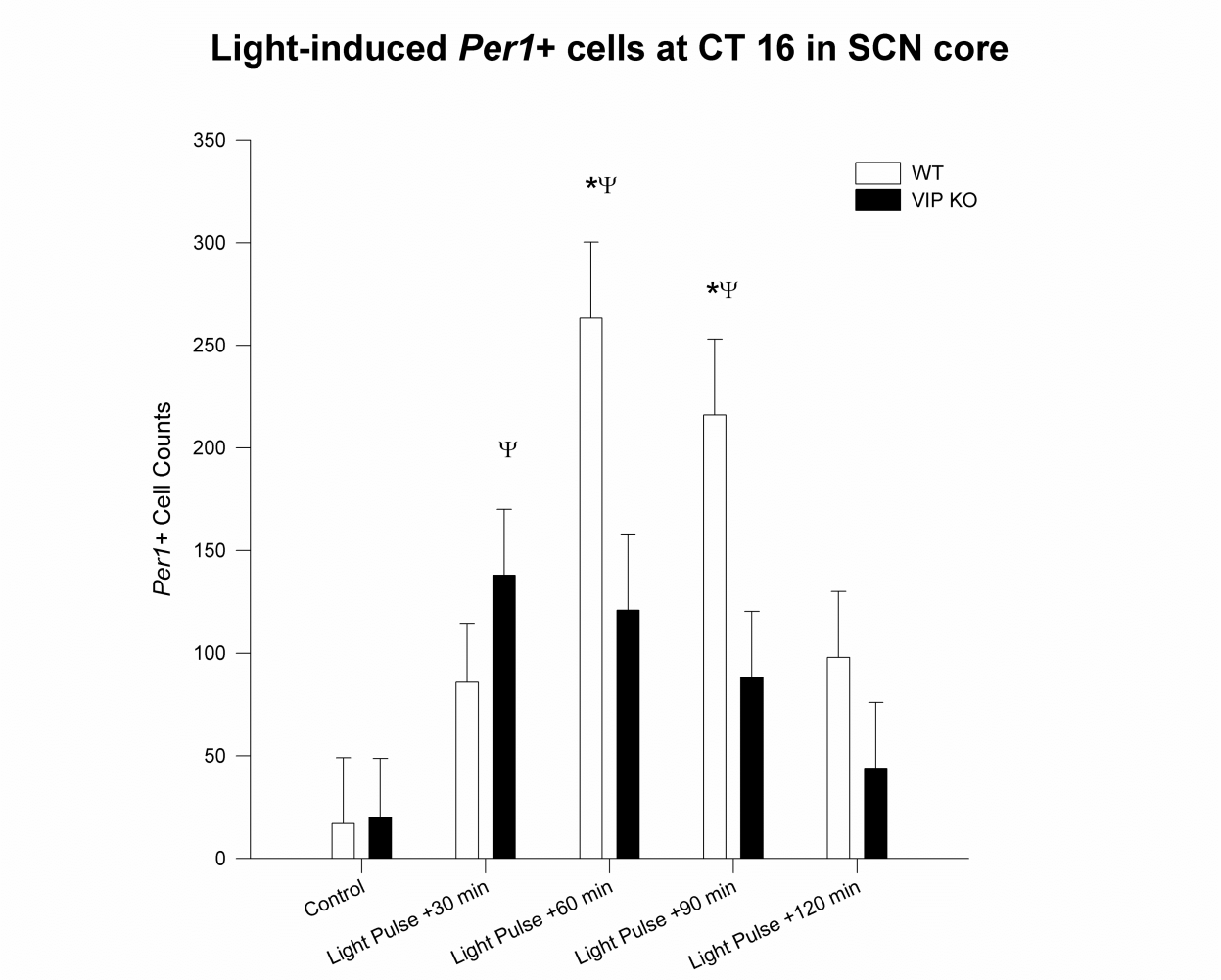

Cell counting of *Per1*+ cells in the SCN core following hybridization histochemsitry reveals that *Per1* is significantly induced by a CT 16 light pulse at 60 and 90 minutes post pulse in WT mice, but only at 30 minutes post pulse in VIP KO mice (denoted by ψ). *Post hoc* analyses reveal greater *Per1*+ cell counts in WT mice compared with VIP KO mice at both 60 and 90 minutes following the light pulse (denoted by *).

Fig. 10. *Per1*+ cell count quantification shows no *Per1* induction in the shell of VIP KO mice

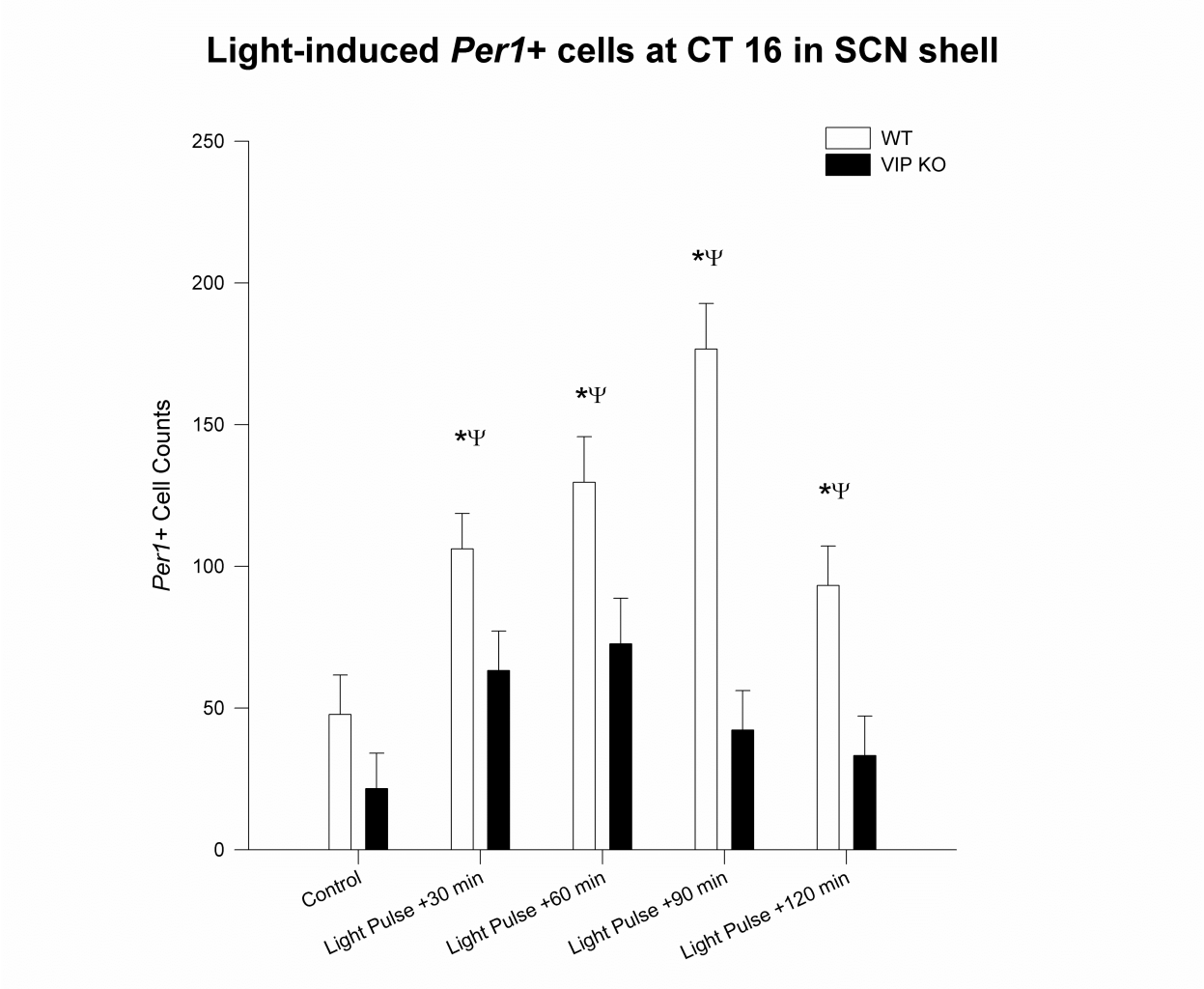

Cell counting of *Per1*+ cells in the SCN shell following hybridization histochemsitry reveals that *Per1* is significantly induced by a CT 16 light pulse at all time points measured following a CT 16 light pulse in WT mice, and not at all in VIP KO mice (denoted by ψ). *Post hoc* analyses reveal greater *Per1*+ cell counts in WT mice compared with VIP KO mice at all time points following the light pulse (denoted by *).

Fig. 11. VIP KO mice show reduced magnitude SCN c-FOS expression to a CT 16 light pulse

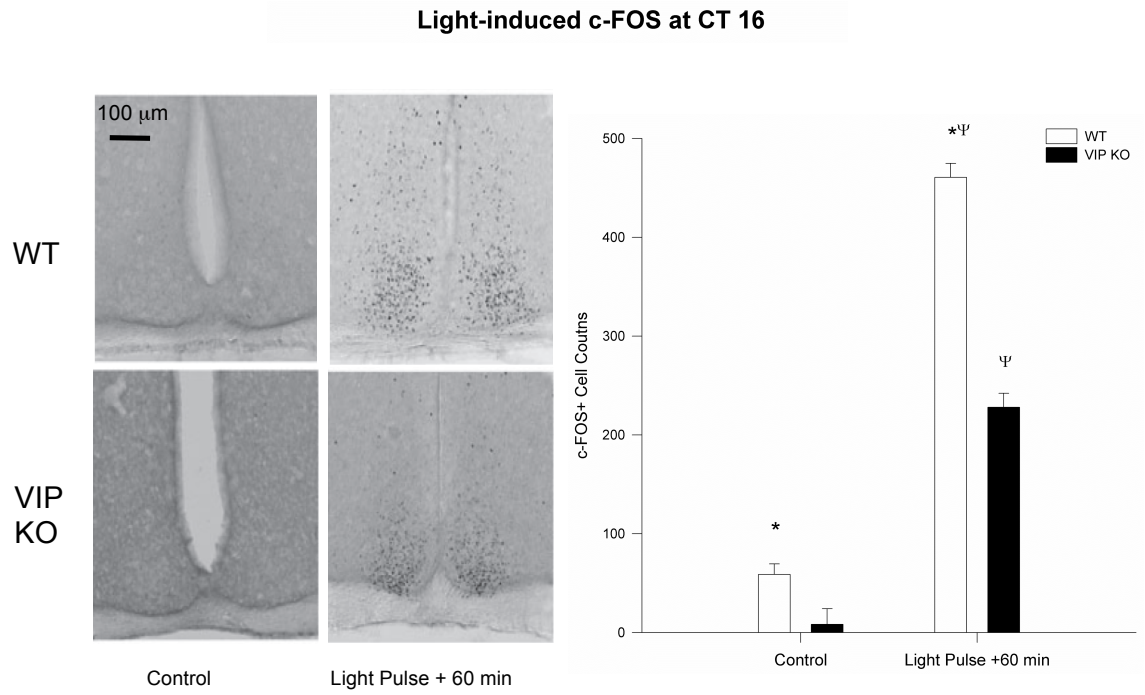

Chromogenic revelation of immunohistochemistry against c-FOS shows an induction in c-FOS protein in response to a CT 16 light pulse in both WT and VIP KO mice. (A) Photomicrographs taken from SCN in mice one hour after a 10 minute light pulse at CT 16, alongside SCN from time-matched control mice receiving no light. (B) While both WT and VIP KO mice show a significant induction of *Per1* from the light pulse compared to controls (denoted by ψ), WT mice show significantly higher levels of c-FOS compared to VIP KO mice (denoted by *).

Fig. 12. SCN c-FOS expression shows a characteristic spatio-temporal profile following a CT 16 light pulse in WT mice

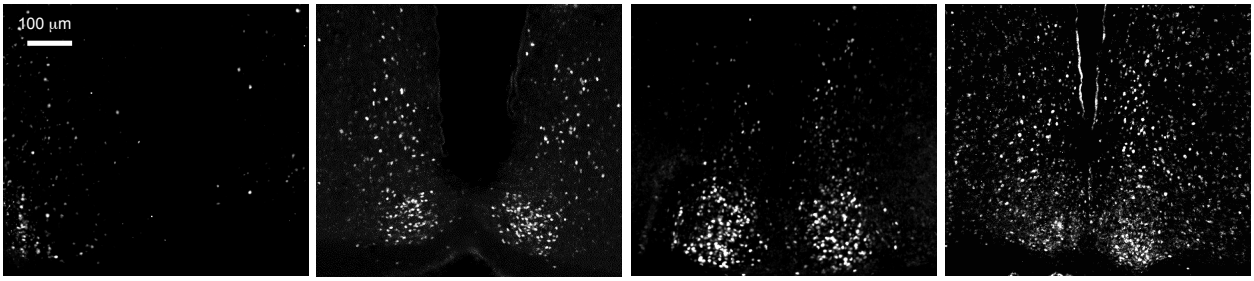

Grayscale SCN photomicrographs following immunofluorescence against c-FOS reveal a time course of induction in WT mice at CT 16. Protein expression begins to appear around 45 minutes after the beginning of the light pulse, with well-defined expression in a subpopulation of cells in the ventro-middle region of the nucleus around 60 to 90 minutes after the initial pulse. Protein expression spreads across the nucleus by 2 hours after the initial pulse.

Fig. 13. VIP is essential for sustained SCN c-FOS expression following a CT 16 light pulse

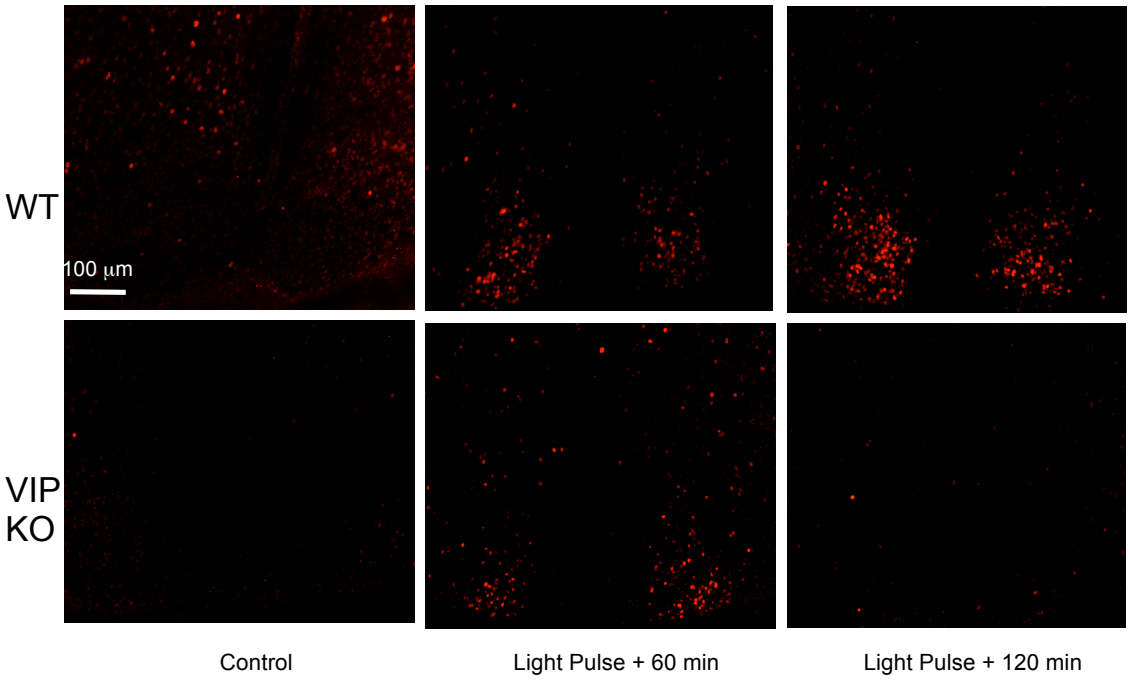

Photomicrographs from c-FOS immunofluorescence show a time course of relative protein expression in the SCN of WT and VIP KO mice following a CT 16 light pulse. There was an initial induction of *Per1* in response to the light pulse in both WT and VIP KO mice. However, only in the WT mice is this signal sustained and strongly concentrated in the ventro-middle SCN subregion.

Fig. 14. c-FOS is propagated in parallel core and shell waves in WT, but not in VIP KO mice

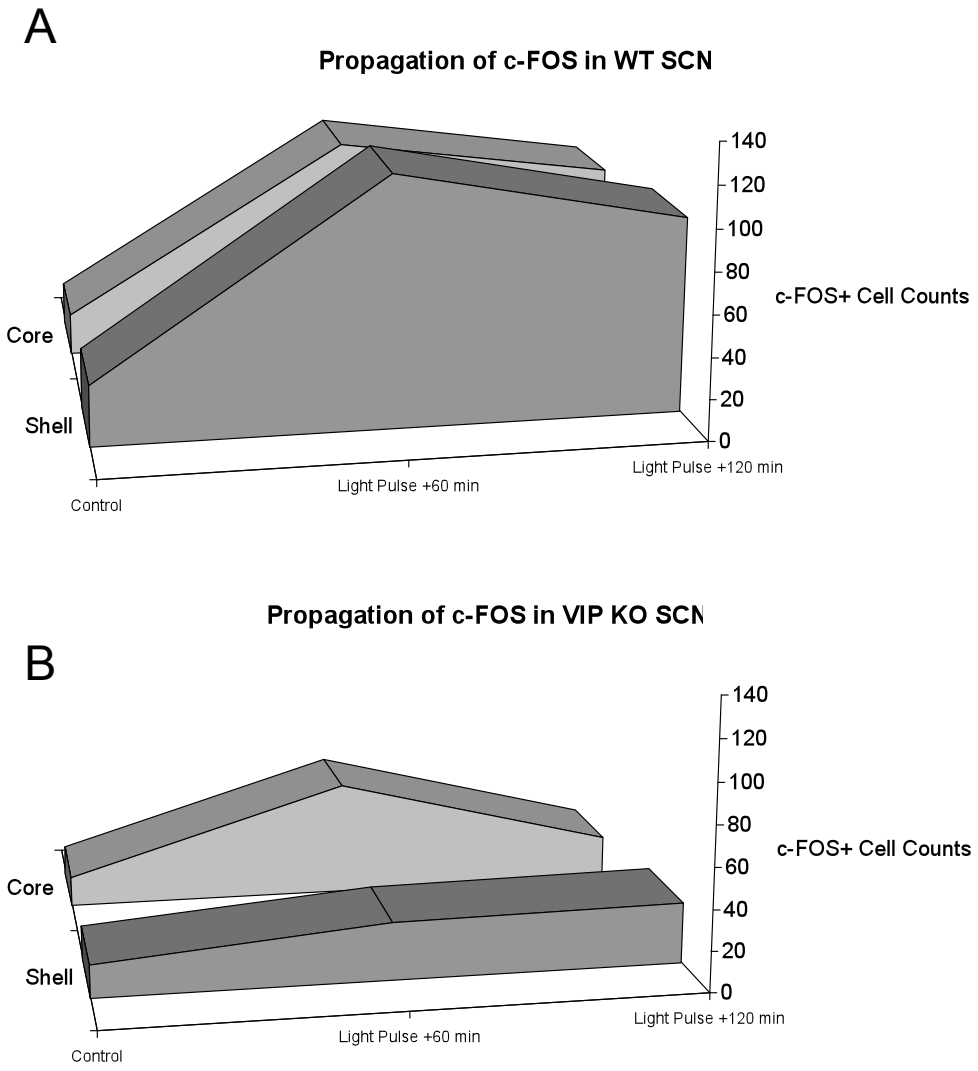

Graphical representation of c-FOS spread shows differences in signal propagation between WT and VIP KO mice. (A) After a CT 16 light pulse, WT mice show high amplitude waves of c-FOS expression in both the core and shell. (B). VIP KO mice, however, show a blunted, brief wave of c-FOS expression in the core and a near complete lack of c-FOS induction in the shell.

Fig. 15. C-FOS+ cell count quantification shows a lower magnitude c-FOS induction in the core that is not sustained in VIP KO mice

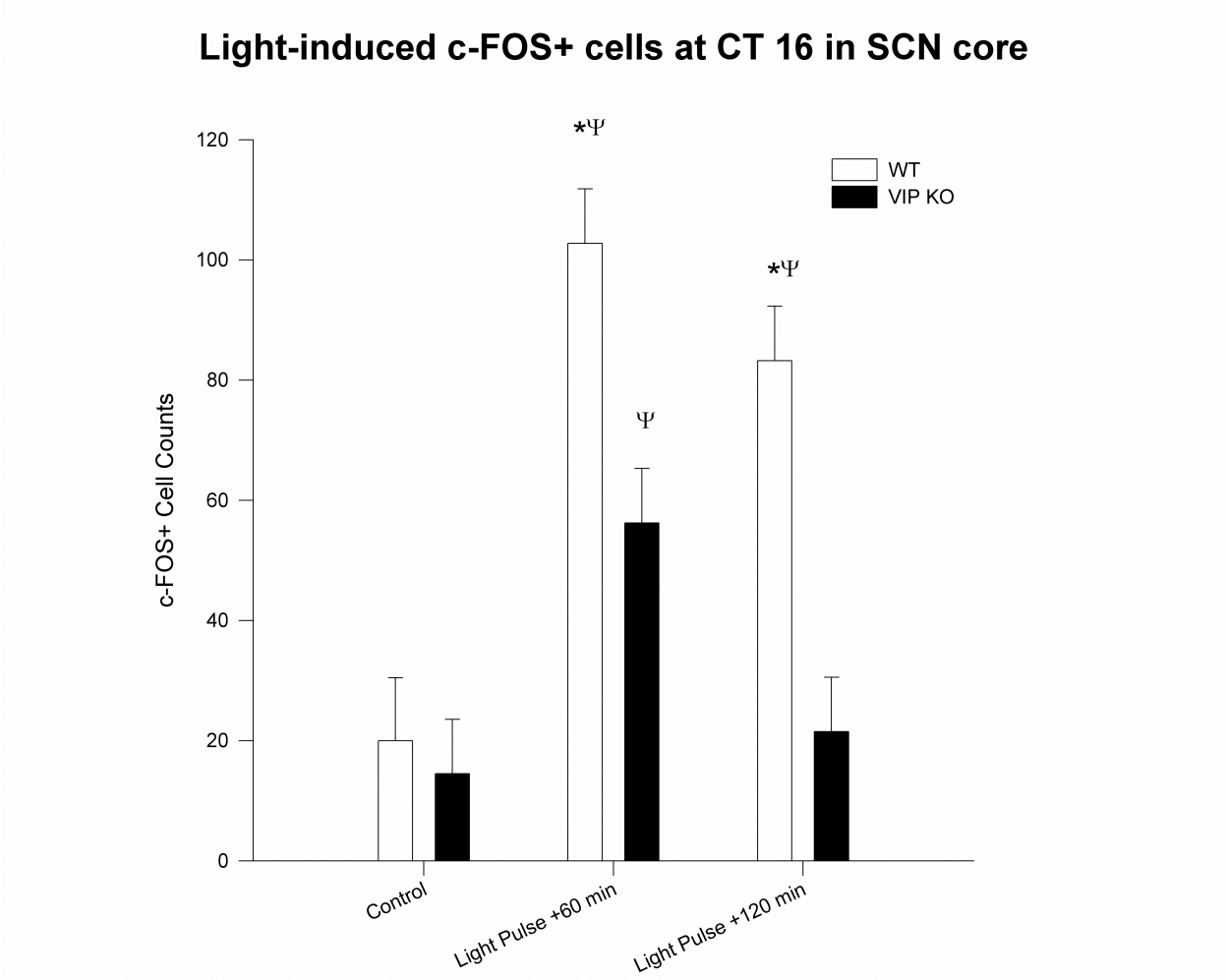

Cell counting of c-FOS+ cells in the SCN core following immunofluorescence reveals that c-FOS is significantly induced by a CT 16 light pulse at all time points measured following the pulse in WT mice, but only at 60 minutes post pulse in VIP KO mice (denoted by ψ). *Post hoc* analyses reveal greater c-FOS+ cell counts in WT mice compared with VIP KO mice at both 60 and 120 minutes following the light pulse (denoted by *).

Fig. 16. C-FOS+ cell quantification shows no c-FOS induction in the shell of VIP KO mice

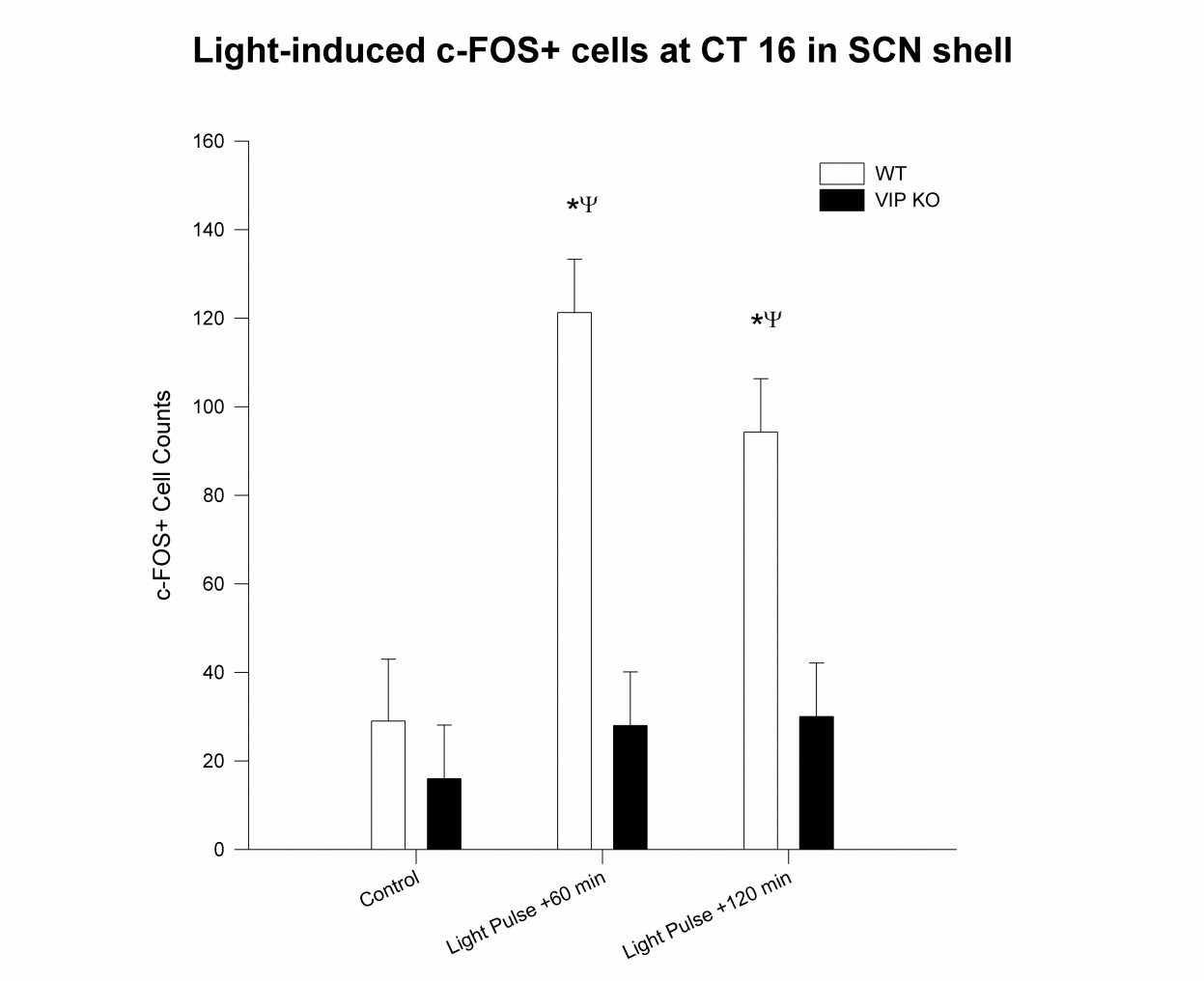

Cell counting of c-FOS+ cells in the SCN shell following immunofluorescence reveals that c-FOS is significantly induced by a CT 16 light pulse at all time points measured following a CT 16 light pulse in WT mice, and not at all in VIP KO mice (denoted by ψ). *Post hoc* analyses reveal greater *Per1*+ cell counts in WT mice compared with VIP KO mice at all time points following the light pulse (denoted by *).

Abrahamson, E.E. & Moore, R.Y. (2001) Suprachiasmatic nucleus in the mouse: retinal innervation, intrinsic organization and efferent projections. *Brain Res*, **916**, 172-191.

Akiyama, M., Kouzu, Y., Takahashi, S., Wakamatsu, H., Moriya, T., Maetani, M., Watanabe, S., Tei, H., Sakaki, Y. & Shibata, S. (1999) Inhibition of light- or glutamate-induced mPer1 expression represses the phase shifts into the mouse circadian locomotor and suprachiasmatic firing rhythms. *J Neurosci*, **19**, 1115-1121.

Albrecht, U., Zheng, B., Larkin, D., Sun, Z.S. & Lee, C.C. (2001) MPer1 and mper2 are essential for normal resetting of the circadian clock. *J Biol Rhythms*, **16**, 100-104.

Antle, M.C. & Silver, R. (2005) Orchestrating time: arrangements of the brain circadian clock. *Trends Neurosci*, **28**, 145-151.

Aronin, N., Sagar, S.M., Sharp, F.R. & Schwartz, W.J. (1990) Light regulates expression of a Fos-related protein in rat suprachiasmatic nuclei. *Proc Natl Acad Sci U S A*, **87**, 5959-5962.

Aton, S.J. & Herzog, E.D. (2005) Come together, right...now: synchronization of rhythms in a mammalian circadian clock. *Neuron*, **48**, 531-534.

Benloucif, S., Masana, M.I. & Dubocovich, M.L. (1997) Light-induced phase shifts of circadian activity rhythms and immediate early gene expression in the suprachiasmatic nucleus are attenuated in old C3H/HeN mice. *Brain Res*, **747**, 34-42.

Berson, D.M. (2003) Strange vision: ganglion cells as circadian photoreceptors. *Trends Neurosci*, **26**, 314-320.

Chen, D., Buchanan, G.F., Ding, J.M., Hannibal, J. & Gillette, M.U. (1999) Pituitary adenylyl cyclase-activating peptide: a pivotal modulator of glutamatergic regulation of the suprachiasmatic circadian clock. *Proc Natl Acad Sci U S A*, **96**, 13468-13473.

Colwell, C.S. (2010) Preventing dehydration during sleep. *Nat Neurosci*, **13**, 403-404.

Colwell, C.S. & Foster, R.G. (1992) Photic regulation of Fos-like immunoreactivity in the suprachiasmatic nucleus of the mouse. *J Comp Neurol*, **324**, 135-142.

Colwell, C.S., Michel, S., Itri, J., Rodriguez, W., Tam, J., Lelievre, V., Hu, Z., Liu, X. & Waschek, J.A. (2003) Disrupted circadian rhythms in VIP- and PHI-deficient mice. *Am J Physiol Regul Integr Comp Physiol*, **285**, R939-949.

Colwell, C.S., Michel, S., Itri, J., Rodriguez, W., Tam, J., Lelievre, V., Hu, Z. & Waschek, J.A. (2004) Selective deficits in the circadian light response in mice lacking PACAP. *Am J Physiol Regul Integr Comp Physiol*, **287**, R1194-1201.

Curran, T., Miller, A.D., Zokas, L. & Verma, I.M. (1984) Viral and cellular fos proteins: a

comparative analysis. *Cell*, **36**, 259-268.

Czeisler, C.A., Richardson, G.S., Zimmerman, J.C., Moore-Ede, M.C. & Weitzman, E.D. (1981) Entrainment of human circadian rhythms by light-dark cycles: a reassessment. *Photochem Photobiol*, **34**, 239-247.

Deurveilher, S. & Semba, K. (2005) Indirect projections from the suprachiasmatic nucleus to major arousal-promoting cell groups in rat: implications for the circadian control of behavioural state. *Neuroscience*, **130**, 165-183.

Dunlap, J.C. (2004) Kinases and circadian clocks: per goes it alone. *Dev Cell*, **6**, 160-161.

Falktoft, B., Georg, B. & Fahrenkrug, J. (2009) Calmodulin interacts with PAC1 and VPAC2 receptors and regulates PACAP-induced FOS expression in human neuroblastoma cells. *Neuropeptides*, **43**, 53-61.

Francl, J.M., Kaur, G. & Glass, J.D. (2010) Regulation of vasoactive intestinal polypeptide release in the suprachiasmatic nucleus circadian clock. *Neuroreport*, **21**, 1055-1059.

Gau, D., Lemberger, T., von Gall, C., Kretz, O., Le Minh, N., Gass, P., Schmid, W., Schibler, U., Korf, H.W. & Schutz, G. (2002) Phosphorylation of CREB Ser142 regulates light-induced phase shifts of the circadian clock. *Neuron*, **34**, 245-253.

Golombek, D.A. & Rosenstein, R.E. (2010) Physiology of circadian entrainment. *Physiol Rev*, **90**, 1063-1102.

Gooley, J.J., Lu, J., Chou, T.C., Scammell, T.E. & Saper, C.B. (2001) Melanopsin in cells of origin of the retinohypothalamic tract. *Nat Neurosci*, **4**, 1165.

Hamada, T., Antle, M.C. & Silver, R. (2004) Temporal and spatial expression patterns of canonical clock genes and clock-controlled genes in the suprachiasmatic nucleus. *Eur J Neurosci*, **19**, 1741-1748.

Hamada, T., LeSauter, J., Venuti, J.M. & Silver, R. (2001) Expression of Period genes: rhythmic and nonrhythmic compartments of the suprachiasmatic nucleus pacemaker. *J Neurosci*, **21**, 7742-7750.

Han, S., Yu, F.H., Schwartz, M.D., Linton, J.D., Bosma, M.M., Hurley, J.B., Catterall, W.A. & de la Iglesia, H.O. (2012) Na(V)1.1 channels are critical for intercellular communication in the suprachiasmatic nucleus and for normal circadian rhythms. *Proc Natl Acad Sci U S A*, **109**, E368-377.

Hannibal, J., Moller, M., Ottersen, O.P. & Fahrenkrug, J. (2000) PACAP and glutamate are co-stored in the retinohypothalamic tract. *J Comp Neurol*, **418**, 147-155.

Harmar, A.J., Marston, H.M., Shen, S., Spratt, C., West, K.M., Sheward, W.J., Morrison, C.F.,

Dorin, J.R., Piggins, H.D., Reubi, J.C., Kelly, J.S., Maywood, E.S. & Hastings, M.H. (2002) The VPAC(2) receptor is essential for circadian function in the mouse suprachiasmatic nuclei. *Cell*, **109**, 497-508.

Harrington, M.E. & Rusak, B. (1986) Lesions of the thalamic intergeniculate leaflet alter hamster circadian rhythms. *J Biol Rhythms*, **1**, 309-325.

Hattar, S., Liao, H.W., Takao, M., Berson, D.M. & Yau, K.W. (2002) Melanopsin-containing retinal ganglion cells: architecture, projections, and intrinsic photosensitivity. *Science*, **295**, 1065-1070.

Hedstrom, A.K., Akerstedt, T., Hillert, J., Olsson, T. & Alfredsson, L. Shift work at young age is associated with increased risk for multiple sclerosis. *Ann Neurol*, **70**, 733-741.

Honrado, G.I., Johnson, R.S., Golombek, D.A., Spiegelman, B.M., Papaioannou, V.E. & Ralph, M.R. (1996) The circadian system of c-fos deficient mice. *J Comp Physiol A*, **178**, 563-570.

Hoogerwerf, W.A. (2009) Role of biological rhythms in gastrointestinal health and disease. *Rev Endocr Metab Disord*, **10**, 293-300.

Hughes, A.T., Fahey, B., Cutler, D.J., Coogan, A.N. & Piggins, H.D. (2004) Aberrant gating of photic input to the suprachiasmatic circadian pacemaker of mice lacking the VPAC2 receptor. *J Neurosci*, **24**, 3522-3526.

Johnson, C.H., Elliott, J.A. & Foster, R. (2003) Entrainment of Circadian Programs. *Chronobiology International*, **20**, 741-774.

Kalsbeek, A., Perreau-Lenz, S. & Buijs, R.M. (2006) A network of (autonomic) clock outputs. *Chronobiol Int*, **23**, 521-535.

Karatsoreos, I.N. & Silver, R. (2007) Minireview: The neuroendocrinology of the suprachiasmatic nucleus as a conductor of body time in mammals. *Endocrinology*, **148**, 5640-5647.

Karatsoreos, I.N., Yan, L., LeSauter, J. & Silver, R. (2004) Phenotype matters: identification of light-responsive cells in the mouse suprachiasmatic nucleus. *J Neurosci*, **24**, 68-75.

Keller, M., Mazuch, J., Abraham, U., Eom, G.D., Herzog, E.D., Volk, H.D., Kramer, A. & Maier, B. (2009) A circadian clock in macrophages controls inflammatory immune responses. *Proc Natl Acad Sci U S A*, **106**, 21407-21412.

Kolker, D.E., Fukuyama, H., Huang, D.S., Takahashi, J.S., Horton, T.H. & Turek, F.W. (2003) Aging alters circadian and light-induced expression of clock genes in golden hamsters. *J Biol Rhythms*, **18**, 159-169.

Kornhauser, J.M., Nelson, D.E., Mayo, K.E. & Takahashi, J.S. (1990) Photic and circadian regulation of c-fos gene expression in the hamster suprachiasmatic nucleus. *Neuron*, **5**, 127-134.

LeSauter, J. & Silver, R. (1998) Output signals of the SCN. *Chronobiol Int*, **15**, 535-550.

Lewy, A.J., Lefler, B.J., Emens, J.S. & Bauer, V.K. (2006) The circadian basis of winter depression. *Proc Natl Acad Sci U S A*, **103**, 7414-7419.

Lutz, E.M., Sheward, W.J., West, K.M., Morrow, J.A., Fink, G. & Harmar, A.J. (1993) The VIP2 receptor: molecular characterisation of a cDNA encoding a novel receptor for vasoactive intestinal peptide. *FEBS Lett*, **334**, 3-8.

Maywood, E.S., O'Neill, J.S., Chesham, J.E. & Hastings, M.H. (2007) Minireview: The circadian clockwork of the suprachiasmatic nuclei--analysis of a cellular oscillator that drives endocrine rhythms. *Endocrinology*, **148**, 5624-5634.

Meijer, J.H. & Schwartz, W.J. (2003) In search of the pathways for light-induced pacemaker resetting in the suprachiasmatic nucleus. *J Biol Rhythms*, **18**, 235-249.

Michel, S., Itri, J., Han, J.H., Gniotczynski, K. & Colwell, C.S. (2006) Regulation of glutamatergic signalling by PACAP in the mammalian suprachiasmatic nucleus. *BMC Neurosci*, **7**, 15.

Moore, R.Y., Speh, J.C. & Leak, R.K. (2002) Suprachiasmatic nucleus organization. *Cell Tissue Res*, **309**, 89-98.

Morin, L.P. (2007) SCN organization reconsidered. *J Biol Rhythms*, **22**, 3-13.

Nagano, M., Adachi, A., Nakahama, K., Nakamura, T., Tamada, M., Meyer-Bernstein, E., Sehgal, A. & Shigeyoshi, Y. (2003) An abrupt shift in the day/night cycle causes desynchrony in the mammalian circadian center. *J Neurosci*, **23**, 6141-6151.

Nielsen, H.S., Hannibal, J. & Fahrenkrug, J. (2002) Vasoactive intestinal polypeptide induces per1 and per2 gene expression in the rat suprachiasmatic nucleus late at night. *Eur J Neurosci*, **15**, 570-574.

O'Neill, J.S., Maywood, E.S., Chesham, J.E., Takahashi, J.S. & Hastings, M.H. (2008) cAMP-dependent signaling as a core component of the mammalian circadian pacemaker. *Science*, **320**, 949-953.

Piggins, H.D., Antle, M.C. & Rusak, B. (1995) Neuropeptides phase shift the mammalian circadian pacemaker. *J Neurosci*, **15**, 5612-5622.

Reed, H.E., Meyer-Spasche, A., Cutler, D.J., Coen, C.W. & Piggins, H.D. (2001) Vasoactive intestinal polypeptide (VIP) phase-shifts the rat suprachiasmatic nucleus clock in vitro.

Eur J Neurosci, **13**, 839-843.

Reghunandanan, V. & Reghunandanan, R. (2006) Neurotransmitters of the suprachiasmatic nuclei. *J Circadian Rhythms*, **4**, 2.

Reppert, S.M. & Weaver, D.R. (2002) Coordination of circadian timing in mammals. *Nature*, **418**, 935-941.

Rusak, B., Guido, M.E. & Semba, K. (2002) Chapter VI Immediate-early gene expression in the analysis of circadian rhythms and sleep. In Kaczmarek, L., Robertson, H.A. (eds) *Handbook of Chemical Neuroanatomy*. Elsevier, pp. 147-170.

Saper, C.B., Scammell, T.E. & Lu, J. (2005) Hypothalamic regulation of sleep and circadian rhythms. *Nature*, **437**, 1257-1263.

Schernhammer, E.S., Kroenke, C.H., Laden, F. & Hankinson, S.E. (2006) Night work and risk of breast cancer. *Epidemiology*, **17**, 108-111.

Schwartz, W.J., Carpino, A., Jr., de la Iglesia, H.O., Baler, R., Klein, D.C., Nakabeppu, Y. & Aronin, N. (2000) Differential regulation of fos family genes in the ventrolateral and dorsomedial subdivisions of the rat suprachiasmatic nucleus. *Neuroscience*, **98**, 535-547.

Shen, S., Spratt, C., Sheward, W.J., Kallo, I., West, K., Morrison, C.F., Coen, C.W., Marston, H.M. & Harmar, A.J. (2000) Overexpression of the human VPAC2 receptor in the suprachiasmatic nucleus alters the circadian phenotype of mice. *Proc Natl Acad Sci U S A*, **97**, 11575-11580.

Shibata, S., Ono, M., Tominaga, K., Hamada, T., Watanabe, A. & Watanabe, S. (1994) Involvement of vasoactive intestinal polypeptide in NMDA-induced phase delay of firing activity rhythm in the suprachiasmatic nucleus in vitro. *Neurosci Biobehav Rev*, **18**, 591-595.

Shigeyoshi, Y., Taguchi, K., Yamamoto, S., Takekida, S., Yan, L., Tei, H., Moriya, T., Shibata, S., Loros, J.J., Dunlap, J.C. & Okamura, H. (1997) Light-induced resetting of a mammalian circadian clock is associated with rapid induction of the mPer1 transcript. *Cell*, **91**, 1043-1053.

So, W.V. & Rosbash, M. (1997) Post-transcriptional regulation contributes to Drosophila clock gene mRNA cycling. *EMBO J*, **16**, 7146-7155.

Travnickova-Bendova, Z., Cermakian, N., Reppert, S.M. & Sassone-Corsi, P. (2002) Bimodal regulation of mPeriod promoters by CREB-dependent signaling and CLOCK/BMAL1 activity. *Proc Natl Acad Sci U S A*, **99**, 7728-7733.

Travnickova, Z., Sumova, A., Peters, R., Schwartz, W.J. & Illnerova, H. (1996) Photoperiod-dependent correlation between light-induced SCN c-fos expression and resetting of

circadian phase. *Am J Physiol*, **271**, R825-831.

Van den Pol, A.N. (1980) The hypothalamic suprachiasmatic nucleus of rat: intrinsic anatomy. *J Comp Neurol*, **191**, 661-702.

Vosko, A.M., Schroeder, A., Loh, D.H. & Colwell, C.S. (2007) Vasoactive intestinal peptide and the mammalian circadian system. *Gen Comp Endocrinol*, **152**, 165-175.

Wang, H.Y., Xin, Z., Tang, H. & Ganea, D. (1996) Vasoactive intestinal peptide inhibits IL-4 production in murine T cells by a post-transcriptional mechanism. *J Immunol*, **156**, 3243-3253.

Welsh, D.K., Takahashi, J.S. & Kay, S.A. (2010) Suprachiasmatic nucleus: cell autonomy and network properties. *Annu Rev Physiol*, **72**, 551-577.

Wilsbacher, L.D., Yamazaki, S., Herzog, E.D., Song, E.J., Radcliffe, L.A., Abe, M., Block, G., Spitznagel, E., Menaker, M. & Takahashi, J.S. (2002) Photic and circadian expression of luciferase in mPeriod1-luc transgenic mice invivo. *Proc Natl Acad Sci U S A*, **99**, 489-494.

Wollnik, F., Brysch, W., Uhlmann, E., Gillardon, F., Bravo, R., Zimmermann, M., Schlingensiepen, K.H. & Herdegen, T. (1995) Block of c-Fos and JunB expression by antisense oligonucleotides inhibits light-induced phase shifts of the mammalian circadian clock. *Eur J Neurosci*, **7**, 388-393.

Yan, L., Karatsoreos, I., Lesauter, J., Welsh, D.K., Kay, S., Foley, D. & Silver, R. (2007) Exploring spatiotemporal organization of SCN circuits. *Cold Spring Harb Symp Quant Biol*, **72**, 527-541.

Yan, L. & Silver, R. (2002) Differential induction and localization of mPer1 and mPer2 during advancing and delaying phase shifts. *Eur J Neurosci*, **16**, 1531-1540.

Chapter 3

Vasoactive intestinal peptide shapes the anatomical organization of the retino-recipient circadian circuit

Introduction

The mammalian circadian system, which is hierarchically organized to track and communicate temporal information across large networks of individually oscillating cells, functions primarily by 1) ensuring that individual cells maintain the capacity to keep circadian time, and 2) providing a way for these cells to synchronize to the external environment (Davidson *et al.*, 2003). The suprachiasmatic nucleus of the hypothalamus (SCN) sits at the top of this hierarchy, receiving environmental time information via the retina and communicating temporal information through its many neural connections and diffusible signals (LeSauter & Silver, 1998). While in the past, the SCN was considered the "master pacemaker" of the circadian system (Reppert & Weaver, 2002), recent work suggests that the SCN acts more like a "master synchronizer" of rhythms (Tahara *et al.*, 2012). The most robust external force that entrains the mammalian circadian system is light (Czeisler *et al.*, 1981).

The circadian visual system utilizes two direct pathways to detect and code irradiance information from environmental light. First, like in the classical phototransduction pathway, light reaches the back of the retina to rod and cone cells, where photopigments undergo a conformational change and hyperpolarization occurs (Hubbell & Bownds, 1979). This electrical change is communicated to bipolar cells, which then send electrical output signals to adjacent retinal ganglion cells (RGCs). Axons from RGCs project to the hypothalamus, thalamus and midbrain (Hubbell & Bownds, 1979; Hattar *et al.*, 2006), releasing neurotransmitters to activate both the image forming and non-imaging forming (including circadian) visual systems.

The other (and primary) means by which light information is communicated across the circadian visual system bypasses rods, cones and bipolar cells and begins via depolarization of

intrinsically photosensitive retinal ganglion cells (ipRGCs) that contain the photopigment melanopsin (Altimus *et al.*, 2010). These ipRGCs send a dense projection to the SCN via the retinohypothalamic tract (RHT) (Hattar *et al.*, 2002), and ablation of ipRGCs results in a persistence of rhythms without the ability to properly entrain to environmental light-dark (LD) cycles (Guler *et al.*, 2008). While most effects of the circadian visual system appear to be mediated by this pathway, it is only in the absence of both pathways that mammals lose the ability to use light as a timekeeping cue to synchronize rhythms (Hattar *et al.*, 2003).

Retinal axons reach the SCN bilaterally from the ventral aspect of the nucleus, synapsing first in a region known as the retino-recipient core (Abrahamson & Moore, 2001). This region contains vasoactive intestinal peptide-expressing (VIP+) cell bodies whose axons course through the entire SCN, situating them to act as effective agents in synchronizing many SCN neurons to external cues (Abrahamson & Moore, 2001). Studies utilizing VIP-ergic agonists and antagonists suggest a major role for VIP in communicating light-based information across the SCN (see Chapter 1). We have been able to further define this role by using mice genetically deficient in VIP and studying their photically-induced gene expression phenotypes in the SCN (see Chapter 2). These data have lead us to conclude that VIP promotes the magnitude, duration and spread of cellular and molecular responses across the SCN following a phase resetting light cue (see Chapter 2).

The next step in our course of study is to determine where along the circuits in the circadian system the genetic loss of VIP contributes to the dysfunctional light responses in gene expression and behavior. A simple explanation is that the normal release of VIP and co-transmitters in response to light cues alters the membrane properties of the next set of neurons in the SCN circuit via binding to the VPAC2 receptor (VPAC2R), and the light response phenotype

in VIP KO mice results from this loss of acute signaling. The acute effects of VIP-ergic signaling in SCN neurons has been shown *in vitro*, when phase dispersed VIP KO SCN neurons could be resynchronized with acute application of a VPAC2R agonist (Aton *et al.*, 2005). However, these *in vitro* results do not necessarily replicate the physiological environment of the SCN in an intact system, and so other factors must also be considered.

Genetic loss of VIP can have indirect effects on circadian behavior and physiology through alternate pathways. For instance, VIP has been shown to affect a number of different hormones, including cortisol (or corticosterone in mice), oxytocin, prolactin and testosterone (Abe *et al.*, 1985; Bardrum *et al.*, 1987; Cunningham & Holzwarth, 1988; Lacombe *et al.*, 2007). This effect on testosterone is particularly relevant, as castrated male mice have a blunted light-induced c-FOS response, similar to VIP KO mice (Karatsoreos *et al.*, 2007). It has been posited that testosterone acts on the SCN via the androgen receptor (AR), which is expressed strongly in the core subregion. Testosterone deficiency greatly reduces AR expression in the SCN (Iwahana *et al.*, 2008), and VIP KO mice have been shown to have significantly reduced levels of testosterone (Lacombe *et al.*, 2007). Therefore, the light response deficiencies in the circadian system of VIP KO mice may be related to compromised androgen signaling.

Other important effects related to the genetic loss of VIP on the circadian system include a role for VIP in the development of anatomical substrates in the circadian visual circuit. In the spinal cord, VIP has been shown to act as a growth factor (Brenneman *et al.*, 1985), and in other neural systems, VIP has been shown to have protective effects against excitotoxicity (Kaiser & Lipton, 1990; Gressens, 1999). In the retina, the selective perinatal death of RGC axons is strongly affected by the presence of VIP (Kaiser and Lipton, 1990). VIP is normally expressed in a small subpopulation of retinal amacrine cells, and it is thought that a VIP-ergic afferent signal

helps determine the survival of RGCs that project to the brain (Kaiser & Lipton, 1990). Genetic loss of VIP could affect RGC projection to the SCN, and in this way, disrupt the light input signal to the SCN and other targets in the circadian system.

There is a body of evidence to support that VIP-ergic signaling is thoroughly entangled into the architecture and plasticity of the circadian visual system. Animals housed in constant light have significantly depressed concentrations of VIP+ cells in the SCN (Albers *et al.*, 1987). Furthermore, long light pulses cause a decrease in SCN VIP levels as well (Shinohara *et al.*, 1998). Interestingly, many of the effects of light induced changes of VIP studied to date are long-term organizational effects on expression. Animals temporarily housed under constant lighting conditions as pups have lower levels of VIP in the SCN as adults, and they also have higher rhythmic activity amplitude and more stable activity than animals reared in normal light-dark cycles or in constant darkness (DD) (Smith & Canal, 2009). Conversely, when mice have had congenitally interrupted retinal signaling due to a mutation causing anophthalmia, they show more diffuse, ectopic labeling of VIP+ cells and an overall increase in VIP+ cell expression. Therefore, the presence of retinal input appears to pattern SCN expression of VIP+ cells.

Since visual input to the SCN and VIP expression have a complex relationship, it is possible that the photic response phenotypes in VIP KO mice in Chapter 2 are related to changes in retinal signaling to the SCN. Alternatively, VIP may play an important role in organizing connectivity within the SCN, if VIP has a role in promoting neuronal survival and postsynaptic pruning during development. Thirdly, VIP loss may be indirectly affecting photic signaling in the SCN via another pathway. Finally, it is possible that the photic response in VIP KO mice results only from acute effects of VIP transmission via paracrine or synaptic mechanisms. We sought to examine each of these possibilities by using tract tracing, Golgi impregnation, and

immunohistochemistry to examine neuronal characteristics related to connectivity along different points of the circadian visual pathway. In the following studies, we track anatomical differences between WT and VIP KO mice at the levels of retinal afferents, the SCN core and shell, and across the SCN rostro-caudal axis in order to begin explaining the mechanisms by which VIP deficiency leads to dysfunction in circadian light responses.

Materials and Methods

Animals

Adult male (2-5 months) WT C57Bl/6 mice, mice lacking the gene encoding for the neuropeptides VIP and peptide histidine isoleucine (PHI), and both WT and VIP KO mice crossed with *mPer2*^{luc} reporter mice were obtained from a breeding facility at the University of California, Los Angeles. Because *mPer2*^{luc} crossing into either WT or VIP KO lines did not affect circadian behavioral phenotypes, nor did it affect anatomical differences between WT and VIP KO mice, mice were grouped and analyzed as either 'WT' or 'VIP KO,' irrespective of whether or not they were also crossed with the *mPer2*^{luc} line. Tissue obtained from animals used for experiments in Chapter 2 was also used for androgen receptor (AR) and neurofilament medium chain (NF-M) experiments (see below) in the current set of studies. Other tissue was taken from experimental mice that were housed 1-4 animals/cage and kept in 12:12 h light-dark (LD) for at least 2-3 weeks before collection. All collections took place during the light phase.

For immunofluorescence studies, WT and VIP KO mice were culled under isoflurane anesthesia, their brains removed and frozen, slide mounted at 20 μM, and then refrozen until

immunofluorescence was to be performed. A total of 14 mice were used for AR experiments (*n* = 7 WT, *n* = 7 VIP KO) and10 mice were used for NF-M experiments (*n* = 5 WT, *n* = 5 VIP KO). For 1,1'-dioctadecyl-3,3,3'3'-tetramethylindocarbocyanine perchlorate (DiI) experiments, brains were removed and placed in 1.5% paraformaldehyde for 4 hours at 4°C. Brains were then rinsed in phosphate buffered saline (PBS) before DiI crystal placement (described below). A total of 8 brains were analyzed for DiI experiments (*n* = 3 WT, *n* = 5 VIP KO). For Golgi impregnation experiments, brains were removed, briefly rinsed in deionized water, and placed in impregnation solution according to FD Rapid GolgiStain^{TM} kit instructions (FD NeuroTechnologies, Columbia, MD). A total of 11 brains were used for Golgi impregnation (*n* = 5 WT, *n* = 6 VIP KO).

Small silastic capsules (internal diameter: 1.57 mm, outer diameter: 2.41 mm) filled with 5 mm of 4-androsten-17β-OL-3-ONE (Steraloids Inc., Newport, RI) were implanted subcutaneously under isoflurane anesthesia in 2 adult male VIP KO mice for testosterone supplementation and behavioral analysis. Following surgery, animals were monitored and left to recover for 1 week. Afterwards, mice were housed in individual running wheels, and their wheel-running activity was recorded as revolutions per 3 minute interval. Mice were exposed to 12:12 LD for 12 to 14 days (light intensity ≈ 700 lux) and placed into constant dark (DD) for 7-14 days to assess their free-running activity patterns. Running wheel activity records from mice used in experiments described in Chapter 2 were used for comparison. Experimental protocols used in this study were approved by the UCLA Animal Research Committee, and all recommendations for animal use and welfare, as dictated by the UCLA Division of Laboratory Animals and the guidelines from the National Institutes of Health, were followed.

DiI tract tracing

Following light fixation and brief PBS rinsing, brains were blotted dry and optic nerves were bilaterally severed at a 45° angle with iris scissors 1-2 mm rostral to the optic chiasm under a dissecting microscope. DiI crystals (Molecular Probes, Inc., Eugene, OR) collected with the tip of a glass electrode were distributed between each optic nerve slit so that crystals only came into contact with the severed optic nerve surfaces. Brains were placed on their dorsal surface, incubated in a small amount of PBS with 0.01% sodium azide, protected from light and stored at 37°C for 3 weeks. Brains were then embedded in agarose and coronally sliced on a vibratome at 100 μM, slide mounted, and kept, covered, at 4°C until imaged.

Fluorescence images were obtained using a Zeiss Apotome microscope with AxioVision software. Unilateral SCN images were taken across a z-stack through the rostro-caudal focal axis and visualized for reproduction with the software's maximum intensity projection (MIP) command. For analysis of area, Image J software was used to threshold each grayscale image and remove background light based on fluorescence signal within the SCN. The area of fluorescence was then calculated by measuring the area occupied by continuous pixels falling within threshold values.

Sholl-like analysis was carried out by first creating template concentric circles that were superimposed on unilateral SCN images. These circles were centered at a point where RHT axons emerged *en masse* from the chiasm, and they were consistently placed at the same relative area for each image. These circles encompassed nearly the entire dorso-ventral axis of the SCN, and circles at Sholl levels '3' through '6' delineated a reliable range at which individual axons could be separated from each other. Axonal processes that crossed each Sholl level were counted blind to genotype and confirmed by z-stack reference.

NF-M and AR immunofluorescence

Brains were collected and processed as described previously. Prior to immunostaining, sections were fixed in 4% paraformaldehyde at room temperature, washed with PBS, and incubated in blocking solultion (3% normal goat serum (NGS) and 0.1% Triton X-100 in PBS). After blocking, sections were incubated with a rabbit polyclonal antibody raised against androgen receptor (AR) (Santa Cruz Biotechnology, Santa Cruz, CA) diluted to 1:150 in blocking solution at 4^{o}C for 5 days, or a mouse monoclonal antibody raised against medium chain neurofilament (NF-M) (Sigma-Aldrich, Milwaukee, WI) diluted to 1:10,000 in blocking solution at 4^{o}C for 2 days. Sections were then washed and incubated with Cy3-conjugated secondary antibody (Jackson ImmunoResearch Laboratories Inc., West Grove, PA), diluted to 1:200 (in the case of anti-AR), or Cy2-conjugated secondary antibody (Jackson ImmunoResearch Laboratories Inc., West Grove, PA) diluted to 1:400. After incubation with secondary antibody, sections were again washed with PBS, coverslipped with Vectashield Mounting Media containing 4',6-Diamidino-2-Phenylindole, Dihydrochloride (DAPI, Vector Laboratories, Burlingame, CA), and stored in the dark at 4^{o}C until imaged. Images from AR-immunostained sections were taken to optimize the signal to noise ratio of fluorescence signal in each section. Images from NF-M immunostained sections were taken with equal exposure parameters across both genotypes on sections used within the same run.

Golgi impregnation

Golgi impregnation utilized the Golgi-Cox method, which employs the random deposition of metallic mercury among cells to be later developed as a color product by an oxidation reaction. The current study employed the FD Rapid Golgistain^{TM} kit (FD Neurotechnologies, Baltimore, MD) to label neurons. Briefly, after brains were collected, they were rinsed in deionized water and placed in a Golgi-Cox solution containing potassium dichromate, mercuric chloride and potassium chromate that was protected from light. Solution was changed after 24 hours, and brains were left to incubate away from light at RT for another 2 weeks. Following incubation, brains were embedded in agarose, coronally sliced on a vibratome at 100 μM, slide mounted, developed with color reactants, counterstained with cresyl violet, and dehydrated in ethanol. When sections dried, they were coverslipped and protected from light at 4^{o}C until imaged.

Images were obtained using a Zeiss Apotome microscope with AxioVision software. Individual neuron and cluster images were taken across a z-stack through the rostro-caudal focal axis and visualized for reproduction with the software's extended focus command. This allows for the sharp images of each z-plane to be combined into a 2D image that appears focused throughout. Images were taken at the rostral, mid and caudal SCN regions. In the mid SCN, core and shell were determined based on a standardized template overlaid on the section. For analysis of cell classification, cells were first defined according to criteria described in van den Pol (1980). Each neuron was examined across its z-stacks in order to properly identify its characteristics.

Quantification and statistical analysis

In the case of Sholl-like analysis and soma-to-soma appositions, data were analyzed by a

two-way analysis of variance (ANOVA). If significant group differences were detected ($p < 0.05$), then the Holm–Sidak method for pair-wise multiple comparison was used. For DiI area analysis, and AR+ cell counts, data were analyzed via a student's *t*-test. Finally, for neuronal subtype distributions, data were analyzed by multiple logistic regression. For all tests, values were considered significantly different if $p < 0.05$. All parametric tests were performed using SIGMASTAT (version 3.5, Systat Software, San Jose, CA, USA) and all non-parametric tests were performed using SPSS (version 20, IBM SPSS Inc., Chicago, IL). When standard errors are appropriate, values are shown as mean ± SEM.

Results

SCN retinal afferent anatomy is affected by VIP

We first used DiI tract tracing to analyze, in detail, the differences between retinal axon terminals in the SCN of WT and VIP KO mice. DiI implantation to the optic nerves stains only a small subset of RHT axons, but this sparse expression, along with the complete axonal tracing conferred by the lipophilic behavior of DiI, specifically allows for the measurement of fine differences in axon terminals.

In VIP KO mice, there was successful DiI tracing in ≈ 80% of the optic nerves implanted. In WT mice, ≈ 40% of optic nerves implanted resulted in successful DiI tracing. Success was determined by an ability to identify single neurons among clusters from the ventro-lateral aspect of the SCN under high power (40X) magnification using either epifluorescence or Apotome-based microscopy.

In both WT and VIP KO mice, the vast majority of retinal afferents entered the SCN in a highly ordered fashion, from the optic chiasm into the ventro-lateral aspect of the SCN at the mid and mid-posterior levels of the nucleus along its rostro-caudal axis (Fig. 1). There was very sparse labeling in the anterior SCN. Nearly all retinal axons terminated in the middle-most region of the SCN, coinciding with what is most likely the SCN core (based on optic chiasm and other peri-SCN landmarks). Some axon terminals extended beyond the putative core and extended either dorsally or laterally into the SCN shell (Fig. 1). This occurred in both WT and VIP KO brains. A few retinal axons also coursed outside of the SCN and appeared to terminate in other hypothalamic areas adjacent to the SCN.

The mid SCN area innervated by the RHT did not appear to differ between WT and VIP KO mice ($p = 0.19$). Although the area of innervation did not appear to differ between the two genotypes, images suggested a brighter tracer signal from VIP KO compared to WT mice. This could have been due to either: 1) differences at a more subtle level of analysis, such as in number of fine branching terminals within the SCN, or 2) differences in axonal size or makeup between the two genotypes. A third possibility is a difference in initial tracer placement, but this is less likely in that DiI crystal placement was done blind to genotype. Both of the first two possibilities are addressed below.

High power images of SCN were super-imposed with concentric circles centered at the middle-most point where RHT axons emerged from the optic chiasm to implement a Sholl-like analysis that measured retinal branching complexity within the SCN (Fig. 2A). Two-way ANOVA revealed an increase in branching complexity in VIP KO compared to WT mice ($p = 0.028$), but there were no significant effects on Sholl-level ($p = 0.42$) nor an interaction effect of genotype and Sholl-level ($p = 0.92$).

Although the number of retinal branches terminating in the SCN was relatively increased in VIP KO mice, it is also possible that there were differences in axon composition between genotypes, resulting in different tracing profiles. This could be related to the different success rates of DiI tracing in WT and VIP KO mice. In order to investigate this possibility, sections of mouse SCN (collected from experiments in Chapter 2) were subjected to immunofluorescent staining of NF-M, a major molecule in axonal architecture.

Compared to surrounding brain regions, the SCN only lightly expresses NF-M. In the mid SCN of both WT and VIP KO mice, there were long, patterned axonal clusters stained in the dorsal-most region that extended dorsally toward the hypothalamic subparaventricular zone (SPVZ) (Fig. 3). In the ventral-most SCN, small, punctuate clusters expressing NF-M were scattered just dorsal to the optic chiasm, often concentrated around its medial aspect. The middle region of the mid SCN, which predominantly consists of the SCN core, was largely devoid of NF-M staining in both genotypes (Fig. 3). There was heterogeneity in expression of NF-M across rostro-caudal SCN slices, with mid SCN showing consistently the phenotype described above.

In coronal sections, VIP KO mice expressed a particularly robust NF-M signal in the SCN and adjacent structures compared to WT mice. There also were specifically noticeable differences in NF-M expression in the dorsal region of the SCN. Here, WT mice expressed thin, filamentous, vertically-oriented clusters (Fig. 3). In 4 out of 5 VIP KO mice, however, these clusters appeared wider and also had more variability in their orientation, oftentimes coursing laterally rather than dorsally (Fig. 3). The remaining VIP KO mouse appeared similar to the other WT mice in its NF-M expression of the dorsal SCN, but it had particularly long vertically-oriented clusters compared to all other animals.

SCN core organization is affected by VIP

Following RGC axon terminal analysis, the retino-recipient SCN core was then examined as a next target along the circadian visual pathway. To analyze core differences in WT and VIP KO mice, we used AR immunofluorescence to determine if typical core chemoarchitecture differed between genotypes. Unilateral cell counts evaluated by a student's *t*-test revealed that the SCN of WT mice have nearly twice as many AR+ cells as VIP KO mice (Fig. 4). AR expression is confined to the same subregion in each genotype (the ventro-middle aspect of the mid SCN), but the number of AR+ cells is significantly decreased in VIP KO mice.

Since VIP KO mice are known to have low levels of testosterone (Lacombe *et al.*, 2007), we implanted VIP KO mice with testosterone to supplement levels. Following implantation, light entrainment was monitored in WT, VIP KO and VIP KO + testosterone mice. While WT mice showed an activity onset predicted by the previous LD cycle when released into constant conditions, both VIP KO and VIP KO + testosterone mice showed similarly abnormal entrainment to the previous LD cycle, with a phase advance in activity onset between 8 and 10 hours (Fig. 5). Thus, testosterone supplementation alone was not sufficient to restore this particular light-based deficiency in VIP KO mice.

SCN morphological substrates of intercellular communication

We then used Golgi impregnation for analysis of SCN neuron morphological characteristics in order to infer differences in structure related to intercellular communication. As is the case with DiI, Golgi impregnation only fills a small subset of SCN neurons, but usually

does so completely, providing fine, cellular detail. A total of 267 Golgi impregnated neurons were analyzed across the SCN rostro-caudal axis (WT: 140 neurons, VIP KO: 127 neurons).

The neuronal cell soma ranged similarly in shape and size in both genotypes. These soma appeared along a spectrum of morphologies containing three basic shapes: 1) rounded, 2) oblong, or 3) semi-rounded with numerous protrusions (see Figs. 6, 8-11). Most oblong soma were smooth and did not contain spines or protuberances. The semi-rounded cells, on the other hand, expressed a diverse mix of spines and protrusions. These included long, thin 'lollipop'-like spines, shorter stump-like spines, and long and thin filamentous spines. The surface areas of the soma ranged from ≈ 100-300μm^2.

Throughout the SCN, there were many clusters of neurons that appeared to make soma-to-soma contact with each other in groups of 2-5 (Fig. 6). In addition to neuron-to-neuron contact, many of these clusters included other impregnated parts of cells that appeared non-neuronal, such as glial (smaller cell body) and vascular (very thick processes) in origin. Two way ANOVA revealed no effect of genotype ($p = 0.70$), rostro-caudal axis ($p = 0.77$), or interaction effects ($p = 0.95$) on the number of soma-to-soma clusters found per section (Fig. 7.) Since there were small numbers of clusters in the mid SCN, analyzing core to shell distribution differences in genotypes was not feasible.

Golgi impregnated axons are not highly visible in SCN neurons, possibly in part because SCN axons are much shorter and thinner than SCN dendrites (Fig. 8). In both WT and VIP KO mice, axons were found to be about half the thickness as dendrites from the same neurons, and they extended only ≈ 10 μm from the soma in the plane of the reconstructed photomicrograph (Fig. 8). While axons arising from SCN neurons appear highly localized close to the soma, axons from outside the SCN have been reported at a variety of sizes, including those that are much

wider and course along much larger distances (Van den Pol, 1980). Indeed, our SCN show a number of "orphan" processes that travel through the nucleus, and these could be axons originating from outside the nucleus (Fig. 8). Because the nature of these processes was unknown, they were not further compared across the two genotypes.

Dendrites are the most visualizable feature of SCN neurons due to their thickness and reach across the nucleus. In the mid SCN, impregnated neurons showed that long, dendritic processes reached into the SCN around its core from neuronal soma distal in the shell (Fig. 8). Other long dendritic processes outline the boundaries of the SCN, both coursing dorso-ventrally along its oblong sides and curling around to trace the dorsal and ventral boundaries of the nucleus.

Unlike in other structures, dendritic morphology of the SCN (or the hypothalamus in general) does not easily distinguish neurons as has been the case in such areas as the cerebellum, striatum, or cortex. However, there have been a few attempts at classification schemes created in the past, the most comprehensive of which comes from work in the rat SCN and divides neuronal subtypes into five different categories (Van den Pol, 1980). Golgi impregnated neurons revealed a similar classification scheme of these five subtypes in our study of the mouse SCN as well. These classifications are: monopolar, simple bipolar, curly bipolar, radial multipolar, and spiny. The terms monopolar, bipolar and multipolar are in reference to the total number of dendrites and not to the total number of processes.

There were very few monopolar neurons found in the SCN of both WT and VIP KO mice. These neurons sometimes had a dendritic bifurcation close to the soma that made them appear bipolar in nature. Monopolar neurons had some spines around their soma and dendrites, but comparatively, spines were only lightly expressed. Monopolar neurons also tended to have soma

that were rounder than they were oblong (Fig. 9A).

Simple bipolar neurons were common throughout both genotypes. These tended to be long and thin, both in terms of processes and soma. Simple bipolar neurons expressed spines rather sparsely. Although most simple bipolar neurons were uniformly long and thin (Fig. 9B), some bipolar neurons also had somewhat rounded soma.

Curly bipolar neurons were the most common neuronal subtype found in the SCN of both WT and VIP KO mice. The major distinguishing characteristic of these neurons from simple bipolar neurons is that their processes appear to curl or travel perpendicular to each other (Fig. 9C). Additionally, curly bipolar neurons tended to have higher expression of spines and rounder soma than simple bipolar neurons. Because of the lower number of processes and spines in curly bipolar, simple bipolar and monopolar neurons, these three categories of neurons were further pooled and classified as having 'simple' connectivity.

There were also very few radial multipolar neurons found among the SCN of each genotype. These neurons were so named due to their appearance, in which at least 3 dendritic processes arose out of a central soma, oftentimes equilaterally (Fig. 10A). Not all of these neurons were uniformly radial, but were classified as such to maintain continuity with the classification scheme of van den Pol. The soma of this type of neuron was generally round.

The last group classified, the spiny neurons, were so named because of their heavy spine expression along the dendrites and soma. These neurons were relatively common in the SCN of both genotypes. The spiny neurons had the greatest heterogeneity in the number and directionality of their dendritic processes (Fig. 10B). Furthermore, although most spiny neurons had round soma, a round cell body was not a pre-requisite for this classification. Because of the higher number of processes and spines found in the radial multipolar and spiny neurons, these

two categories were pooled and further classified as having 'complex' connectivity.

SCN distributions of these five neuronal subtypes were very similar across the rostro-caudal axis in both WT and VIP KO mice (Fig. 11). Multiple logistic regression showed no statistically significant effects of genotype on simple vs. complex neuronal expression ($p = 0.99$). Furthermore, there were no statistically significant effects of rostro-caudal level ($p = 0.64$), nor an interaction effect of genotype and level, on neuronal subtype expression ($p = 0.21$).

SCN distribution of simple and complex neurons also showed similar profiles across the core and shell in WT and VIP KO mice (Fig. 12). Multiple logistic regression showed no statistically significant effects of genotype on simple vs. complex neuronal expression ($p =0.44$) nor of an interaction effect between genotype and level ($p = 0.42$). However, there was a statistically significant effect of shell-core distribution of neuronal subtype ($p = 0.037$).

Discussion

In this set of studies, we investigated how VIP deficiency affects the anatomy of the SCN network involved in the light response pathways necessary for environmental light-dark synchronization. Since VIP KO mice exhibit impaired photic entrainment and phase shifting responses, we sought to find out how genetic loss of VIP can alter structure and morphology: from afferents in circadian visual input pathways through the local circuitry within the SCN. In this way, we aimed to uncover a role for VIP in the circadian system involving long-term effects in an anatomical area that is rarely studied from a developmental perspective.

Our experiments suggest that there are, in fact, differences in the organization of the circadian visual system arising when VIP is absent ubiquitously and congenitally. Specifically, it

appears that: 1) both RHT axons and other SCN axons have altered organization when VIP is absent, 2) chemoarchitecture of the SCN core is altered when VIP is absent, and 3) dendritic and somatic correlates of SCN connectivity are not affected by VIP absence. This is the first set of morphological studies to report any anatomical changes in the SCN in response to the genetic loss of VIP. These findings will provide useful targets to understand mechanisms underlying how anatomical changes can result from VIP deficiency, and also examine how these changes can further affect physiological and behavioral circadian phenotypes.

Both RHT axons and other SCN axons have altered organization when VIP is absent

Through using both DiI tract tracing and NF-M immunostaining, we show that axonal organization is altered in the circadian system that is lacking VIP (Figs. 2, 3). Tracing retinal ganglion cell terminals in the SCN provided a means to study how the number of neurotransmitter release sites (and possibly synapses) was altered in the SCN of VIP KO mice. The lack of an overall change in area of retinal innervation fits with the observation that light-induced *Per1* and c-FOS expression in VIP KO mice persists in the retino-recipient regions of the SCN (Fig. 1; Chapter 2 Figs. 9, 15). However, this response is blunted, and this could be explained, in part, by a change in the number of RHT terminal branches.

For branching studies, the DiI tracing technique is ideal because only some neurons take up the dye, and DiI-lined axon terminals are clearly visible at the level of a single branch. Because this method is not normally used to trace RHT innervation of the SCN, the finding that successful tracing was found in half as many WT as VIP KO mice had not been previously documented. The most commonly used tracing method to look at RHT innervation is cholera

toxin, but for the sake of studying branches, cholera toxin results would be difficult to measure due to its lack of fine, spatial detail. Each technique has its own characteristic properties which are advantageous for tracing the retinal pathways. For one, cholera toxin is actively transported in living cells, rather than passively diffused like DiI in postmortem tissue. In this way, it would be less affected by variables such as axon caliber, than would passive diffusion. If factors that affected diffusion were related to the differences in tracing success rate, data from cholera toxin injections would provide useful clues to determine the source of RHT differences in WT and VIP KO mice.

Effects on RGC survival by pharmacologically blocking VIP have been documented in the past *in vitro* (Kaiser & Lipton, 1990). This model suggests that VIP found in some amacrine cells regulates the postsynaptic survival of RGCs by a use-dependent mechanism. In our experiment, a decrease in the total number of axons was not observed, as inferred by the similar terminal retinal innervation area in the SCN of WT and VIP KO mice. However, the increased number of axonal branches (Fig. 2) in VIP KO mice seems opposite to what would be expected if VIP were a neurotrophic or neuroprotective signal for RGCs. These differences in the action of VIP may result from *in vivo* vs. *in vitro* paradigms as well as pharmacological vs. genetic manipulation.

Interestingly, in sympathetic ganglionic neurons, VIP has been shown to inhibit dendritic growth via acting on the PAC1 receptor (PAC1R) (Drahushuk *et al.*, 2002). The PAC1R is also expressed in RGCs (Seki *et al.*, 2000), and so it is feasible that VIP could act to inhibit neuronal growth, and in this way, its absence would permit the increased branching found in VIP KO mice. While VIP-ergic signaling through the PAC1R was shown to be specific to dendritic growth and not to axonal growth, this study did not specifically look at terminal branching, where effects of

total axon number could conceivably exist independently of branching complexity.

Functionally, the finding that increased retinal terminal branching is found in the VIP KO mouse SCN is unexpected, as RHT axons are excitatory and would most likely have action potential generating effects in postsynaptic SCN cells. In a simple model, increased glutamatergic release from RHT axons activated by a light pulse should elicit higher c-FOS and *Per1* responses. As just the opposite appears true, there must be some other mechanism that can account for this discrepancy. One possibility is that with increased branching, there is increased glutamatergic tone at the synapse, and thus in VIP KO mice, there could be a lower signal to noise ratio of excitatory input that actually blunts c-FOS and *Per1* responses when a phase resetting light pulse occurs. In order to test this idea, mircodialysis with HPLC or glutamate biosensors could be used to track glutamatergic levels around the SCN following a light pulse. Electrophysiological studies could also be carried out to determine the resting membrane potential of SCN core neurons, the effects of tonic glutamate on this resting membrane potential, and the responses of these neurons to a pharmacological 'light pulse' of NMDA.

In these experiments, not only was branching complexity modestly increased, but NF-M-immunoreactivity was increased as well (Fig. 3). NF-M is a 160kDA subunit of neurofilament, an intermediate filament specific to neurons that provides structure for the cytoskeleton and promotes axonal growth (Al-Chalabi & Miller, 2003). Neurofilament is comprised of subunits formed by heavy and light chain neurofilament (NF-H and NF-L) combinations, or medium and light chain neurofilament (NF-M and NF-L) combinations (Al-Chalabi & Miller, 2003). Qualitatively, there was a stronger NF-M signal in all sections from VIP KO mice, which were run in parallel and their images were taken at the same exposure as in WT mice. Furthermore, this difference appeared both within and outside of the SCN. These results need to be further

quantified by western blot and compared with relative expression levels of NF-H and NF-L. Furthermore, in order to address questions of individual axon caliber changes, electron microscopy studies would be needed. These experiments will be important for showing how VIP deficiency affects axonal organization both within the SCN and in other brain regions.

It is also worth noting that the orientation of VIP KO axons appears more variable than in WT mice. If axons are misrouted, then both the behavior and gene expression phenotypes we observe in response to light resetting may be explained by a mis-wired circuit. In terms of the ventral aspects of the SCN, where retino-recipient axons would be important for conveying visual information to shell neurons, there were not robust differences in NF-M expression. It was only in the dorsal part, where the SCN is either receiving afferent signals, or more likely, sending output signals from its robust oscillatory neurons. Thus information coming from shell neurons might be specifically sensitive to the loss of VIP, and this might account for the specific deficiencies in shell *Per1* and c-FOS expression in response to photic cues found in VIP KO mice.

Chemoarchitecture of the SCN core is altered when VIP is absent

Our analysis of AR expression found a clear difference in AR+ cell counts in the SCN core, with VIP KO mice having about 60% of the levels that WT mice express (Fig. 4). This difference has a number of implications. First, it suggests that the cell signaling that occurs in the WT mouse core differs from that of the VIP KO mouse. AR is a nuclear receptor hormone that, upon binding by testosterone, translocates to the nucleus and binds to androgen response elements to initiate transcription (Janne & Bardin, 1984). *Per1* contains an androgen response

element in its promoter region and *Per1* expression increases in response to activated AR (Gery & Koeffler, 2010), and so it is quite possible that androgen signaling deficits could be related to the VIP KO phenotype in gene expression. Another pathway by which AR acts is via a non-DNA binding route where the AR receptor activates mitogen-activated protein kinase (MAPK) and the subsequent phosphorylation of cyclic-AMP response element binding protein (CREB) at ser133 (Fix *et al.*, 2004). In this state, pCREB can initiate the transcription of both *c-fos* and *Per1*. In support of this model, data from castrated male mice show greatly diminished AR expression in the SCN core and further show reduced c-FOS responses to a nighttime light pulse (Karatsoreos *et al.*, 2007; Iwahana *et al.*, 2008). Because VIP KO mice also have been shown to have lower levels of testosterone (Lacombe *et al.*, 2007), androgen signaling is a good mechanistic target to explain the photic gene expression differences in VIP KO and WT mice.

In our study, testosterone-supplemented VIP KO mice showed the same phase advance (8-10 hrs) as non-implanted VIP KO mice had shown (Fig. 5). It is important to note that this experiment had a small *n*, did not examine the phenotype of single light pulse phase shifts and did not look at the core anatomy to confirm that AR expression was restored. However, our results, demonstrating a complete lack of effect of testosterone supplementation in photo-entrainment, suggest that testosterone by itself is not mediating the circadian system's altered response to light in VIP KO mice.

Another possibility is that lower AR expression is actually reflective of fewer cells in the core itself. In order to address this possibility, stereological methods would be necessary to first determine the total number of neurons in the SCN. If the total number of cells differs, then this would suggest that VIP deficiency has effects at the gross organizational level of the SCN. In mid-SCN sections, we would also then use such methodology to calculate the total number of

AVP+ neurons. If the AVP+: total neuron ratio differs between the genotypes, this would further suggest that VIP absence has an effect specific to the number of cells in the SCN core. Functionally, a smaller core region could account for the blunted *Per1* and c-FOS responses found here, and could further affect the transmission of the core-shell phase resetting signal that is deficient in VIP KO mice.

Dendritic and somatic correlates of SCN connectivity are not affected by VIP absence

Using Golgi impregnation, VIP KO mice did not appear to have major differences in the morphological properties related to connectivity of their SCN neurons. The parameters measured in this way utilized a scheme where SCN neurons were first classified based on their dendritic organization, and the distributions of these neuronal subtypes were compared across different levels of the SCN and between genotypes. This type of analysis was also carried out along with a qualitative description of impregnated neurons. Of five published reports on Golgi impregnation in the rodent SCN to date (Silver, 1977; Guldner & Wolff, 1978; Silver & Brand, 1979; Van den Pol, 1980; Sugita *et al.*, 1996), only one in the rat (Van den Pol, 1980) has gone into detail on the properties of SCN neurons. This study was used as the basis for classifying neurons in the current experiments.

SCN neurons in both the VIP KO and WT mouse could be classified similarly based on dendritic and somatic morphological profiles into five major categories: monopolar, simple bipolar, curly bipolar, radial multipolar and spiny (Fig. 9, 10). Of these subtypes, the most common in the SCN were the bipolar and spiny. Other structures, like the cortex, hippocampus and cerebellum, have strongly defined neuronal subtypes where dendritic morphology can be

correlated with connectivity and neuronal function. Morphological differences in SCN neurons, however, are less robust, and inference about connectivity and function remains inductive. Thus it is possible that with a different classification scheme, Golgi impregnated SCN neurons would show differences between WT and VIP KO mice.

In order to statistically compare the distributions of the different neuronal subtypes in SCN neurons, a distinction was made between simple and complex neurons based on their dendritic complexity. Using these divisions, there were no reported differences based on genotype in the distribution profiles of the different neuronal subtypes in the rostro-caudal axis or between the core and the shell (Figs. 11, 12). However, there was a difference in both genotypes that a higher proportion of simple neurons were distributed in the core than in the shell.

Most descriptive results from our study are in line with the findings of other Golgi studies in the SCN (Silver, 1977; Guldner & Wolff, 1978; Silver & Brand, 1979; Van den Pol, 1980; Sugita *et al.*, 1996). These primarily stress the dendritic aspects of the neurons, pointing out that SCN axons are comparatively short and localized (Van den Pol, 1980). Examples of shell dendrites that extend well into the SCN core provide a useful picture in understanding how information from one SCN sub-region reaches another (Fig. 8). This organization would suggest that within the SCN, it is the connections made by the distal targeting of postsynaptic efferent dendrites that organizes the connectivity within the heterogeneous circuit.

In addition to classical axonal-dendritic synapses, other Golgi studies have noted putative synapses arising between dendrites and also from dendrites to soma (Guldner & Wolff, 1978; Van den Pol, 1980). Furthermore, the rat SCN has been shown to include ‘autapses’ where axons originating from a single neuron actually form a synapse with its own dendritic process (Guldner & Wolff, 1978). These synaptic properties are unusual and would confer a unique connectivity in

the SCN that could be affected by genetic manipulation. Electron microscopy would be necessary to verify such properties in the mouse as well, but once carried out, would provide an interesting target to understand circadian properties in the SCN for both WT and mutant models.

The morphology of SCN soma shape varies on a continuum from round to ovoid. Our analysis included the quantification of soma-to-soma contacts, in that they may represent microcircuits that reflect specific connective properties within the SCN. It is possible that our analysis underestimated these appositions, however, as very tight clusters could have been mistaken for single neurons. Surface area from soma measured in the current study ranged from 100 to 300 μm^2, whereas they have been reported to average around 100 μm^2 in other reports (Silver, 1977; Van den Pol, 1980). Thus, the 2-3X surface area increase we observed in some neurons could be from multiple neurons clustering tightly.

Close somatic appositions may reflect somato-somatic synapses, ephaptic communication (where a localized change in membrane potential in one neuron affects the electrophysiological properties of an adjacent neuron without chemical signaling), or gap junctions between SCN neurons. In the past, gap junctions have been found in the SCN and they are thought to play a role in its functioning as a robust oscillator (Colwell, 2000). If Golgi impregnation fully incorporates into an individual neuron, and if two neurons are connected by an open channel, as is the case with gap junctions, then it is conceivable that Golgi impregnated clusters of neurons represent neurons joined by gap junctions. This idea could be further confirmed with connexin immunostaining.

There were no reported differences in the distribution of soma-to-soma clusters between WT and VIP KO mice across the SCN rostro-caudal axis. This type of analysis has not been quantified in any study to date, but van den Pol (1980) did note that similar clusters were more

common in the SCN shell rather than core. Such a comparison was not feasible with our data, however, as there were relatively few clusters in the mid SCN, and dividing them up into core and shell would have thinned out their distribution to a point that statistical results would have been difficult to interpret.

Taken together, data from the current study point to a number of individual anatomical parameters in the circadian system affected in the VIP KO mouse model. Therefore, while the VIP KO mouse has been used to determine a role for VIP in the circadian system from the standpoint of acute and targeted pharmacology, our data show a number of other roles that VIP can play in the circadian system. It will be important for future studies to determine how these anatomical changes can then affect physiological and behavioral parameters as well. Not only will this provide us with an understanding of how genetic knockout of VIP affects a system at different levels, this type of anatomical analysis can also be incorporated into other knockout models to better characterize the role of individual genes across the nervous system.

Fig. 1. DiI tracing shows similar RHT innervation of the SCN in WT and VIP KO mice

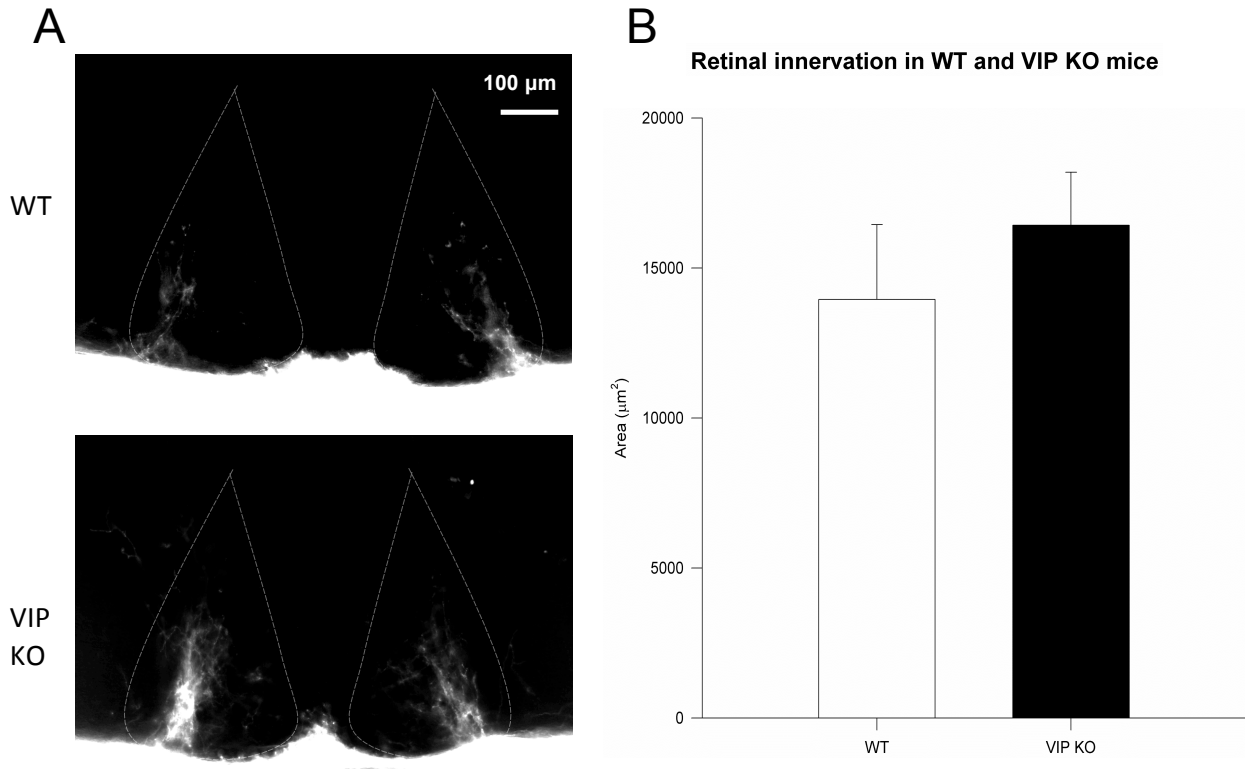

WT and VIP KO mice do not differ in retinal innervation area in the SCN. (A) Photomicrographs of mid SCN sections in which optic nerves had been implanted with the anterograde tracer DiI contain SCN boundary outlines determined by optic chiasm and third ventricle expression (dashed lines). Retinal axons enter the SCN from the ventrolateral aspect of the nucleus and innervate its ventro-middle portion. Some axons can be seen extending further dorsally into the putative shell, and a few axons terminate outside of the SCN in other hypothalamic areas. (B) Using Image J, area of retinal innervation was determined in mid SCN slices by thresholding optical density values and measuring the area of DiI signal relative to background. Student's *t*-test analysis reveals no statistically significant differences in retinal innervation area of the SCN between the two genotypes ($\alpha = 0.05$).

Fig. 2. Increased branching complexity in the SCN of VIP KO mice

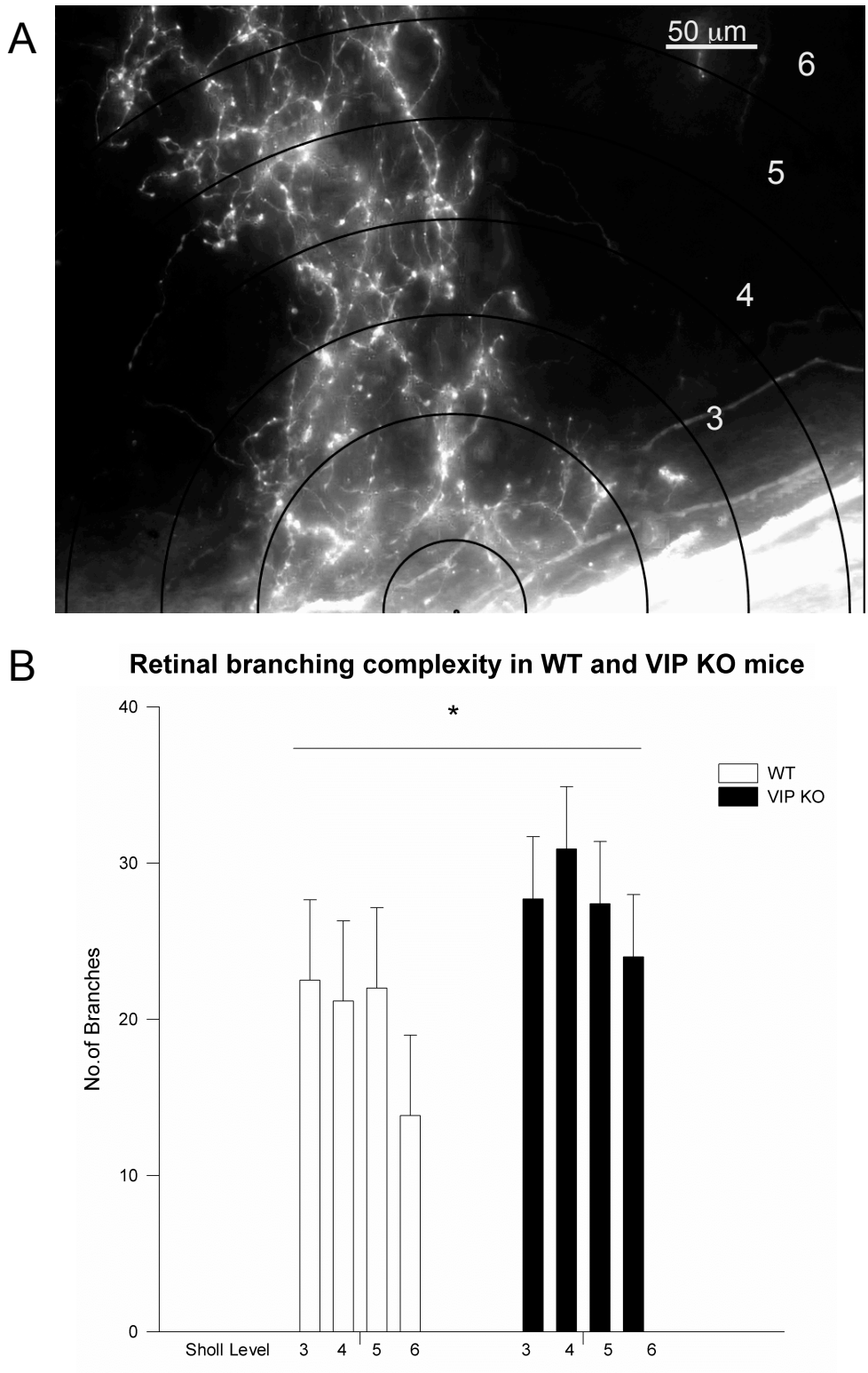

Using a Sholl-like analysis on high magnification, unilateral SCN images, branching complexity from retinal axons was determined by counting branch crossings through different

levels distal to the focal point of SCN entry via the optic chiasm. This analysis shows an increase in branching complexity in VIP KO mice. (A) A photomicrograph of the SCN where retinal axons exit the chiasm and project through different levels of the nucleus. Concentric circles were superimposed on each image, and levels 3-6 were used for a Sholl-like analysis. (B) Analysis by two-way ANOVA shows an effect of genotype on the number of branch crossings at each level ($p < 0.05$).

Fig. 3. NF-M expression suggests that there are differences in axonal properties in the SCN of WT and VIP KO mice

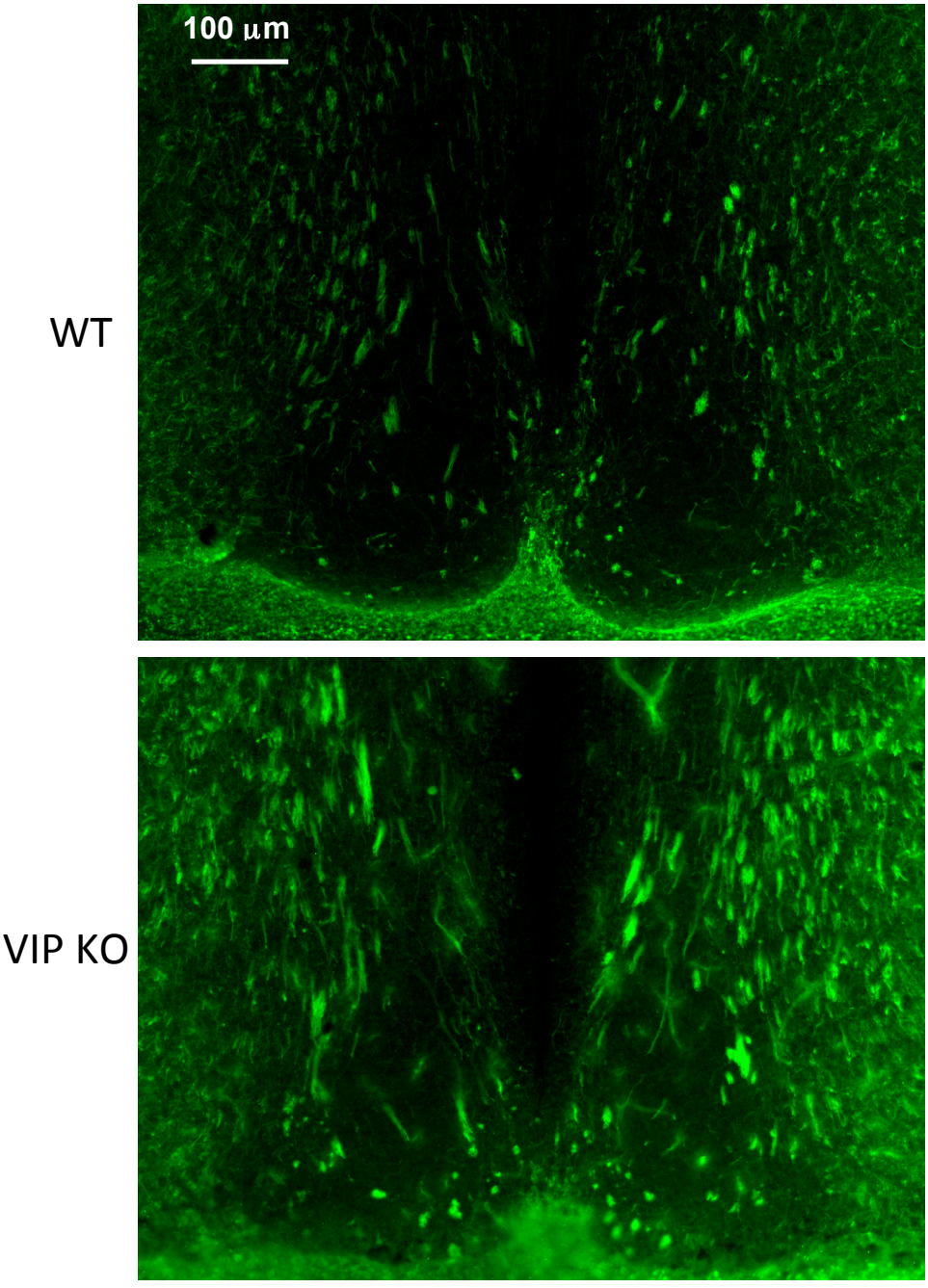

Photomicrographs of WT and VIP KO SCN immunostained for NF-M show stronger expression

of NF-M both in and around the SCN of VIP KO mice compared with WT mice. In both genotypes, NF-M is expressed in punctuate clusters in the ventral SCN just dorsal to the optic chiasm, and in the dorsal SCN, longer chains of NF-M-expressing fibers course dorsally toward the subparaventricular zone (SPVZ). VIP KO mice show more variable orientation of these longer chains compared with WT mice.

Fig. 4. AR expression is decreased in the core of VIP KO mice

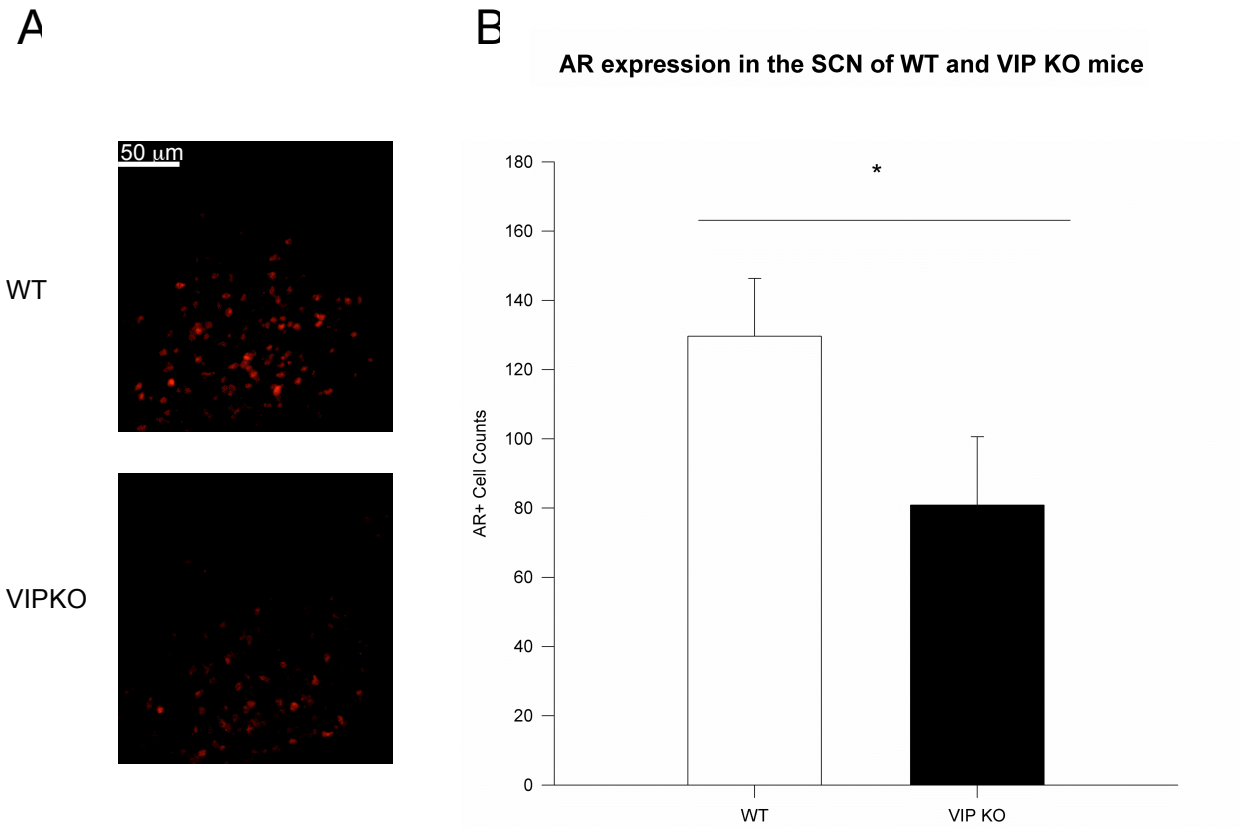

Immunostaining for AR reveals that VIP KO mice have fewer AR+ cells than WT mice in the SCN. (A) Photomicrographs of the unilateral SCN core in WT and VIP KO mice and (B) statistical quantification show that there is ≈40% reduction in the number of AR+ cells in the SCN core in VIP KO mice.

Fig. 5. Testosterone supplementation in VIP KO mice does not restore impaired entrainment to the LD cycle

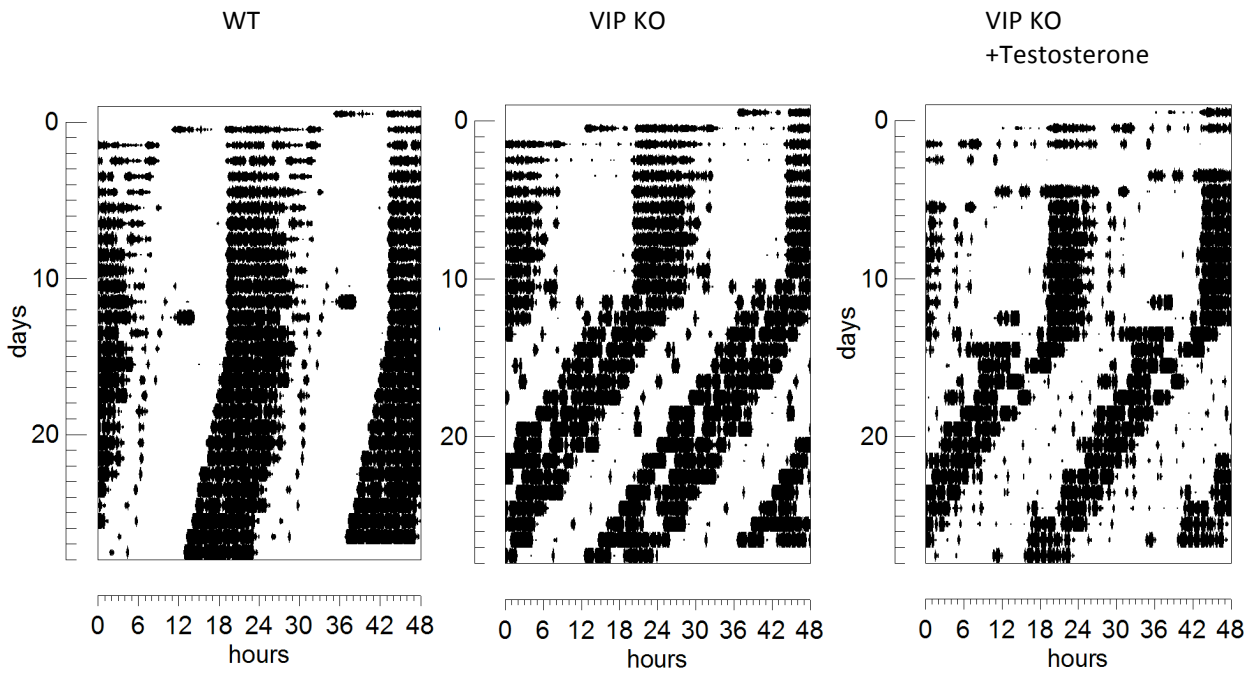

Actograms of locomotor activity from mice subjected to 10-14 days in a 12:12 light-dark (LD) cycle and then released into constant darkness (DD). As reported earlier, WT mice began their phase of activity in constant conditions from a phase predicted by the prior LD cycle. VIP KO mice, however, showed a ≈ 8 hr phase advance when released into DD. VIP KO mice that were implanted with testosterone capsules showed the same impairment as non-treated VIP KO mice.

Fig. 6. Cluster of SCN neurons showing soma-to-soma appositions

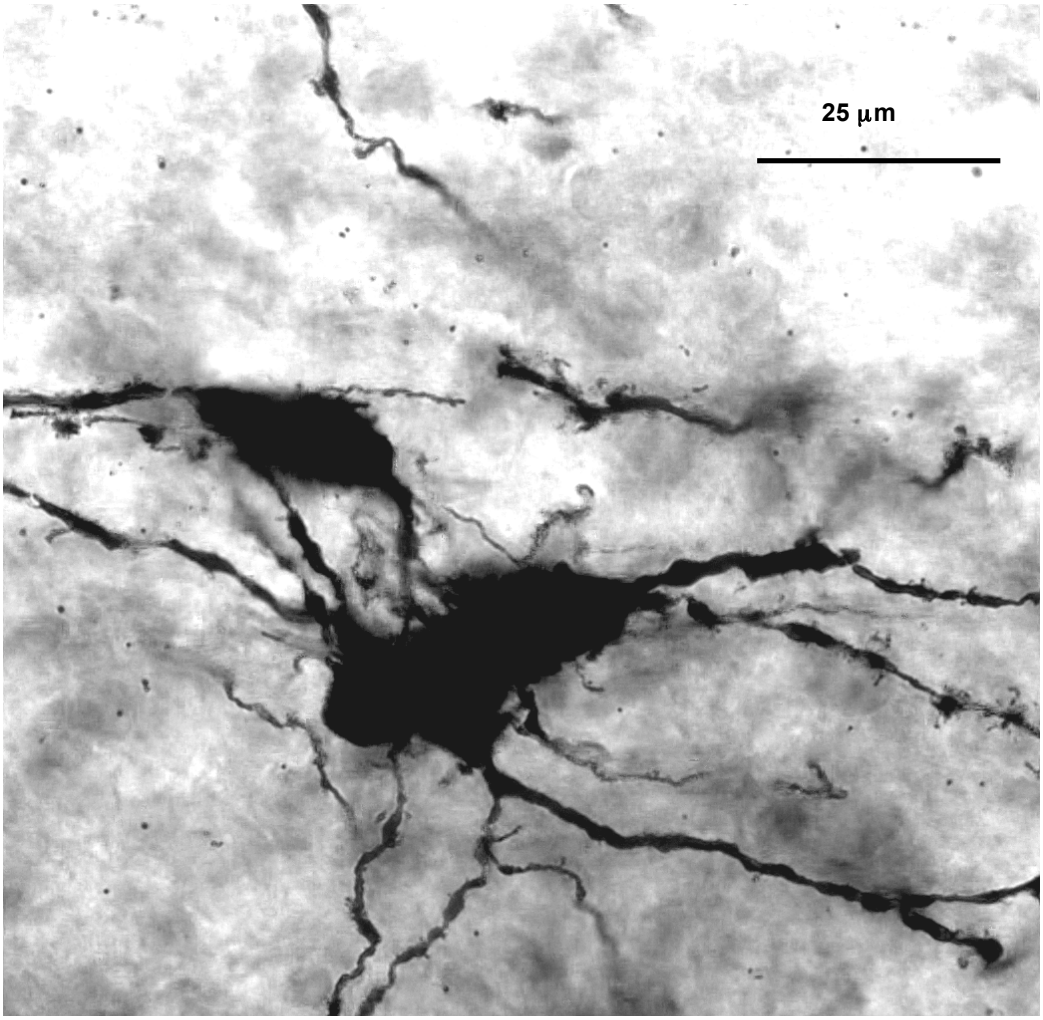

Many SCN neurons were found in clusters, specifically with soma-to-soma apposition. In this example, there are at least three neurons that seem to make somatic contact with each other. Other processes are found in this cluster as well, such as the dendrite from the curly bipolar neuron sitting just dorsally to the cluster.

Fig. 7. No significant differences in the distribution of soma-to-soma appositions in the SCN of WT and VIP KO mice

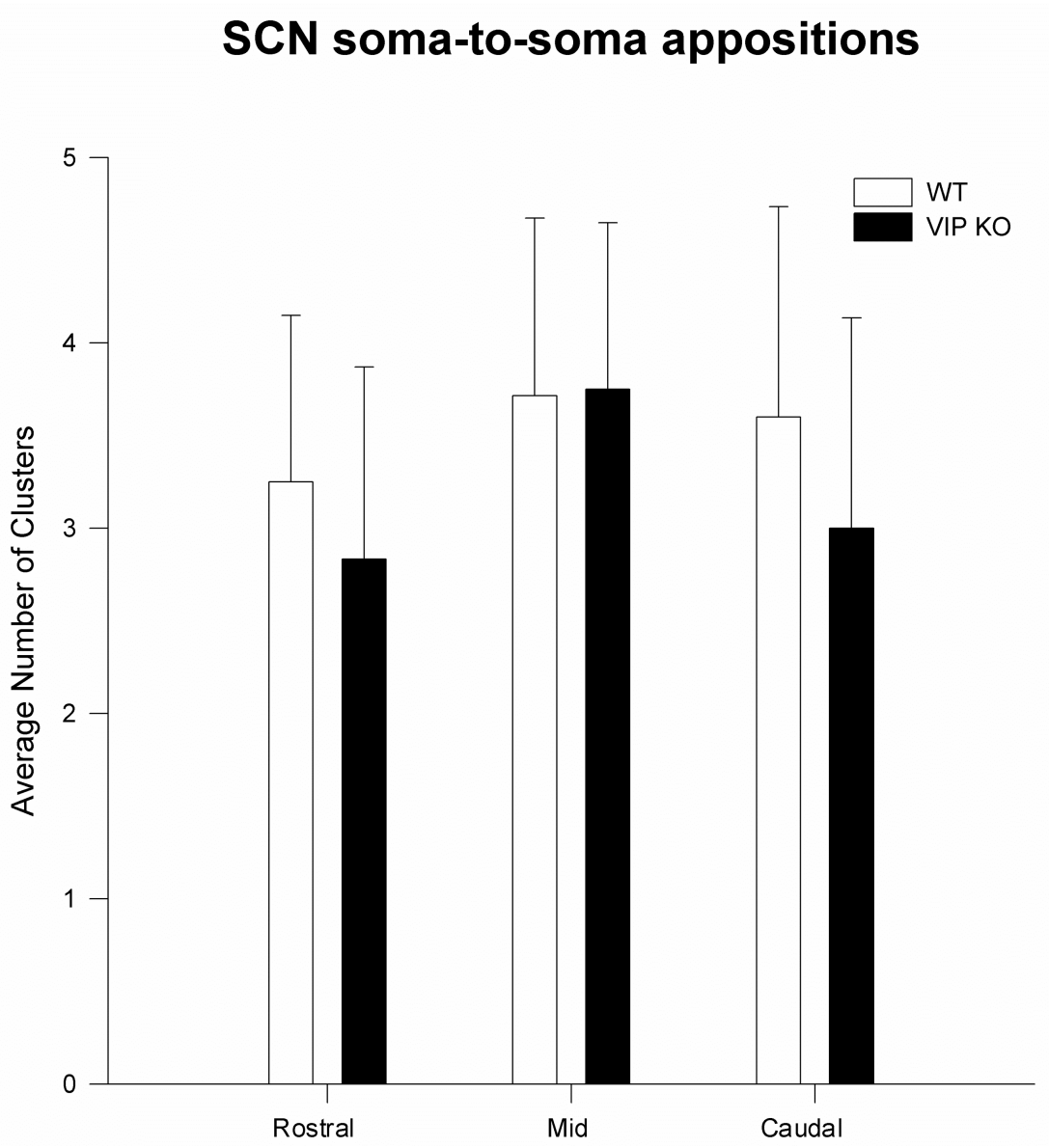

Quantification of clusters by two-way ANOVA in which 2 or more soma contact each other across the rostro-caudal axis shows no effect of genotype on the amount or distribution of clusters ($\alpha = 0.05$).

Fig. 8. Processes in the SCN comprise orphan axons and dendrites as well as SCN-derived axons and dendrites

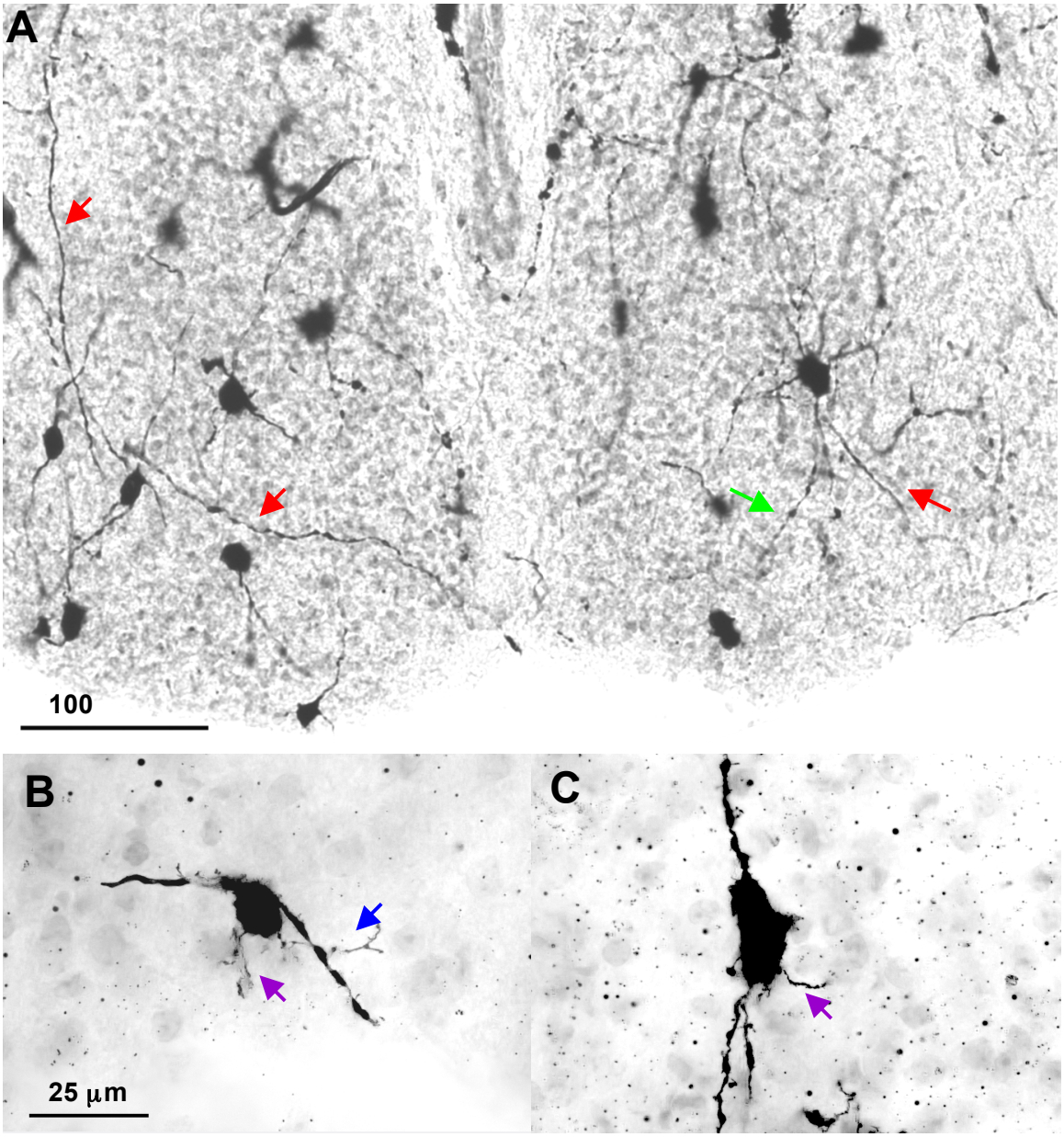

Both axons and dendrites are visible with Golgi-Cox impregnation, with axons from SCN neurons being less prominent. (A) Orphan processes are found throughout the SCN (denoted by red arrows). These may be axons or dendrites, and their origin may be from neurons whose cell soma lie in another plane of the SCN or from extra-SCN regions. A demonstrated pathway from the core to the shell is also seen with a long dendritic process extended from a neuron localized in the shell (denoted by a green arrow). (B) and (C) The two types of bipolar neurons show small, thin axons protruding ≈ 10 µm from the soma (denoted by purple arrows). An orphan process

(denoted by a blue arrow) also makes contact with the curly bipolar neuron in (B).

Fig. 9. Simple connectivity SCN neurons found in both WT and VIP KO mice

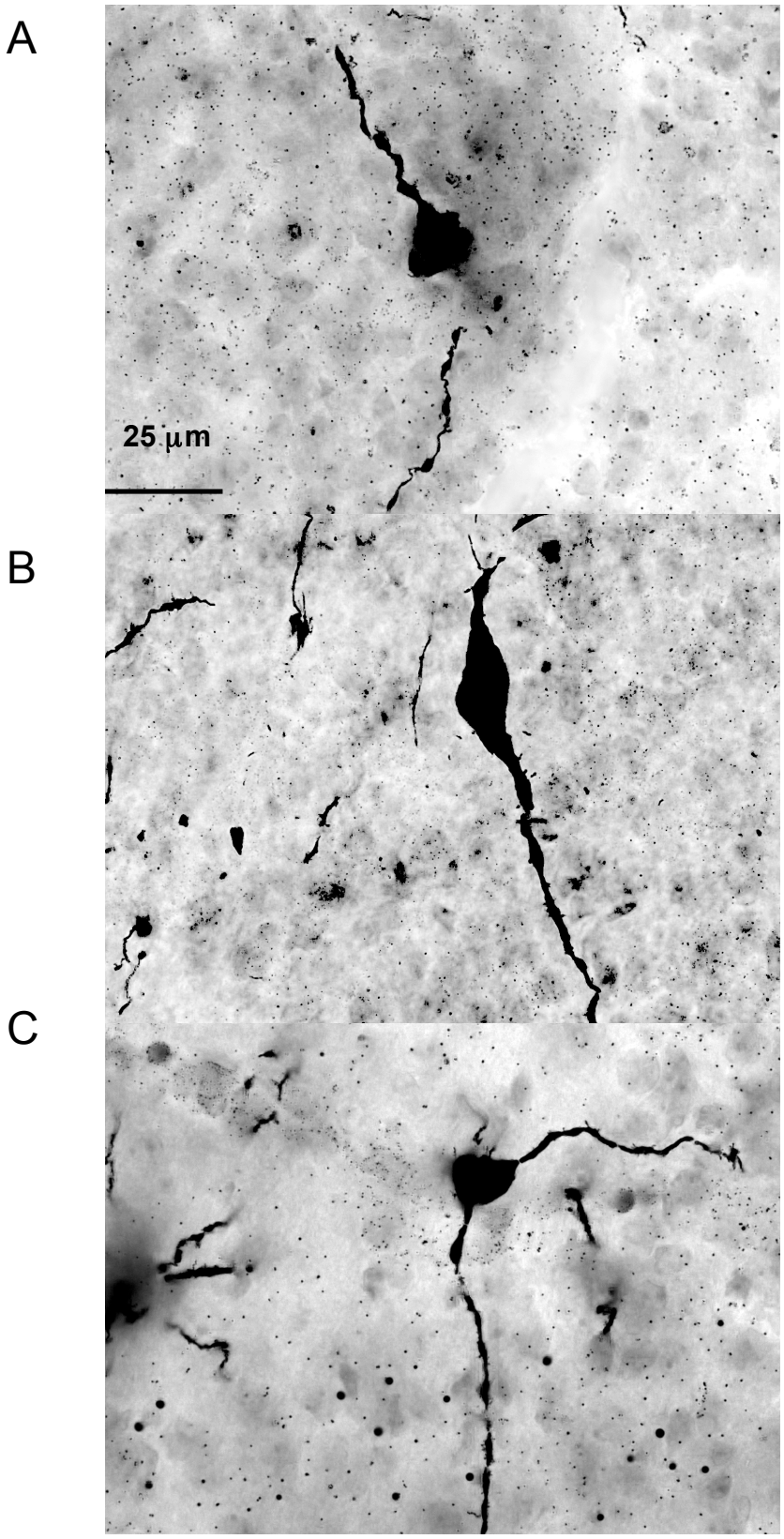

Photomicrogrpahs of representative (A) monopolar, (B), simple bipolar and (C) curly bipolar neurons based on descriptions from van den Pol (1980). Nomenclature is based on dendritic properties of neurons.

Fig. 10. Complex connectivity SCN neurons found in both WT and VIP KO mice

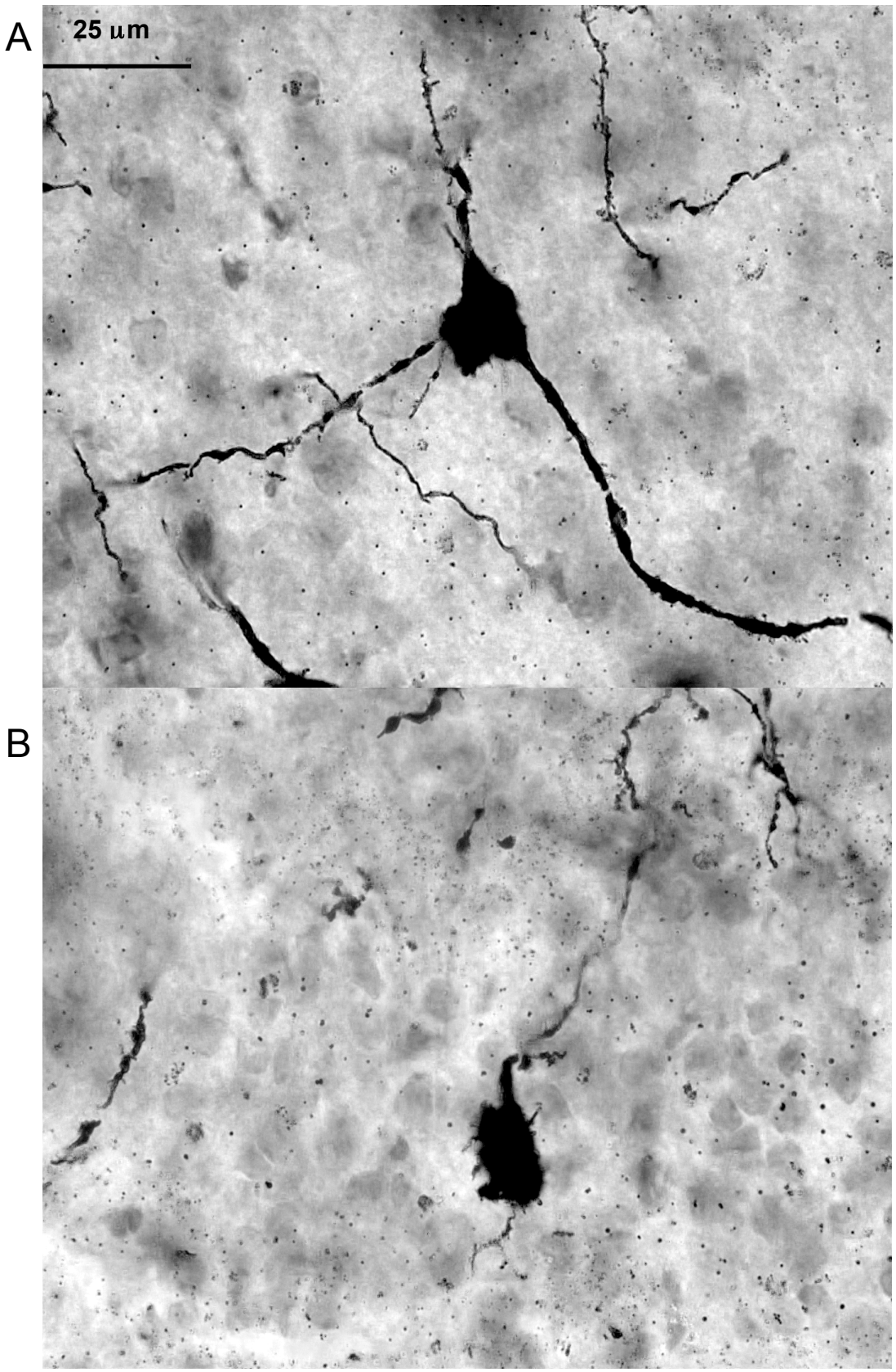

Photomicrogrpahs of representative (A) radial multipolar and (B) spiny neurons based on descriptions from van den Pol (1980). Nomenclature is based on dendritic properties of neurons.

Fig. 11. WT and VIP KO neuronal complexity distributions across the SCN rostro-caudal axis not differ

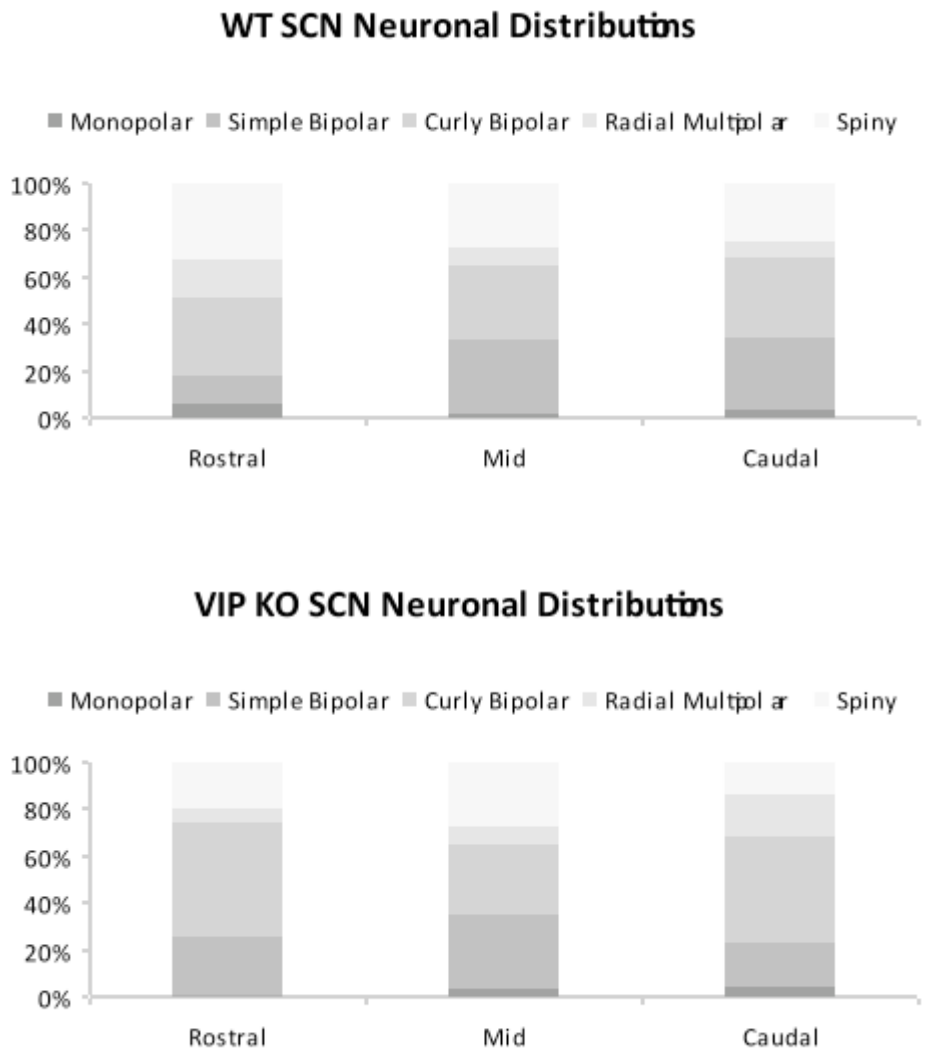

Using z-stacks of individual neurons throughout the mid SCN, neuronal subtypes were tallied based on the 5 different categories described in the text. For statistical analysis, the simple and complex classification schema were used with multiple logistic regression. This analysis showed no significant effects of genotype, rostro-caudal level, or interaction on neuronal subtype distribution ($\alpha = 0.05$).

Fig. 12. WT and VIP KO neuronal complexity distributions in the SCN core and shell do not differ

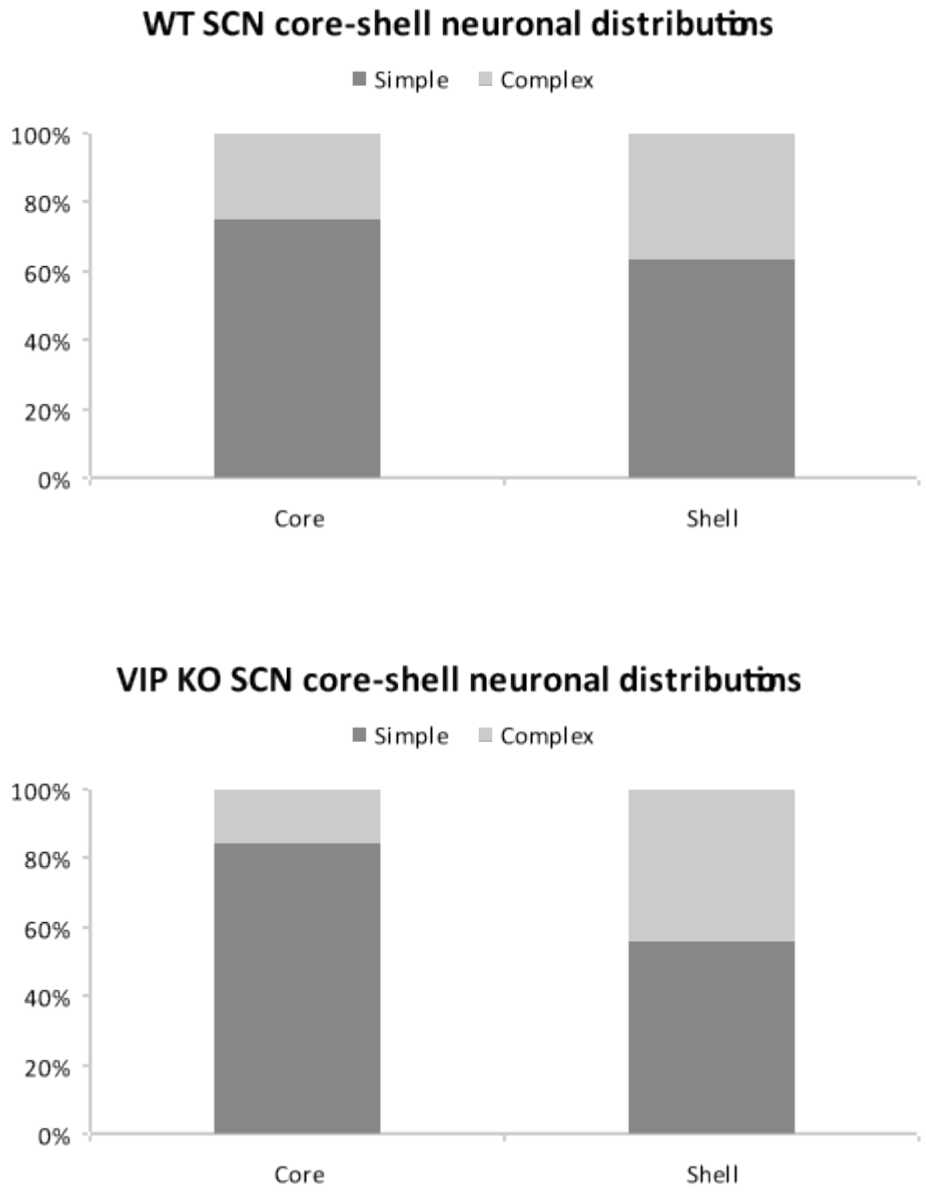

Using z-stacks of individual neurons throughout the mid SCN, neuronal subtypes were tallied based on the simple and complex classification schema described in the text. Core and shell delineations were determined from a standard template that was created from a representative SCN section used in Chapter 2. Analysis with multiple logistic regression showed no effects of genotype on distribution, however there was an effect of core vs. shell location that affected distribution of simple and complex neurons ($p = 0.037$).

Abe, H., Engler, D., Molitch, M.E., Bollinger-Gruber, J. & Reichlin, S. (1985) Vasoactive intestinal peptide is a physiological mediator of prolactin release in the rat. *Endocrinology*, **116**, 1383-1390.

Abrahamson, E.E. & Moore, R.Y. (2001) Suprachiasmatic nucleus in the mouse: retinal innervation, intrinsic organization and efferent projections. *Brain Res*, **916**, 172-191.

Al-Chalabi, A. & Miller, C.C. (2003) Neurofilaments and neurological disease. *Bioessays*, **25**, 346-355.

Albers, H.E., Minamitani, N., Stopa, E. & Ferris, C.F. (1987) Light selectively alters vasoactive intestinal peptide and peptide histidine isoleucine immunoreactivity within the rat suprachiasmatic nucleus. *Brain Res*, **437**, 189-192.

Altimus, C.M., Guler, A.D., Alam, N.M., Arman, A.C., Prusky, G.T., Sampath, A.P. & Hattar, S. (2010) Rod photoreceptors drive circadian photoentrainment across a wide range of light intensities. *Nat Neurosci*, **13**, 1107-1112.

Aton, S.J., Colwell, C.S., Harmar, A.J., Waschek, J. & Herzog, E.D. (2005) Vasoactive intestinal polypeptide mediates circadian rhythmicity and synchrony in mammalian clock neurons. *Nat Neurosci*, **8**, 476-483.

Bardrum, B., Ottesen, B. & Fuchs, A.R. (1987) Preferential release of oxytocin in response to vasoactive intestinal polypeptide in rats. *Life Sci*, **40**, 169-173.

Brenneman, D.E., Eiden, L.E. & Siegel, R.E. (1985) Neurotrophic action of VIP on spinal cord cultures. *Peptides*, **6 Suppl 2**, 35-39.

Colwell, C.S. (2000) Rhythmic coupling among cells in the suprachiasmatic nucleus. *J Neurobiol*, **43**, 379-388.

Cunningham, L.A. & Holzwarth, M.A. (1988) Vasoactive intestinal peptide stimulates adrenal aldosterone and corticosterone secretion. *Endocrinology*, **122**, 2090-2097.

Czeisler, C.A., Richardson, G.S., Zimmerman, J.C., Mooreede, M.C. & Weitzman, E.D. (1981) Entrainment of human circadian rhythms by light-dark cycles-a reassessment. *Photochemistry and Photobiology*, **34**, 239-247.

Davidson, A.J., Yamazaki, S. & Menaker, M. (2003) SCN: ringmaster of the circadian circus or conductor of the circadian orchestra? *Novartis Found Symp*, **253**, 110-121; discussion 121-115, 281-114.

Drahushuk, K., Connell, T.D. & Higgins, D. (2002) Pituitary adenylate cyclase-activating polypeptide and vasoactive intestinal peptide inhibit dendritic growth in cultured sympathetic neurons. *J Neurosci*, **22**, 6560-6569.

Fix, C., Jordan, C., Cano, P. & Walker, W.H. (2004) Testosterone activates mitogen-activated protein kinase and the cAMP response element binding protein transcription factor in Sertoli cells. *Proc Natl Acad Sci U S A*, **101**, 10919-10924.

Gery, S. & Koeffler, H.P. (2010) Circadian rhythms and cancer. *Cell Cycle*, **9**, 1097-1103.

Gressens, P. (1999) VIP neuroprotection against excitotoxic lesions of the developing mouse brain. *Ann N Y Acad Sci*, **897**, 109-124.

Guldner, F.H. & Wolff, J.R. (1978) Self-innervation of dendrites in the rat suprachiasmatic nucleus. *Exp Brain Res*, **32**, 77-82.

Guler, A.D., Ecker, J.L., Lall, G.S., Haq, S., Altimus, C.M., Liao, H.W., Barnard, A.R., Cahill, H., Badea, T.C., Zhao, H., Hankins, M.W., Berson, D.M., Lucas, R.J., Yau, K.W. & Hattar, S. (2008) Melanopsin cells are the principal conduits for rod-cone input to non-image-forming vision. *Nature*, **453**, 102-105.

Hattar, S., Kumar, M., Park, A., Tong, P., Tung, J., Yau, K.W. & Berson, D.M. (2006) Central projections of melanopsin-expressing retinal ganglion cells in the mouse. *J Comp Neurol*, **497**, 326-349.

Hattar, S., Liao, H.W., Takao, M., Berson, D.M. & Yau, K.W. (2002) Melanopsin-containing retinal ganglion cells: architecture, projections, and intrinsic photosensitivity. *Science*, **295**, 1065-1070.

Hattar, S., Lucas, R.J., Mrosovsky, N., Thompson, S., Douglas, R.H., Hankins, M.W., Lem, J., Biel, M., Hofmann, F., Foster, R.G. & Yau, K.W. (2003) Melanopsin and rod-cone photoreceptive systems account for all major accessory visual functions in mice. *Nature*, **424**, 76-81.

Hubbell, W.L. & Bownds, M.D. (1979) Visual transduction in vertebrate photoreceptors. *Annu. Rev. Neurosci.*, **2**, 17-34.

Iwahana, E., Karatsoreos, I., Shibata, S. & Silver, R. (2008) Gonadectomy reveals sex differences in circadian rhythms and suprachiasmatic nucleus androgen receptors in mice. *Horm Behav*, **53**, 422-430.

Janne, O.A. & Bardin, C.W. (1984) Androgen and antiandrogen receptor binding. *Annu Rev Physiol*, **46**, 107-118.

Kaiser, P.K. & Lipton, S.A. (1990) VIP-mediated increase in cAMP prevents tetrodotoxin-induced retinal ganglion cell death in vitro. *Neuron*, **5**, 373-381.

Karatsoreos, I.N., Wang, A., Sasanian, J. & Silver, R. (2007) A role for androgens in regulating circadian behavior and the suprachiasmatic nucleus. *Endocrinology*, **148**, 5487-5495.

Lacombe, A., Lelievre, V., Roselli, C.E., Muller, J.M., Waschek, J.A. & Vilain, E. (2007) Lack of vasoactive intestinal peptide reduces testosterone levels and reproductive aging in mouse testis. *J Endocrinol*, **194**, 153-160.

LeSauter, J. & Silver, R. (1998) Output signals of the SCN. *Chronobiol Int*, **15**, 535-550.

Reppert, S.M. & Weaver, D.R. (2002) Coordination of circadian timing in mammals. *Nature*, **418**, 935-941.

Seki, T., Izumi, S., Shioda, S., Zhou, C.J., Arimura, A. & Koide, R. (2000) Gene expression for PACAP receptor mRNA in the rat retina by in situ hybridization and in situ RT-PCR. *Ann N Y Acad Sci*, **921**, 366-369.

Shinohara, K., Tominaga, K. & Inouye, S.T. (1998) Luminance-dependent decrease in vasoactive intestinal polypeptide in the rat suprachiasmatic nucleus. *Neurosci Lett*, **251**, 21-24.

Silver, J. (1977) Abnormal development of the suprachiasmatic nuclei of the hypothalamus in a strain of genetically anophthalmic mice. *J Comp Neurol*, **176**, 589-606.

Silver, J. & Brand, S. (1979) A route for direct retinal input to the preoptic hypothalamus: dendritic projections into the optic chiasm. *Am J Anat*, **155**, 391-401.

Smith, L. & Canal, M.M. (2009) Expression of circadian neuropeptides in the hypothalamus of adult mice is affected by postnatal light experience. *J Neuroendocrinol*, **21**, 946-953.

Sugita, S., Minematsu, M., Nagai, K. & Sugahara, K. (1996) Morphological changes in the hypothalamic suprachiasmatic nucleus and circadian rhythm of locomotor activity in hereditary microphthalmic rats. *Exp Anim*, **45**, 115-124.

Tahara, Y., Kuroda, H., Saito, K., Nakajima, Y., Kubo, Y., Ohnishi, N., Seo, Y., Otsuka, M., Fuse, Y., Ohura, Y., Komatsu, T., Moriya, Y., Okada, S., Furutani, N., Hirao, A., Horikawa, K., Kudo, T. & Shibata, S. (2012) In Vivo Monitoring of Peripheral Circadian Clocks in the Mouse. *Curr Biol*.

Van den Pol, A.N. (1980) The hypothalamic suprachiasmatic nucleus of rat: intrinsic anatomy. *J Comp Neurol*, **191**, 661-702.

Chapter 4

Vasoactive intestinal peptide and a new model to explain its role in circadian phase shifting

Introduction

In the biological organization of complex systems, network hierarchies provide a means to efficiently and reliably carry out necessary functions and permit that system the essential capacity to adapt. Circadian rhythms are generated across such a hierarchy, and while we have identified some of the major physiological hubs in this network, we are also beginning to understand how these hubs influence each other. The suprachiasmatic nucleus (SCN) of the hypothalamus is a well-studied hub in the mammalian circadian system that both provides timekeeping cues for the entire body and integrates environmental timing information from the ambient light-dark cycle (see Chapter 1).Within the SCN, the neuropeptide vasoactive intestinal peptide (VIP) mediates both the intercellular communication of these timekeeping cues and the integration of environmental timing information. Because of this dual role, VIP is indispensible both for a functional SCN and more broadly, the circadian system as a whole.

VIP expression within the hypothalamus was discovered a short time after it was first isolated in the porcine intestine (Said & Mutt, 1969; Larsson *et al.*, 1976). When the discovery of the SCN as a pacemaker occurred around the same time (Moore & Lenn, 1972; Stephan & Zucker, 1972), the identification of large amounts of VIP- and VPAC2 receptor (VPAC2R)-containing neurons in the SCN later followed (Besson *et al.*, 1986; Vertongen *et al.*, 1997). The perikarya of VIP+ cells were largely confined to the middle 1/3rd of the SCN along its rostro-caudal axis, almost entirely within the same ventral region that first makes contact with retinal afferents from the optic chiasm (Sims *et al.*, 1980; van den Pol, 1991; Abrahamson & Moore, 2001). VIP+ neurons in this retino-recpieint area send projections throughout the SCN (van den

Pol, 1991; Abrahamson & Moore, 2001), and VPAC2R expression was found equally dispersed with very high concentration throughout the SCN (Vertongen *et al.*, 1997). Thus, from early on, anatomical expression studies had pointed to VIP-ergic signaling as an important locus for controlling the circuits that comprise the SCN.

With progress in transgenic technology, new mouse models had become available to understand the role of VIP-ergic signaling *in vivo* (Shen *et al.*, 2000; Harmar *et al.*, 2002; Colwell *et al.*, 2003). Two important ideas came from these studies: 1) VIP played a major role in the maintenance of circadian rhythmicity (expressed across multiple physiological and behavioral levels), and 2) VIP played a major role in normal entrainment of the circadian system (Aton & Herzog, 2005; Vosko *et al.*, 2007). Because these findings coincided with key advances in understanding how individual SCN cells oscillated (Welsh *et al.*, 2004), the focus of subsequent research was on the effects of VIP absence on intercellular rhythmicity between SCN cells *in vitro* (Aton *et al.*, 2005; O'Neill *et al.*, 2008; Maywood *et al.*, 2011). These studies were important for establishing VIP as a vital synchronizing agent, specifically by affecting cyclic AMP (cAMP) rhythms, between SCN neurons (O'Neill *et al.*, 2008).

The same type of *in vitro*, mechanistic, studies, have not been carried out to define the role of VIP in photoentrainment. In part, this is likely because of the absence of a photoreceptive organ in the *in vitro* model. Furthermore, even though entrainment can be studied from the perspective of pharmacologically induced, acute phase shifts (see Chapter 1), the entire SCN, rather than individual cells or even a cross-section of a slice culture, would be necessary to recreate the appropriate circuitry. Therefore, the work of this dissertation focused on the mechanisms by which VIP affects photoentrainment, using an appropriate and available tool: snapshots across different parameters of the SCN circuit taken *in vivo* from the VIP KO mouse.

Using an acute phase shifting paradigm in VIP KO mice to study normal mechanisms of entrainment, experiments in Chapter 2 revealed three important characteristics in the SCN:

1) VIP KO mice have blunted molecular responses of intracellular signaling (c-FOS) and clock resetting (*Per1*) pathways

2) VIP KO mice do not sustain molecular responses of intracellular signaling and clock resetting pathways

3) VIP KO mice specifically lack molecular responses of intracellular signaling and clock resetting pathways in the SCN shell.

A new model to explain VIP and phase shifting mechanisms in SCN neurons

At a functional level, this first finding has been previously implicated in phase shifting differences between young and aged rodents (Benloucif *et al.*, 1997; Kolker *et al.*, 2003). As animals, including humans, age, circadian disturbances can arise, and many of these are specific to entrainment-related dysfunctions (Gibson *et al.*, 2009). Interestingly, retinal innervation to the SCN has also been shown to decrease with age (Lupi *et al.*, 2010), as has expression of VIP and other neuropeptides (Swaab *et al.*, 1985). These independent observations can all be linked together to create a hypothesis for why there are circadian rhythm deficiencies among the aged, but the single time point analysis carried out in VIP KO (and also VPAC2R KO mice) does not further define the mechanisms by which VIP deficiency affects the pathways triggered during a phase shifting response.

Conversely, the finding that VIP KO mice do not <u>sustain</u> nor <u>propagate</u> molecular

responses to a phase shifting light stimulus provides clues to the types of cellular and molecular processes that are affected by the loss of VIP. Firstly, *Per1* is only increased in response to a phase shifting light pulse for about an hour before levels begin to fall again (see Chapter 2, Figs. 3, 8). Because levels are not sustained as they are in WT mice, a decrease in transcriptional activity on *Per1* is quite possible. That there is an early increase in *Per1* also suggests that the cellular machinery necessary for inducing normal gene responses to photic stimuli is intact in VIP KO mice. Because the magnitude of the initial *Per1* response is nearly the same between genotypes, this later decrease in transcriptional activity would likely be specific to events independent of initial promoter activity and transcriptional initiation.

The idea that there is a transcriptional decrease is further supported by the similar, temporally-confined c-FOS response in VIP KO mice. Since these mice show both c-FOS and *Per1* to have similar temporal response phenotypes, it is likely that transcriptional pathways activated by phase shifting light are affected through global events upstream of targeted transcription. For instance, it is thought that the cell signaling pathways involved with phase shifting and entrainment involve the phosphorylation of histones and chromatin modification, and these chromatin conformational changes are necessary to provide exposure to large strands of DNA for subsequent transcription (Crosio *et al.*, 2000). Therefore a diminished window for transcription could be explained by decreased histone phosphorylation and could account for the shortened induction of both *Per1* and c-FOS in the VIP KO SCN.

There is other experimental evidence to suggest that VIP deficiency has effects upstream of the transcriptional initiation of *Per1* and *c-fos*. These come from mitogen activated protein kinase (MAPK) expression, Ca^{2+} imaging and electrophysiological studies. Before evidence will be discussed, it is first important to remember that phase shifts are mediated by excitatory

neurotransmission from retinal afferents that alter the electrical activity of retino-recipient SCN neurons, leading to an activation of different intracellular signaling cascades and transcriptional activation (Reppert & Weaver, 2002). Specifically, glutamatergic signals acting through NMDA receptors trigger an influx of Ca^{2+} that initiates a number of signal transduction pathways, including protein kinase A (PKA), mitogen-activated protein kinase (MAPK), and calcium-calmodulin dependent protein kinase II (CAMKII). These signaling pathways converge on the phosphorylation of cAMP response element binding protein (CREB) at both Ser133 and Ser142 (Gau *et al.*, 2002), leading to the nuclear translocation and transcriptional activity of phosphorylated CREB upon certain genes carrying a cAMP response element (CRE) in their promoter regions like *c-fos* and *Per1* (Rusak *et al.*, 2002; Travnickova-Bendova *et al.*, 2002).

In VIP KO mice, phosphorylated MAPK (pMAPK) expression is greatly reduced compared to WT mice 30 minutes after exposure to a phase shifting light pulse (Dragich *et al.*, 2010). In WT animals, glutamate from retinal afferents leads to the phoshporylation of MAPK in the SCN during a phase shifting light pulse early along the cell signaling pathway that phosphorylates CREB and triggers transcriptional initiation (Obrietan *et al.*, 1998). Importantly, MAPK, acting through mitogen- and stress- activated protein kinases (MSKs), is also thought to act as a major player in the histone phosphorylation and chromatin remodeling that have been observed in SCN responses to light (Crosio *et al.*, 2000; Soloaga *et al.*, 2003; Butcher *et al.*, 2005). Again, in both WT and VIP KO mice, there is pMAPK expression in response to phase-shifting light, but in the VIP KO mice, this expression is blunted. Thus, in the order of cell signaling events involved in phase shifting, the differences in phosphorylation of MAPK could be the convergent point that limits the transcription of *Per1* and *c-fos*.

According to the canonical MAPK signaling cascade, MAPK is closely coupled to cell

membrane events through a small GTP-ase known as Ras (Cheng & Obrietan, 2006). In the SCN, there is expression of a Ras-family protein, Dexras1, which is activated via Ca^{2+} influx through NMDA receptor channels and phosphorylation of CAMKII (Rosen *et al.*, 1994; Fang *et al.*, 2000; Takahashi *et al.*, 2003). An interesting observation is that mice deficient in Dexras1 lack the ability to gate their circadian phase shifting responses to light at night, a phenotype also found in VIP KO mice (Cheng *et al.*, 2006; Dragich *et al.*, 2010).

There is also a pathway by which VIP-ergic signaling could affect MAPK, and this is through cAMP activation of the exchange protein activated by cAMP (EPAC). Recently, it was reported that cAMP promotes molecular rhythmicity in SCN neurons by an EPAC-dependent mechanism (O'Neill *et al.*, 2008). When VIP binds to the VPAC2 receptor, it couples to adenylyl cyclase and converts ATP to cAMP (Vosko *et al.*, 2007). cAMP then has two actions, one promotes the phosphorylation of PKA and the other promotes the association of a small GTP-ase, Rap1, to B-Raf via EPAC. This association results in the phosphorylation of MAPK (Waltereit & Weller, 2003). Between the Dexras1 and EPAC arms of the MAPK signaling cascade, the photic phenotypes observed in VIP deficiency can be explained, and because both arms are involved, it is likely that an event upstream of both of these routes is a regulator of SCN responses to phase shifting stimuli. The common upstream point of convergence for both of these pathways is Ca^{2+} influx.

We now also have preliminary data to suggest that Ca^{2+} signaling is affected by VIP deficiency. When parsing the SCN into a dorsal region, which contains the SCN shell, and a ventral region, which predominantly contains the SCN core, it appears that there is an inhibited Ca^{2+} response to NMDA application that is specifically pronounced in the dorsal SCN in VIP KO mice (data not shown). Furthermore, our lab has also collected preliminary data on the

electrophysiological responses of VIP neurons using a similar dorsal-ventral division of the SCN, and it was found again that there was an inhibited electrical response to neurons specifically in the dorsal SCN (data not shown). These data together suggest that the light response deficiencies in VIP KO mice can be tracked back to membrane events at the level of neurotransmitter binding and ionic flux in SCN neurons. In other words, VIP normally regulates photic phase shifting information through affecting transmission between SCN neurons. I hypothesize that in the circadian visual system, VIP acts to modulate glutamatergic signaling in order to promote the proper postsynaptic responses to retinal input.

The phase shifting signals that utilize glutamate can act across the SCN broadly, not just on a confined region of a core. The usefulness of a 'core' distinction is that the majority of retino-recipient synapses take place in this region, but retinal innervation, to a lesser extent, has been shown in the shell as well (Hattar *et al.*, 2002). NMDA receptor subunits have been found all throughout the SCN (Mikkelsen *et al.*, 1993), and VGLUT-expressing terminal afferents have been shown to make synaptic contact with both shell and core neurons (Kiss *et al.*, 2008). Additionally, within the SCN core there is heterogeneity, with only a subset of neurons expressing VIP, and others expressing gastrin releasing peptide (GRP) or calbindin (Antle & Silver, 2005). A characteristic important for VIP+ perikarya is that they are located in the ventral-most region of the SCN, where the majority of retinal afferents will contact them by their proximity to the vast number of retinal axons that are traveling through and dorsally out of the optic chiasm. It is likely that because of this proximity, VIP+ perikarya are exposed to more glutamatergic signals than any other cell population in the SCN.

At a functional level, there is an established body of literature to suggest that VIP potentiates glutamatergic signaling in the cortex (Magistretti *et al.*, 1998). At the level of gene

expression, VIP has been shown to potentiate *c-fos* levels in response to glutamate (Martin *et al.*, 1995). In the SCN acute slice preparation, application of VIP together with glutamate has dramatic effects in increasing the number of neurons that respond with increased firing compared to either glutamate or VIP alone (Huang & Pan, 1993). Furthermore, co-administration also has potentiating effects on individual neuronal responses (Huang & Pan, 1993). It would make sense that if VIP were a potentiating agent for glutamate in the SCN, then areas with the greatest glutamatergic input are less likely to rely on the presence of both molecules, whereas areas with less glutamatergic input would require more of a VIP-ergic presence to achieve postsynaptic responses required for circadian phase resetting. This is illustrated concretely in the SCN of VIP KO mice, where there is almost a complete lack of gene expression responses of *Per1* or c-FOS to a phase-shifting light pulse in the SCN shell. Conversely, in part of the SCN core, there are gene expression responses in VIP KO mice because perikarya of cells that would otherwise be expressing VIP are still receiving postsynaptic glutamatergic signals, just as they do in WT animals. Note that the magnitude of this response is still affected, possibly because in the dorsal aspects of the core, neurons are not as strongly innervated by glutamatergic fibers as the VIP+ perikarya are, and these areas normally require some potentiation by VIP. In this model of phase resetting, it is the ventral-most VIP+ neurons that are the first to receive retinal afferent signals, and then these neurons subsequently release VIP to coincide with glutamate release from retinal afferents onto postsynaptic targets in the dorsal aspect of the SCN. As the circuit continues dorsally and the glutamatergic signals become weaker, VIP plays a more prominent role in recruiting the appropriate postsynaptic responses (see Fig. 1).

The gene expression studies in this dissertation add a critical understanding to this model by examining the spatio-temporal profile of photic responses in the SCN. This type of analysis

allowed us to separate the SCN across its different axes and record changes in gene expression through time with all of the necessary circuitry intact. Without the knowledge that the SCN shell was nearly devoid of gene expression responses, or the observation that gene expression responses are not sustained in VIP KO mice, it would not have been possible to create a systems-based explanation for how the SCN is capable of its multi-tasking role. Based on this work and that from others utilizing transgenic models of VIP-ergic signaling, it is possible to summarize the two essential roles of VIP in the SCN: 1) to synchronize individually oscillating neurons via cAMP activation through VIP-ergic signaling alone (Aton *et al.*, 2005; Aton *et al.*, 2006) or concomitant with GABA-ergic signaling (Liu & Reppert, 2000; Itri & Colwell, 2003); and 2) to modulate phase shifting responses from the external environment by postsynaptic potentiation of glutamatergic responses from retinal afferents. Before beginning work on these studies, I had posited that 'VIP is necessary for integration of photic information through the SCN'. This hypothesis is now refined with a very specific model that is testable in numerous future experiments.

Subsequent experiments can examine if VIP potentiates glutamatergic phase shifting responses *in vivo* by using a number of pharmacological means. This approach has been used in the past to determine the identities of many of the players in the signaling pathways regulating behavioral phase shifts and would be appropriate here as well. Firstly, VPAC2R agonists could be infused to the third ventricle in the VIP KO mouse during a nighttime light pulse as an attempted rescue study. A reasonable hypothesis would be that when applied together with a VPAC2R agonist, the behavioral effects of a phase shifting light pulse would be restored in VIP KO mice. Since no antagonist for VPAC2R is available for the mouse, adenylyl cyclase inhibitors could be infused into WT mice during a nighttime light pulse to phenocopy the phase

shifting impairments in VIP KO mice. Following, instead of a light pulse, nighttime infusion of NMDA agonists at varying concentrations, together with a VPAC2R agonist (or without in control conditions), can also be used to elicit and measure behavioral phase shifts in VIP KO mice. This dose-response of NMDA against the presence of VIP-ergic signaling would establish *in vivo* how NMDA mediated behavioral responses are potentiated by VIP.

Independently of these findings, mechanistic studies can also be carried out to determine the *in vivo* cell signaling differences between WT and VIP KO mice that are responsible for their behavioral phase shifting light phenotypes. As Chapter 2 has set up an experimental paradigm for exposing mice to a light pulse and mapping the spatial expression of proteins or mRNA within the SCN, this established system can be applied to analyze the SCN expression patterns of pCAMKII, pMAPK, pCREB, pH3 (phosphorylated histone protein), PKA and EPAC. I propose the topographically specific activity of each of these molecular signals is responsible for the differential expression of *Per1* and c-FOS in WT mice, and since VIP-ergic signaling is integral for normal photoentrainment and phase shifting, VIP KO mice will show differential, spatially-specific activity of these signaling molecules compared to WT mice.

Immunohistochemistry can be used with antibodies directed against pCaMKII, pMAPK, pCREB and pH3 to map out their distribution in the SCN in their 'activated state'. Only one time point will need to be analyzed for these initial studies, but analysis will include core and shell distribution patterns. For PKA and EPAC, an autoradiographic distribution analysis will be used on SCN sections bound by radiolabeled cAMP. With pCaMKII, there should be high expression in both WT and VIP KO mice in the core and low expression in the shell. For pMAPK, since the signal is boosted in the shell due to EPAC-related activity, WT mice are expected to show high levels in both the core and shell, whereas VIP KO mice will only show high levels in the core.

Similarly, since the pMAPK pathway contributes to both CREB and H3 phosphorylation, WT mice and VIP KO mice will show pCREB and pH3 expression patterns that will respectively mirror the predicted pMAPK expression patterns. In the autoradiography experiments, both WT and VIP KO mice are expected to show low levels of cAMP binding in the core, but only WT mice will show high binding levels in the shell.

To tie these studies together, pharmacological inhibitors of CaMKII, MAPK and PKA can be infused into the third ventricle of WT and VIP KO mice and both light induced behavioral phase shifts and gene expression responses can be compared. I hypothesize that with all three of these infusions, WT mice will mimic the phenotypes of VIP KO mice. Also, blocking CaMKII and MAPK will result in a complete block of photic gene induction in both genotypes, and PKA inhibition will bring WT photic gene induction back down to the levels of VIP KO mice that were seen in Chapter 2. PKA inhibition should have no major affect on photic gene induction in VIP KO mice, as this pathway is assumed to be largely inactive without VPAC2R-mediated signaling.

In addition to experiments outlined in this model, there is one major difference in the c-FOS phenotype of VIP KO mice that is also worth further investigation. Because c-FOS protein is supposed to have a half-life of about 2 hours (Curran *et al.*, 1984), it is unexpected that VIP KO mice show a large reduction in c-FOS expression within 60 minutes (see Chapter 2, Fig. 15). It is therefore possible that in the VIP KO mouse, there are differences affecting either protein stability or protein degradation. Either of these effects could explain previous work in the VPAC2R KO mouse reporting that PER1 protein does not appear to increase as it should to a phase shifting light pulse, whereas there is a noticeable, albeit blunted, *Per1* mRNA response (Harmar *et al.*, 2002; Maywood *et al.*, 2007). Since it has been noted that MAPK can

phosphorylate and stabilize several clock proteins (Hirota & Fukada, 2004), one mechanism by which c-FOS levels show more rapid degradation in VIP KO mice could be through diminished MAPK activation. In this line of experiments, it would be useful to determine the spatial differences in degradation rates. If VIP is necessary for modulating MAPK signaling in sparsely innervated glutamatergic targets, then shell neurons would be expected to express a more severe phenotype than core neurons in the VIP KO SCN. Since this type of experiment would be difficult to carry out *in vivo*, it may be useful to use laser micro-dissection to isolate core and shell sub-populations of neurons and quantify protein degradation rates *in vitro*. This could be done using something like a Bradford assay to determine total protein amounts and compare how they change over time in VIP KO and WT mice.

An acute interpretation

The transgenic approach has allowed for new insights in understanding the mechanisms by which circadian circuits can produce sustained rhythmicity and adapt to changing environmental light cues. In the past, the advantage to using a ligand knockout animal was that exogenous reintroduction of that ligand could be used to rescue the mutant phenotype and establish temporally and spatially specific actions of that gene. This experimental paradigm was carried out in two important studies that helped define a specific role for VIP in circadian rhythm generation in the SCN.

The first of these studies utilized SCN neurons from VIP KO mice in a dispersed microelectrode array (Aton *et al.*, 2005). Compared with WT neurons, VIP KO neurons showed low amplitude firing rate rhythms with dispersed phases across the array. When a VPAC2R

agonist was added to the neurons, the phases of the neurons became more coherent and unified, and the firing rate rhythm amplitude across the array was increased. The authors of this study noted 'no morphological differences' in the neurons of the VIP KO mice compared to WT mice and concluded that VIP acted acutely to synchronize individual SCN neuron electrical rhythms and boost the SCN firing rhythm amplitude across the circuit as a whole. While this study established a new, testable model by which VIP acted as a synchronizing agent, its results were not quite definitive for the role of VIP. This is because the study was carried out *in vitro*, pharmacological agonists might have had non-specific effects, and only a gross comparison of neuronal morphology was used as evidence supporting an acute effect of VIP.

It is important to remember that VIP is not released at constitutive levels in the SCN across the light-dark cycle (Francl *et al.*, 2010). Although it maintains largely consistent levels throughout the day, VIP has a very confined window of elevated release during the middle of the light period (Francl *et al.*, 2010). Therefore, acute application of an agonist to neurons that have a baseline VIP tone of zero is not going to necessarily replicate the actions of VIP *in vivo* in a WT SCN. This limitation on the dynamic, temporal importance of rescue studies has made interpretation of such results considerably more difficult.

Another recent study addressed some of these issues by looking at real-time gene expression rhythms of the clock gene *Per2* in VIP KO mice (Maywood *et al.*, 2011). In this study, a paracrine action for VIP-based synchronization was suggested, as individually phase-dispersed SCN neurons in the VIP KO SCN were shown to become synchronized when an SCN explant graft from a WT mouse was placed on it. Furthermore, this occurred while direct contact was prevented by a semi-permeable membrane. Not only did the WT explant restore rhythmicity, other neuropeptidergic signaling targets were pharmacologically tested as well, and a hierarchy

was established where VIP had the most robust effects of all the peptides in promoting phase synchrony and SCN rhythm amplitude. While this study did not examine any morphological characteristics of VIP KO neurons, it was valuable for providing more direct evidence of an acute role for VIP in synchronizing SCN neurons.

A congenital and ubiquitous interpretation

Because the transgenic models for VIP-ergic signaling are both congenital and ubiquitous, interpretation of results from VIP KO studies need to be considered beyond an acute context. This interpretation includes roles for VIP in organizing circadian system connectivity and indirect actions via pathways that feedback to the circadian system. VIP-ergic pathways are particularly difficult to place into a category of acute, chronic, or organizational, not necessarily because VIP is any more pleiotropic than other transmitters or peptides, but its identification over half a century ago has allowed for a large research effort and the characterization of a diverse set of actions of VIP across multiple developmental and physiological systems. These roles include vasodilation, neural development, neuroprotection, neural repair, glial metabolism, steroidogenic signaling, immunomodulation and cellular transformation, just to name a few. Any one of these VIP-ergic effects could contribute or account for the circadian phenotypes seen in VIP KO mice. Furthermore, since conditional knockout models of VIP have not yet been created for testing effects of VIP in the adult circadian system, it was necessary to take another anatomical approach to address the possibility that the congenital and ubiquitous loss of VIP resulted in important changes in connectivity along different points in the circadian visual pathway.

VIP-ergic and retinal afferent input are modulated in opposite and complimentary directions

To start, there have been many observations of VIP-ergic expression in the SCN being responsive to changes in light input levels reaching the hypothalamus. These include studies of VIP expression in retinally degenerate or anophthalmic animals (Laemle & Rusa, 1992; Ruggiero *et al.*, 2010) as well as in those housed in specific lighting conditions (Albers *et al.*, 1987; Smith & Canal, 2009). Nearly all of these studies report the same trend: when light input is high, VIP expression in the SCN is low. The opposite trend has also been demonstrated when light levels are low. Therefore, it appears that VIP signaling in the SCN is organized by a mechanism that is both plastic and responsive to ambient lighting.

This trend fits well into the model I have created to explain the role of VIP in photic gene expression (see Fig. 1). In this model, VIP plays a more prominent role in recruiting the appropriate postsynaptic responses when glutamatergic signaling from retinal afferents is weaker. If more neurons begin to express VIP in response to lower glutamatergic tone, then the SCN circuit can maintain homeostatic levels of its postsynaptic responses. The first major finding in Chapter 3 of this dissertation work suggests that the opposite relationship can also exist: in response to VIP deficiency, glutamatergic input from retinal axon terminals could be increased to maintain postsynaptic homeostasis. Specifically, this trend was illustrated in the form of increased retinal axon branching in the SCN of VIP KO mice (Chapter 3, Fig. 2).

While an observed increase in the number of terminal branches from glutamatergic inputs would make sense as a compensatory mechanism to maintain postsynaptic responses in the

absence of VIP, further work would be useful to determine if this branching results in more synapses or has other functional implications. It is quite possible that as a compensatory response to a genetic deletion, the functionality of increased branching is minimal. This is likely, given that there are profound deficits in the light response phenotypes in the VIP KO mice. Regardless of functional interpretations, one key point to keep in mind is that there appears to be some kind of communication and plasticity between the organization of the VIP-ergic and glutamatergic circuits in the SCN. As one pathway increases its output, the other seems to decrease.

To follow up with the experiments on retinal branching, functional experiments should be carried out to verify the effects of increased branching found in VIP KO mice. First, in order to determine whether or not increased branching further implies more synapses, synaptophysin immunohistochemistry can be used to quantify differences in synaptic number between WT and VIP KO mice. Second, in order to verify that more branches indicates higher glutamatergic input, third ventricle microdialysis with high performance liquid chromotgraphy, or alternatively, glutamate biosensors, can be used to quantify the amount of glutamate released in response to a phase shifting light pulse. If there is a reciprocal relationship between glutamate and VIP, then VIP KO mice should show relatively higher glutamate release than WT mice in response to a phase shifting light pulse. Since intracellular signaling pathways have been altered in VIP KO mice, this increase in glutamate would be insufficient to induce a phase shift or induce *Per1* or c-FOS to appropriate levels. Finally, to relate these findings to previous work, WT and VIP KO mice could be reared in constant light environments, and then as adults, the DiI and Sholl-like analysis from Chapter 3 could be used to determine if retinal branching complexity is altered. Since WT mice show a reduction in VIP expression from this paradigm (Smith & Canal, 2009), it is predicted that they will show increased branching akin to that of VIP KO mice. According to

my model, the VIP KO mice will most likely be unaffected by this environment at the level of retinal branching, as the postsynaptic homeostasis that the glutamatergic neurons attempt to induce by increased branching would have already been induced in VIP KO mice without any further environmental manipulation.

Axonal properties affected by VIP loss

Results from the DiI tract tracing study have to be interpreted with the consideration that axonal properties could also be affected by VIP loss. In fact, subsequent immunostaining for the neurofilament medium subunit (NF-M) showed increased expression in VIP KO mice in the SCN and in other brain areas (see Chapter 3, Fig. 3). A similar observation has also come from one study in which a VIP antagonist was injected to pregnant mice, and subsequent cortical NF-M expression was shown to increase in offspring (Zupan *et al.*, 2000). In addition to NF-M effects, cortical expression of NMDA-R1 (a subunit necessary for normal NMDA receptor function) was also shown to increase in this model of VIP-ergic blockade. Thus, in maternally-targeted VIP disruption, we can see another example of a homeostatic regulation to balance VIP-ergic and glutamatergic signaling. Furthermore, since these effects were specifically mediated by maternal VIP, it is important to consider using VIP KO mice from heterozygous breeding pairs in future experiments in order to determine the origin of developmentally-specific phenotypes found in VIP KO brains.

A specific, functional implication for NF-M expression differences most likely would involve differences in axonal transport and radial growth, as these are the major roles played by neurofilaments (Julien, 1999; Al-Chalabi & Miller, 2003). In a simple interpretation, the higher

NF-M expression is reflective of larger diameter axons, and since larger diameter, myelinated axons have higher relative conduction velocities, then VIP KO mice could also have faster conduction through the optic nerves, SCN and other brain regions. These NF-M observations need to be further quantified by western blot and compared with relative expression levels of NF-H and NF-L. Furthermore, in order to address questions of individual axon caliber changes, electron microscopy studies would be needed. Finally, electrophysiological experiments would be necessary to test the hypothesis that conduction velocities are faster in VIP KO mice.

Differences in conduction velocities in VIP KO mice would be an important finding, as brain white matter abnormalities have been linked with many psychiatric disorders, and it is hypothesized that these abnormalities alter nerve conduction velocities responsible for some disease characteristics (Fields, 2008). In schizophrenia, for instance, it has been hypothesized that conduction delays may account for a mistiming in neural signals that result in hallucinations and passivity experience (Whitford *et al.*, 2012). Also in schizophrenia, it was recently reported that there is a strong association with an increased copy number variant in the *VIPR2* gene, which codes for the VPAC2R (Vacic *et al.*, 2011). Since the increased *VIPR2* expression also increased VIP-ergic signaling (Vacic *et al.*, 2011), an interesting target for future research would be to establish if there is a relationship between VIP, conduction velocity and schizophrenia. In this way, the findings from the work in Chapter 3 could be applicable as pointing out either circadian-related biomarkers or mechanistic targets for research that extend outside of the field of biological rhythms.

Androgen signaling as an indirect pathway affected by VIP loss

Another important finding from Chapter 3 is that there was a specific loss of androgen receptor (AR) expression in the VIP KO mouse. Mechanistically, this fits well into a model based on data from other studies on the role of androgen signaling in the circadian system. In male rodents, androgen receptor expression is regulated by testicular hormones, as castration results in greatly diminished SCN AR expression, and testosterone supplementation restores this expression (Iwahana *et al.*, 2008). In these mice, the effects of castration and testosterone supplementation are directly related to the amount of c-FOS expressed in the SCN in response to phase shifting light pulses (Karatsoreos *et al.*, 2007). In terms of a mechanism, there is evidence that AR binding can trigger a rapid, non-genomic response that begins with Ca^{2+} influx. This influx recruits the MAPK signaling pathway (Heinlein & Chang, 2002), providing a mechanistic pathway to account for this c-FOS response deficiency. In addition to altered control by a disrupted MAPK signaling pathway, castrated mice would have deficiencies in the direct nuclear actions of the androgen receptor. *Per1* contains an androgen response element in its promoter region, and AR activity has been reported to induce *Per1* expression (Gery & Koeffler, 2010). Taken together, testicular hormones signaling through AR receptors can modulate photic gene expression responses in the SCN.

As young adults, VIP KO mice have diminished levels of testosterone compared to WT mice (Lacombe et al., 2007). As mice age, they normally undergo a reduction in testosterone levels, usually to around the same numbers as found in young VIP KO mice. Also, testosterone levels do not significantly change across the lifespan of VIP KO mice. These changes in testosterone levels in WT mice parallel changes in photic responsivity and VIP expression in aged animals. Thus, the VIP KO mouse could be a useful model to study some of the androgenic mechanisms underlying an age-related decline in circadian photic responses.

For these reasons, we supplemented testosterone levels in VIP KO mice with the goal of rescuing photic response deficiencies. As a starting point, we first tested how testosterone supplementation would affect the strikingly altered entrainment that VIP KO mice exhibit once released into constant conditions. As this did not result in any behavioral changes in the VIP KO mice, this line of experiments was discontinued. It is important to note that this experiment had a small *n*, did not examine the phenotype of single light pulse phase shifts (which could be affected differently than stable entrainment), and did not look at the core anatomy to confirm that AR expression was restored. However, our results, demonstrating a complete lack of effect of testosterone supplementation in photoentrainment, suggest that testosterone by itself is not mediating the circadian system's altered response to light in VIP KO mice.

The idea that testosterone could potently affect light-responsive properties of the circadian system needs to be explored further. As was already mentioned, the testosterone supplementation experiments could be expanded upon. Since testosterone supplementation involved adding more testosterone to a system that already had moderate levels, it is possible that this setup actually increased testosterone to super-physiological doses causing added difficulty in the interpretation of results. To avoid this in future studies, male VIP KO mice could be castrated, along with WT mice, and both photoentrainment and phase shifting parameters can be compared. Afterwards, these mice can then receive testosterone supplementation, and the same circadian parameters can be again compared. This would allow us to control for testosterone levels between both genotypes. If castration and supplementation affect these parameters differently in WT and VIP KO mice, then our studies would suggest that an interaction of VIP and testosterone affects the circadian visual system differently than either does by itself.

Another interesting aspect of androgenic signaling in the circadian system is that it can

have effects that are organizational, in addition to activational. In rats, it was found that if castration occurred before an early postnatal surge in testosterone, animals advanced the phase angle of entrainment in their core body temperature to the LD cycle as adults. Adult testosterone supplementation did not rescue the phenotype, but injecting testosterone around the time of castration to mimic the normal surge earlier in life normalized the phase angle (Zuloaga *et al.*, 2009). Therefore, if the activational effects of androgenic signaling in VIP KO mice do not account for any of their photic response phenotypes, we would still have to rule out that testosterone could be playing an organizational role in the circadian visual system.

Neuronal distribution patterns consistent despite loss of VIP

From the experiments using Golgi impregnation, we found that VIP KO mice did not significantly differ from WT mice in SCN neuronal connectivity. The parameters measured in this way required classification based on dendritic characteristics, and the distributions of these different neuronal subtypes were compared across genotypes. Morphological differences in SCN neurons are not as robust as in other brain areas, however, and inference about connectivity and function has been scarcely, if at all, experimentally tested. Therefore, while no differences in distribution were found from our studies, there are many other anatomical correlates of connectivity that should additionally be tested before we can conclude that SCN neuronal connectivity does not differ between WT and VIP KO mice. Since the parameters one can measure from Golgi impregnation are comparatively as diverse as the number of Golgi studies that have been published, honing in on another target is the most challenging step for further analysis.

One suggested target for further Golgi impregnation analysis would be the orientation and extension of dendrites in the SCN of VIP KO mice. Since it appears that axonal inputs to the SCN are more numerous in the VIP KO mouse, one reasonable expectation is that dendritic fields within the SCN could also be affected. In a mouse carrying a mutation that causes anophthalmia, one study reported specific differences in SCN dendritic orientation and size (Silver, 1977). In WT mice, these dendrites had one major, dorsally-oriented apical process and one basal process that coursed toward visual input axons around the optic chiasm. In anophthalmic mice, many of these neurons showed normal apical dendrites, but basal dendrites were often diminished in size or oriented along an 'irregular course' (Silver, 1977). Using these dendrites for further analysis can easily be accomplished and would be a logical next step for this study. I hypothesize that because anophthalmic animals have increased VIP expression in the SCN relative to WT mice, VIP KO mice will have basal dendrites that are even longer than in the WT SCN. If this hypothesis is supported, we could then employ electrophysiological analysis specifically on NMDA-evoked responses in SCN dendrites in VIP KO mice to determine a functional outcome of this possible anatomical correlate of connectivity.

Conclusion

As was stated in the first chapter, temporal organization is a fundamental property that has evolved multiple mechanisms in its regulation. One such mechanism involving the mammalian circadian timekeeping system is the action of VIP to 'mark time' between neurons. VIP unifies individual oscillators to allow robust and consistent timekeeping across SCN cells. Since VIP-ergic activity can be acutely altered by the presence or absence of light, the magnitude

of this synchronizing role can be quickly and efficiently altered to allow for either broad phase dispersion or narrow alignment of individual oscillators. As VIP also acts to potentiate the strength of environmental light signals that are carried by retinal afferents, it performs two essential functions that confer unique properties to the mammalian SCN as both a multi-tasking and self-sustaining network. Not only does it appear that VIP acts acutely, but it also plays a role in the structuring of the SCN to allow for the efficient flow of light-resetting information across the circadian system. While the studies described in this dissertation provide some insight into the mechanisms by which VIP acts in photic resetting, a number of follow up experiments will also be necessary to further define the effects of VIP and its genetic deletion. These studies will lead to progress in our understanding of neural circuits both within the SCN and throughout the nervous system as a whole. This increased understanding of the circadian system will undoubtedly be beneficial for the application of chronobiological interventions to improve quality of life and treat human disease.

Fig. 1. Phase shifting across the SCN uses postsynaptic integration from glutamate and VIP

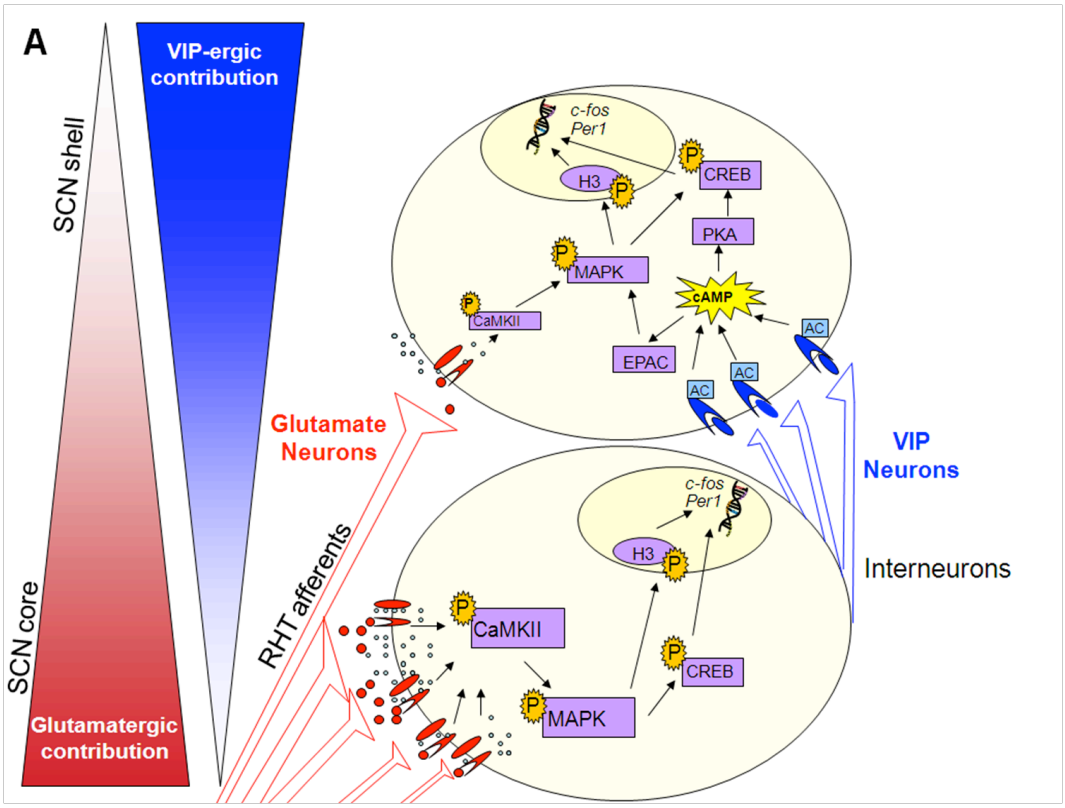

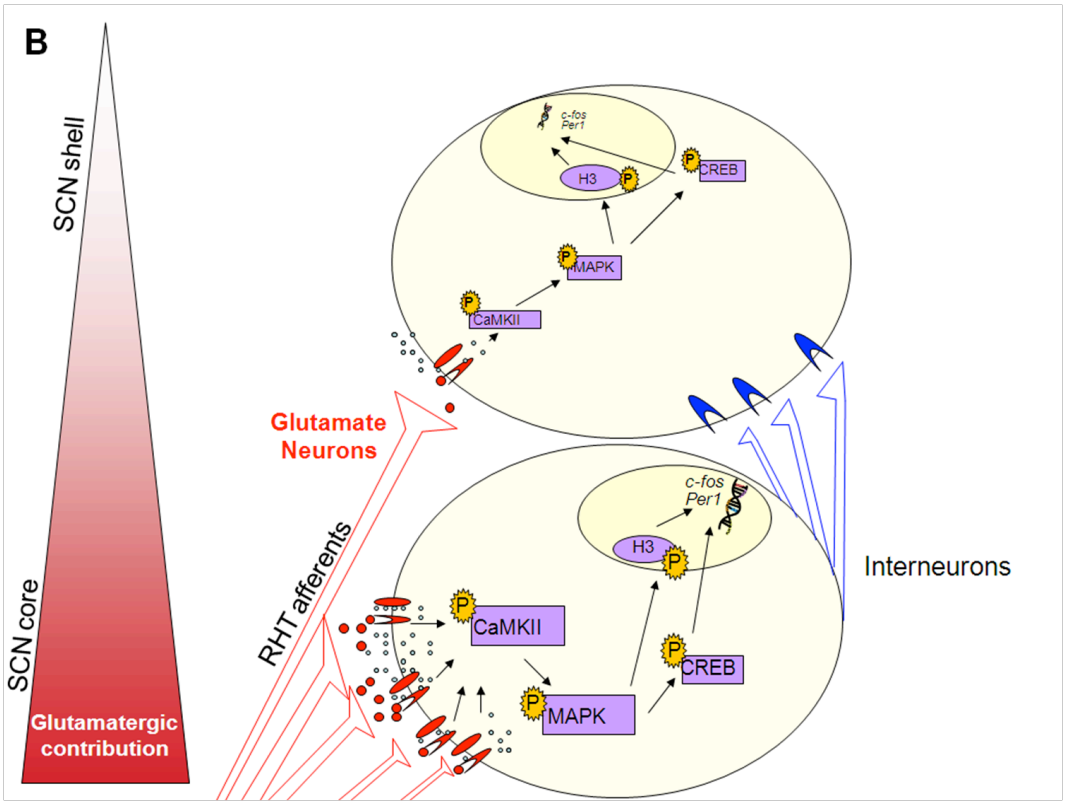

Photic resetting in the SCN requires glutamatergic signaling through retinal hypothalamic tract (RHT) afferents (red). Topographically, there is less glutamatergic input in the more dorsal aspects of the nucleus. (A) In a WT SCN, phase resetting light information first reaches the ventral-most portion of the SCN core where VIP+ perikarya are found (blue). In retino-recipient neurons, glutamate from RHT axons (red circles) binds postsynaptically to NMDA receptors (red), allowing for the influx of Ca^{2+} (as illustrated by tiny circles traveling through NMDA channels). Ca^{2+} influx then leads to the phosphorylation of CaMKII, and through the action of other second messengers, the phosphorylation of MAPK. pMAPK acts through another set of second messengers to phosphorylate a histone subunit to relax the nucleosome and induce chromatin modifications that promote gene expression. pMAPK signaling also promotes CREB phosphorylation, causing CREB to translocate to the nucleus and bind to CRE regions on the promoters of *c-fos* and *Per1* to initiate their transcription. These retino-recipient neurons also release VIP (blue ovals) on more dorsal SCN neurons where postsynaptic binding to VPAC2 receptors (blue) takes place. These dorsal neurons have relatively decreased levels of pCaMKII due to less NMDA-mediated Ca^{2+} influx, but intracellular signaling magnitude is supplemented by VIP-ergic pathways. VIP-VPAC2 binding initiates adenylyl cyclase (AC), activity, which converts ATP to cAMP. The second messenger cAMP induces conformational changes in EPAC and PKA which then promote the phosphorylation of MAPK and CREB, respectively. Thus in more dorsal neurons, the binding of VIP and glutamate together achieve the appropriate levels of cell signaling to initiate proper gene expression responses. (B) In a VIP KO SCN, ventral core neurons receive glutamate from RHT axons just as in the WT SCN, and these neurons utilize cell signaling pathways that effectively induce gene expression changes necessary for phase shifting. However, since retino-recipient neurons no longer can release VIP on more dorsal neurons, intracellular signaling magnitude is no longer supplemented. Because of this deficiency, dorsal core and shell gene expression responses are greatly diminished, as they directly reflect the decreased levels of pCaMKII without the cAMP-mediated bolstering of other cell signaling pathways that converge on the phosphorylation of MAPK and CREB. It is through this proposed mechanism that VIP KO mice show specific deficiencies in photic phase shifting and entrainment.

Abrahamson, E.E. & Moore, R.Y. (2001) Suprachiasmatic nucleus in the mouse: retinal innervation, intrinsic organization and efferent projections. *Brain Res*, **916**, 172-191.

Al-Chalabi, A. & Miller, C.C. (2003) Neurofilaments and neurological disease. *Bioessays*, **25**, 346-355.

Albers, H.E., Minamitani, N., Stopa, E. & Ferris, C.F. (1987) Light selectively alters vasoactive intestinal peptide and peptide histidine isoleucine immunoreactivity within the rat suprachiasmatic nucleus. *Brain Res*, **437**, 189-192.

Antle, M.C. & Silver, R. (2005) Orchestrating time: arrangements of the brain circadian clock. *Trends Neurosci*, **28**, 145-151.

Aton, S.J., Colwell, C.S., Harmar, A.J., Waschek, J. & Herzog, E.D. (2005) Vasoactive intestinal polypeptide mediates circadian rhythmicity and synchrony in mammalian clock neurons. *Nat Neurosci*, **8**, 476-483.

Aton, S.J. & Herzog, E.D. (2005) Come together, right...now: synchronization of rhythms in a mammalian circadian clock. *Neuron*, **48**, 531-534.

Aton, S.J., Huettner, J.E., Straume, M. & Herzog, E.D. (2006) GABA and Gi/o differentially control circadian rhythms and synchrony in clock neurons. *Proc Natl Acad Sci U S A*, **103**, 19188-19193.

Benloucif, S., Masana, M.I. & Dubocovich, M.L. (1997) Light-induced phase shifts of circadian activity rhythms and immediate early gene expression in the suprachiasmatic nucleus are attenuated in old C3H/HeN mice. *Brain Res*, **747**, 34-42.

Besson, J., Sarrieau, A., Vial, M., Marie, J.C., Rosselin, G. & Rostene, W. (1986) Characterization and autoradiographic distribution of vasoactive intestinal peptide binding sites in the rat central nervous system. *Brain Res*, **398**, 329-336.

Butcher, G.Q., Lee, B., Cheng, H.Y. & Obrietan, K. (2005) Light stimulates MSK1 activation in the suprachiasmatic nucleus via a PACAP-ERK/MAP kinase-dependent mechanism. *J Neurosci*, **25**, 5305-5313.

Cheng, H.Y., Dziema, H., Papp, J., Mathur, D.P., Koletar, M., Ralph, M.R., Penninger, J.M. & Obrietan, K. (2006) The molecular gatekeeper Dexras1 sculpts the photic responsiveness of the mammalian circadian clock. *J Neurosci*, **26**, 12984-12995.

Cheng, H.Y. & Obrietan, K. (2006) Dexras1: shaping the responsiveness of the circadian clock. *Semin Cell Dev Biol*, **17**, 345-351.

Colwell, C.S., Michel, S., Itri, J., Rodriguez, W., Tam, J., Lelievre, V., Hu, Z., Liu, X. & Waschek, J.A. (2003) Disrupted circadian rhythms in VIP- and PHI-deficient mice. *Am J Physiol Regul Integr Comp Physiol*, **285**, R939-949.

Crosio, C., Cermakian, N., Allis, C.D. & Sassone-Corsi, P. (2000) Light induces chromatin modification in cells of the mammalian circadian clock. *Nat Neurosci*, **3**, 1241-1247.

Curran, T., Miller, A.D., Zokas, L. & Verma, I.M. (1984) Viral and cellular fos proteins: a comparative analysis. *Cell*, **36**, 259-268.

Dragich, J.M., Loh, D.H., Wang, L.M., Vosko, A.M., Kudo, T., Nakamura, T.J., Odom, I.H., Tateyama, S., Hagopian, A., Waschek, J.A. & Colwell, C.S. (2010) The role of the neuropeptides PACAP and VIP in the photic regulation of gene expression in the suprachiasmatic nucleus. *Eur J Neurosci*.

Fang, M., Jaffrey, S.R., Sawa, A., Ye, K., Luo, X. & Snyder, S.H. (2000) Dexras1: a G protein specifically coupled to neuronal nitric oxide synthase via CAPON. *Neuron*, **28**, 183-193.

Fields, R.D. (2008) White matter in learning, cognition and psychiatric disorders. *Trends Neurosci*, **31**, 361-370.

Francl, J.M., Kaur, G. & Glass, J.D. (2010) Regulation of vasoactive intestinal polypeptide release in the suprachiasmatic nucleus circadian clock. *Neuroreport*, **21**, 1055-1059.

Gau, D., Lemberger, T., von Gall, C., Kretz, O., Le Minh, N., Gass, P., Schmid, W., Schibler, U., Korf, H.W. & Schutz, G. (2002) Phosphorylation of CREB Ser142 regulates light-induced phase shifts of the circadian clock. *Neuron*, **34**, 245-253.

Gery, S. & Koeffler, H.P. (2010) Circadian rhythms and cancer. *Cell Cycle*, **9**, 1097-1103.

Gibson, E.M., Williams, W.P., 3rd & Kriegsfeld, L.J. (2009) Aging in the circadian system: considerations for health, disease prevention and longevity. *Exp Gerontol*, **44**, 51-56.

Harmar, A.J., Marston, H.M., Shen, S., Spratt, C., West, K.M., Sheward, W.J., Morrison, C.F., Dorin, J.R., Piggins, H.D., Reubi, J.C., Kelly, J.S., Maywood, E.S. & Hastings, M.H. (2002) The VPAC(2) receptor is essential for circadian function in the mouse suprachiasmatic nuclei. *Cell*, **109**, 497-508.

Hattar, S., Liao, H.W., Takao, M., Berson, D.M. & Yau, K.W. (2002) Melanopsin-containing retinal ganglion cells: architecture, projections, and intrinsic photosensitivity. *Science*, **295**, 1065-1070.

Heinlein, C.A. & Chang, C. (2002) The roles of androgen receptors and androgen-binding proteins in nongenomic androgen actions. *Mol Endocrinol*, **16**, 2181-2187.

Hirota, T. & Fukada, Y. (2004) Resetting mechanism of central and peripheral circadian clocks in mammals. *Zoolog Sci*, **21**, 359-368.

Huang, S.K. & Pan, J.T. (1993) Potentiating effects of serotonin and vasoactive intestinal peptide

on the action of glutamate on suprachiasmatic neurons in brain slices. *Neurosci Lett*, **159**, 1-4.

Itri, J. & Colwell, C.S. (2003) Regulation of inhibitory synaptic transmission by vasoactive intestinal peptide (VIP) in the mouse suprachiasmatic nucleus. *J Neurophysiol*, **90**, 1589-1597.

Iwahana, E., Karatsoreos, I., Shibata, S. & Silver, R. (2008) Gonadectomy reveals sex differences in circadian rhythms and suprachiasmatic nucleus androgen receptors in mice. *Horm Behav*, **53**, 422-430.

Julien, J.P. (1999) Neurofilament functions in health and disease. *Curr Opin Neurobiol*, **9**, 554-560.

Karatsoreos, I.N., Wang, A., Sasanian, J. & Silver, R. (2007) A role for androgens in regulating circadian behavior and the suprachiasmatic nucleus. *Endocrinology*, **148**, 5487-5495.

Kiss, J., Csaki, A., Csaba, Z. & Halasz, B. (2008) Synaptic contacts of vesicular glutamate transporter 2 fibres on chemically identified neurons of the hypothalamic suprachiasmatic nucleus of the rat. *Eur J Neurosci*, **28**, 1760-1774.

Kolker, D.E., Fukuyama, H., Huang, D.S., Takahashi, J.S., Horton, T.H. & Turek, F.W. (2003) Aging alters circadian and light-induced expression of clock genes in golden hamsters. *J Biol Rhythms*, **18**, 159-169.

Laemle, L.K. & Rusa, R. (1992) VIP-like immunoreactivity in the suprachiasmatic nuclei of a mutant anophthalmic mouse. *Brain Res*, **589**, 124-128.

Larsson, L.I., Fahrenkrug, J., Schaffalitzky De Muckadell, O., Sundler, F., Hakanson, R. & Rehfeld, J.R. (1976) Localization of vasoactive intestinal polypeptide (VIP) to central and peripheral neurons. *Proc Natl Acad Sci U S A*, **73**, 3197-3200.

Liu, C. & Reppert, S.M. (2000) GABA synchronizes clock cells within the suprachiasmatic circadian clock. *Neuron*, **25**, 123-128.

Lupi, D., Semo, M. & Foster, R.G. (2010) Impact of age and retinal degeneration on the light input to circadian brain structures. *Neurobiol Aging*, **33**, 383-392.

Magistretti, P.J., Cardinaux, J.R. & Martin, J.L. (1998) VIP and PACAP in the CNS: regulators of glial energy metabolism and modulators of glutamatergic signaling. *Ann N Y Acad Sci*, **865**, 213-225.

Martin, J.L., Gasser, D. & Magistretti, P.J. (1995) Vasoactive intestinal peptide and pituitary adenylate cyclase-activating polypeptide potentiate c-fos expression induced by glutamate in cultured cortical neurons. *J Neurochem*, **65**, 1-9.

Maywood, E.S., Chesham, J.E., O'Brien, J.A. & Hastings, M.H. (2011) A diversity of paracrine signals sustains molecular circadian cycling in suprachiasmatic nucleus circuits. *Proc Natl Acad Sci U S A*, **108**, 14306-14311.

Maywood, E.S., O'Neill, J.S., Chesham, J.E. & Hastings, M.H. (2007) Minireview: The circadian clockwork of the suprachiasmatic nuclei--analysis of a cellular oscillator that drives endocrine rhythms. *Endocrinology*, **148**, 5624-5634.

Mikkelsen, J.D., Larsen, P.J. & Ebling, F.J. (1993) Distribution of N-methyl D-aspartate (NMDA) receptor mRNAs in the rat suprachiasmatic nucleus. *Brain Res*, **632**, 329-333.

Moore, R.Y. & Lenn, N.J. (1972) A retinohypothalamic projection in the rat. *The Journal of Comparative Neurology*, **146**, 1-14.

O'Neill, J.S., Maywood, E.S., Chesham, J.E., Takahashi, J.S. & Hastings, M.H. (2008) cAMP-dependent signaling as a core component of the mammalian circadian pacemaker. *Science*, **320**, 949-953.

Obrietan, K., Impey, S. & Storm, D.R. (1998) Light and circadian rhythmicity regulate MAP kinase activation in the suprachiasmatic nuclei. *Nat Neurosci*, **1**, 693-700.

Reppert, S.M. & Weaver, D.R. (2002) Coordination of circadian timing in mammals. *Nature*, **418**, 935-941.

Rosen, L.B., Ginty, D.D., Weber, M.J. & Greenberg, M.E. (1994) Membrane depolarization and calcium influx stimulate MEK and MAP kinase via activation of Ras. *Neuron*, **12**, 1207-1221.

Ruggiero, L., Allen, C.N., Brown, R.L. & Robinson, D.W. (2010) Mice with early retinal degeneration show differences in neuropeptide expression in the suprachiasmatic nucleus. *Behav Brain Funct*, **6**, 36.

Rusak, B., Guido, M.E. & Semba, K. (2002) Chapter VI Immediate-early gene expression in the analysis of circadian rhythms and sleep. In Kaczmarek, L., Robertson, H.A. (eds) *Handbook of Chemical Neuroanatomy*. Elsevier, pp. 147-170.

Said, S.I. & Mutt, V. (1969) A peptide fraction from lung tissue with prolonged peripheral vasodilator activity. *Scand J Clin Lab Invest Suppl*, **107**, 51-56.

Shen, S., Spratt, C., Sheward, W.J., Kallo, I., West, K., Morrison, C.F., Coen, C.W., Marston, H.M. & Harmar, A.J. (2000) Overexpression of the human VPAC2 receptor in the suprachiasmatic nucleus alters the circadian phenotype of mice. *Proc Natl Acad Sci U S A*, **97**, 11575-11580.

Silver, J. (1977) Abnormal development of the suprachiasmatic nuclei of the hypothalamus in a strain of genetically anophthalmic mice. *J Comp Neurol*, **176**, 589-606.

Sims, K.B., Hoffman, D.L., Said, S.I. & Zimmerman, E.A. (1980) Vasoactive intestinal polypeptide (VIP) in mouse and rat brain: an immunocytochemical study. *Brain Res*, **186**, 165-183.

Smith, L. & Canal, M.M. (2009) Expression of circadian neuropeptides in the hypothalamus of adult mice is affected by postnatal light experience. *J Neuroendocrinol*, **21**, 946-953.

Soloaga, A., Thomson, S., Wiggin, G.R., Rampersaud, N., Dyson, M.H., Hazzalin, C.A., Mahadevan, L.C. & Arthur, J.S. (2003) MSK2 and MSK1 mediate the mitogen- and stress-induced phosphorylation of histone H3 and HMG-14. *EMBO J*, **22**, 2788-2797.

Stephan, F.K. & Zucker, I. (1972) Circadian rhythms in drinking behavior and locomotor activity of rats are eliminated by hypothalamic lesions. *Proc Natl Acad Sci U S A*, **69**, 1583-1586.

Swaab, D.F., Fliers, E. & Partiman, T.S. (1985) The suprachiasmatic nucleus of the human brain in relation to sex, age and senile dementia. *Brain Res*, **342**, 37-44.

Takahashi, H., Umeda, N., Tsutsumi, Y., Fukumura, R., Ohkaze, H., Sujino, M., van der Horst, G., Yasui, A., Inouye, S.T., Fujimori, A., Ohhata, T., Araki, R. & Abe, M. (2003) Mouse dexamethasone-induced RAS protein 1 gene is expressed in a circadian rhythmic manner in the suprachiasmatic nucleus. *Brain Res Mol Brain Res*, **110**, 1-6.

Travnickova-Bendova, Z., Cermakian, N., Reppert, S.M. & Sassone-Corsi, P. (2002) Bimodal regulation of mPeriod promoters by CREB-dependent signaling and CLOCK/BMAL1 activity. *Proc Natl Acad Sci U S A*, **99**, 7728-7733.

Vacic, V., McCarthy, S., Malhotra, D., Murray, F., Chou, H.H., Peoples, A., Makarov, V., Yoon, S., Bhandari, A., Corominas, R., Iakoucheva, L.M., Krastoshevsky, O., Krause, V., Larach-Walters, V., Welsh, D.K., Craig, D., Kelsoe, J.R., Gershon, E.S., Leal, S.M., Dell Aquila, M., Morris, D.W., Gill, M., Corvin, A., Insel, P.A., McClellan, J., King, M.C., Karayiorgou, M., Levy, D.L., DeLisi, L.E. & Sebat, J. (2011) Duplications of the neuropeptide receptor gene VIPR2 confer significant risk for schizophrenia. *Nature*, **471**, 499-503.

van den Pol, A.N. (1991) The suprachiasmatic nucleus: morphological and cytochemical substrates for cellular interaction. In Klein, D.C., Moore, R.Y., Reppert, S.M., (U.S.), N.I.o.C.H.a.H.D. (eds) *Suprachiasmatic nucleus : the mind's clock*. Oxford University Press, New York, pp. 17-50.

Vertongen, P., Schiffmann, S.N., Gourlet, P. & Robberecht, P. (1997) Autoradiographic visualization of the receptor subclasses for vasoactive intestinal polypeptide (VIP) in rat brain. *Peptides*, **18**, 1547-1554.

Vosko, A.M., Schroeder, A., Loh, D.H. & Colwell, C.S. (2007) Vasoactive intestinal peptide and the mammalian circadian system. *Gen Comp Endocrinol*, **152**, 165-175.

Waltereit, R. & Weller, M. (2003) Signaling from cAMP/PKA to MAPK and synaptic plasticity. *Mol Neurobiol*, **27**, 99-106.

Welsh, D.K., Yoo, S.H., Liu, A.C., Takahashi, J.S. & Kay, S.A. (2004) Bioluminescence imaging of individual fibroblasts reveals persistent, independently phased circadian rhythms of clock gene expression. *Curr Biol*, **14**, 2289-2295.

Whitford, T.J., Ford, J.M., Mathalon, D.H., Kubicki, M. & Shenton, M.E. (2012) Schizophrenia, myelination, and delayed corollary discharges: a hypothesis. *Schizophr Bull*, **38**, 486-494.

Zuloaga, D.G., McGivern, R.F. & Handa, R.J. (2009) Organizational influence of the postnatal testosterone surge on the circadian rhythm of core body temperature of adult male rats. *Brain Res*, **1268**, 68-75.

Zupan, V., Nehlig, A., Evrard, P. & Gressens, P. (2000) Prenatal blockade of vasoactive intestinal peptide alters cell death and synaptic equipment in the murine neocortex. *Pediatr Res*, **47**, 53-63.